Syracuse University
SURFACE

Dissertations - ALL SURFACE

December 2016

Pressure Reduction on Wide Culverts with EPS Geofoam Backfill

Stephen Singh
Syracuse University

Follow this and additional works at: http://surface.syr.edu/etd

 Part of the Engineering Commons

Recommended Citation
Singh, Stephen, "Pressure Reduction on Wide Culverts with EPS Geofoam Backfill" (2016). *Dissertations - ALL*. 548.
http://surface.syr.edu/etd/548

This Thesis is brought to you for free and open access by the SURFACE at SURFACE. It has been accepted for inclusion in Dissertations - ALL by an authorized administrator of SURFACE. For more information, please contact surface@syr.edu.

Abstract

Buried structures may be subjected to excessive stresses that are detrimental to their expected service life. A review of previous design methods shows that there are effective methods to reduce loadings on narrow culverts. The Induced Trench Method introduces compressible fill over a buried structure to mobilize positive arching, and transfer stresses to the side fills. However, this method has not been studied with Bridge Culverts (large spanning culverts). This study evaluates the use of EPS (Expanded Polystyrene, Geofoam) as a compressible/lightweight fill material. The displacements and stresses of the classic narrow trench are examined in detail using the finite difference computer modeling program, FLAC (Fast Lagrangian Analysis of Continua). The narrow trench is then altered to study the overall effect of thickness and width of the compressible zone upon the stresses acting on the buried structure. To extend the service life of the culvert, recommendations are given on how to design with nearly equivalent horizontal and vertical stresses within an Induced Trench. In deeply buried structures, great consideration must also be given to the stresses applied on the geofoam. When geofoam is subjected to large confining axial and confining pressures, it exhibits modulus degradation and can lead to large deformations. This is observed in detail with the case study of the failure of the geofoam within a Bridge Culvert located in Carrs Creek, NY. Proper design methods with geofoam on large spanning, deeply buried culverts are evaluated and outlined. The effects of continuous joints, mixed densities, hydrostatic pressures, overloading, confining stresses, and creep on EPS geofoam are considered. An exponential model that captures the effect of confinement on modulus degradation has been programmed using FISH (FLAC internal coding) and verified with complimentary laboratory testing. A properly designed culvert section is

shown, in which all the design flaws of the culvert at Carrs Creek have been addressed. The stresses in the geofoam and underlying culvert are reduced to tolerable stress levels, while deformations have been greatly reduced. The results of this computer analysis have been presented in such a way that they can be used to aid in proper design of buried structures, using geofoam to reduce stresses and surficial displacements.

PRESSURE REDUCTION ON WIDE CULVERTS WITH EPS GEOFOAM BACKFILL

by

Stephen A. Singh

B.S., Syracuse University, 2011

Thesis
Submitted in partial fulfillment of the requirements for the degree of
Masters of Science in Civil Engineering

Syracuse University
December 2016

Copyright © Stephen Singh 2016
All Rights Reserved

Acknowledgements

First and foremost I offer my sincere gratitude for my thesis advisor, Professor Dawit Negussey, who has supported me throughout my undergraduate and graduate study with his knowledge and patience. Without his encouragement and effort, this thesis would not be complete. Thank you for believing in me and giving me the opportunity to work with you - I have grown as a student and a professional from the lessons you have imparted onto me.

I would like to thank Dr. S.K. Bhatia, Dr. E.M. Lui, Dr. S.P. Clemence, and Dr. J.A. Mandel for their advice and guidance during my time at Syracuse University. Your collective teachings have been essential to the completion of this thesis. I would also like to thank the members of the committee for their time and effort. Thanks to my fellow graduate students, Chen and Luke for their help, accommodations, and friendship. A special thanks to Amsalu, you are a great friend and mentor. I would also like to give thanks to Jared Green and James Delimitros of Langan Engineering for giving me the opportunity and encouragement to complete my thesis.

Finally, I would like to thank my parents Shamia and Ramnarace for working hard to provide this opportunity for me. The love and support of my parents, my "Sister" Sabrina, and my dear girlfriend Julie was vital to the completion of this thesis. Thank you.

Contents

List of Figures

List of Tables

List of Equations

Chapter 1 – Introduction

Rising global temperatures and ocean water levels have been linked to the increase of severe storms. Reports from the National Aeronautics and Space Administration (NASA) indicate that the frequency and severity of these storms are rising due to the elevated latent heat in the atmosphere. There is evidence that extra atmospheric water vapor is present, causing extreme downpours to occur 30% more often. Additionally, approximately 76% of weather stations in the United States have seen increases in extreme precipitation since 1948. Heightened precipitation levels may be problematic for civil infrastructures, primarily buried tunnels and culverts, which are typically low points; directing and controlling water flow (Voiland, 2013).

Buried flow mitigation structures are subjected to more frequent heavy flow interactions and periods of increased groundwater elevation, which could stress the structure beyond design limits. Existing predictions for 50-year and 100-year storms reoccur much sooner, accelerating the deterioration of buried structures, and instigating imminent collapse or failure. This is particularly important when it comes to older structures that have not been designed to endure these increased, more frequent loadings. Furthermore, visual inspections of buried structures are limited due to their submergence beneath fill, and may give insufficient indication of sudden catastrophic failures.

To assess critical conditions under pre-existing overburden pressures, buried structures must be rehabilitated or designed with great attention. Using combinations of properly placed lightweight fill, manipulating load transfer mechanisms, and appropriate guiding of surface

runoff/inlet flow; buried structures can be designed to last for the duration of their intended service life. These design conditions can be altered to accommodate buried structures of different geometries, covering narrow to large spanning bridges, and shallow to deeply buried culverts. The remainder of this thesis will focus strictly on the design of culverts, but concepts can be applied to other types of buried structures.

1.1 **Rapid Construction and the use of Precast Culverts**

As culverts meet their intended service life or need replacement, new culverts must be constructed and installed. Facilities that require rehabilitation or new installations are often below civil infrastructure such as roadways, buildings, and railways. This can impose time restrictions on construction, requiring culvert installations to be done very quickly. To complete projects in a short amount of time, techniques from Rapid Construction (RC) can be used, which is conceptually similar to Accelerated Bridge Construction. The primary objectives of RC are established with scheduling. Innovative construction methods are implemented to accommodate time requirements, while minimizing labor costs, equipment, space, material cost, delay, and environmental impacts. Key design components of RC with culverts include the use of precast sections, minimizing fill compaction time, and minimizing immediate settlements (Culmo, 2011).

Precast culvert sections are beneficial in terms of RC. Constructing culverts with reinforced concrete can prolong the amount of time required to complete the project with a curing time of 7 days with ASTM C 150 Type I Cement. Precast culvert sections can be transported to the project site and installed very quickly. However, this requires prior planning with the supplier

to ensure that the precast culvert is the appropriate size and can support the loadings expected in the scope of the project. The same concept of advanced material preparation is also present in RC with the use of fill. Earth fill is compacted on site, and requires a compaction time proportional to the amount of fill placed since it is typically done in 12inch lifts. By using lightweight fill to replace earth fill while maintaining surface elevation, compaction times can be reduced. For example, Expanded Polystyrene (EPS, Geofoam) blocks can be stacked to replace earth fill, and do not require compaction. More importantly, replacing compacted earth fill with lightweight fill reduces the overburden pressures acting on the culvert.

1.2 Load Reduction on Buried Culverts

I. Classical Buried Structure-Soil Interaction Theory

The mechanisms controlling load reduction on buried culverts are similar to those for buried pipes. Research into buried pipes and interaction with soil was studied by Marston at Iowa State College (Taylor, 1971). Marston analyzed soil pressures on buried concrete and clay pipes underneath roadway embankments to optimize designs and prevent failures. Marston defined two main types of loading conditions: a ditch conduit (trench load condition) and a projecting conduit (embankment condition). The ditch conduit loading condition consists of the installation of a pipe in a narrow trench in undisturbed soil, where the trench is then backfilled to the natural ground surface. In projecting conduits, the pipe is installed underneath an embankment with the top of the pipe projecting above the natural ground surface. Visual representations of a ditch conduit and projecting conduit are shown in Figure 1. The method of installation used will have a significant effect on the loads carried by the pipe (Taylor, 1971).

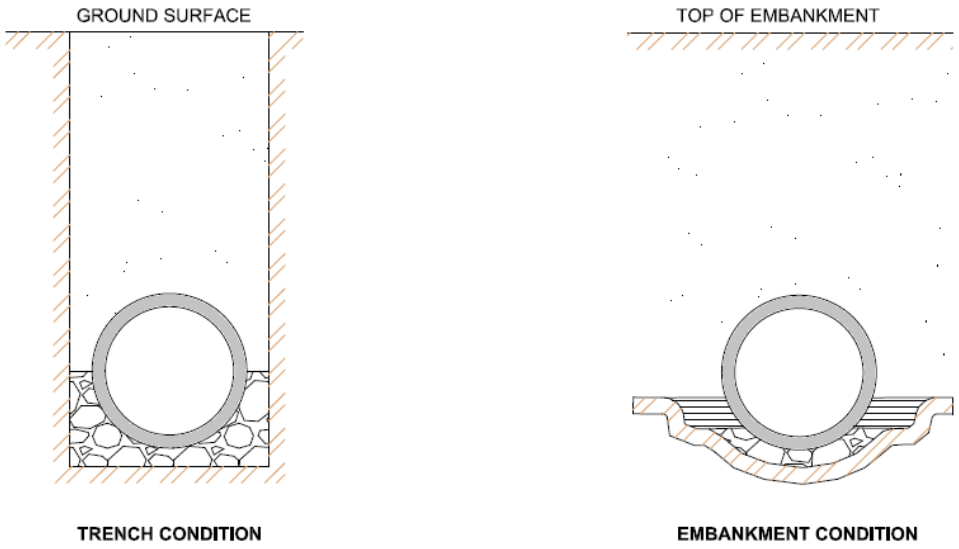

Figure 1: Buried Structure Loading Conditions
(Recreated from American Concrete Pipe Association, 2011)

Marston's load theory suggested that the loadings on a buried pipe vary depending on the relative movement of the prisms of soil adjacent to the pipe or between the trench walls. The movement of the adjacent or overlying prisms of soil generate shear stresses, which alter the distribution of stress (Taylor, 1971). Movement of soil prisms are dependent on the rigidity of the buried materials. The transfer of stresses in a multi-component support system is known as arching. In the case where the buried structure is more rigid than the adjacent soil, arching will be defined as negative arching, where the structure will be exposed to greater pressures relative to the calculated "free-field" pressures from the sum of overburden pressures alone (Taylor, 1971)(Spangler, 1973). Negative arching is demonstrated in Figure 2: Negative Arching.

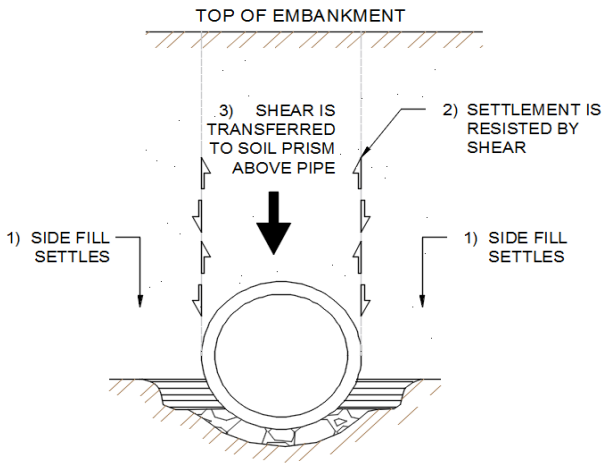

Figure 2: Negative Arching

Marston found that in trench conditions where the trench width is about two times greater than the pipe diameter, negative arching would develop and buried pipes would experience greater stresses. The most critical stress concentrations act along the edge of the culvert. Stresses gradually reduced as measurements were taken heading towards the center of the culvert. At the center of the culvert, stresses were closest to free field stresses (Baoguo Chen & Sun, 2013).

In negative arching conditions under high fill, multiple arches formed and collapsed (Chen et al., 2009), as shown in Figure 3. Stresses in the backfill are represented in the form of the coefficient of earth pressure, which is the ratio of the vertical earth pressure at the top of the culvert to the free-field overburden pressure for the same height of fill. As shown in the figure, the coefficient of earth pressure does not remain constant or increase continually as predicted by models or theory. As the height of fill increases, the coefficient of earth pressure increases non-linearly to a value much higher than linear theory. Then the negative arching zone collapses and stresses return back to levels near linear theory values. When the height of

fill increases, the coefficient of earth pressure increases back to greater values. The collapsing of the arches occurs again at a much smaller level.

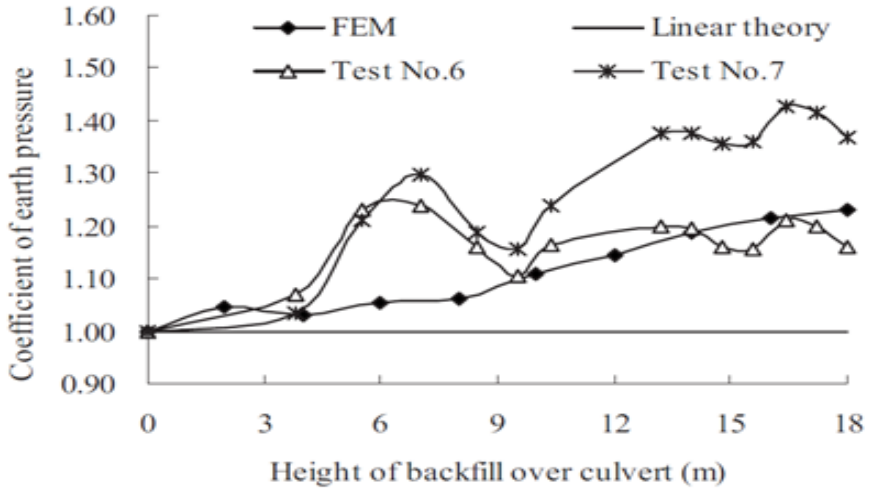

Figure 3: Coefficient of Earth Pressure with Increasing Backfill Height.

To reduce overloading buried structures in negative arching embankment conditions, flexible and semi-rigid pipes have been used. Flexible and semi-rigid pipes are designed to be structurally sound, while being relatively more compressible, which transfers a fraction of the overburden vertical stresses to the neighboring side fill. The reduction of stress on the buried structure due to stress transfer to the adjacent fill is known as positive arching. Flexible pipes may be constructed from materials such as Polyvinyl Chloride (PVC), High Density Polyethylene (HDPE), and corrugated steel pipes. Deflection of non-rigid pipes is an important design consideration as they can be significant and affect the design life of the structure (Spangler, 1941). Although the use of flexible and semi-rigid pipes are an innovative way to reduce stresses with the manipulation of positive arching, it is less likely to be considered on large scale projects such as wide spanning culverts.

Marston developed a third method of pipe installation known as the “induced trench” method (Taylor, 1971). The induced trench is a method of load reduction intended to be used in an embankment condition, where a layer of compressible material was placed within the backfill above the buried structure. Backfilling material above the compressible fill will cause yielding, which in turn induces arching above the buried structure (Taylor, 1971). The reliability of the induced trench method has been questioned in recent years due to uncertainties with design, failures and issues with constructability. However, the New Brunswick Department of Transportation (NBDOT) reported success in over 50 projects incorporating the induced trench over a period of 10 years (McAffee & Valsangkar, 2008). A schematic drawing of the induced trench method is shown in Figure 4.

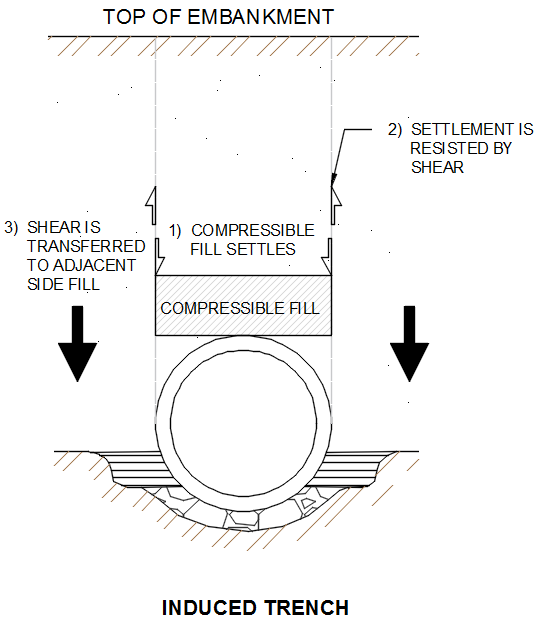

Figure 4: Induced Trench Method

Typical materials used as compressible fill in an induced trench installation are baled hay or straw, leaves, compressible soil and expanded polystyrene (EPS Geofoam). The choice of

compressible material is significant and will have an effect on settlements and long-term behavior. However there is limited research on mechanical properties and the optimum geometry (Sun, et al, 2010). EPS Geofoam has been the focus of recent studies due to its ease of production and light weight. The remainder of this thesis will consider the use of EPS Geofoam as compressible fill.

There are two prevalent approaches for design of induced trench method for culvert installations. The first method was developed by Marston and his student Spangler of Iowa College (Taylor, 1971). Marston and Spangler's method contains empirical formulas and tables based upon field studies to estimate the pressures acting on buried conduits. Research has found Marston and Spangler's method to be conservative in the prediction of experienced stresses (Chen, et al 2009). There have been practical difficulties in determining parameters necessary to estimate the loading on conduits. The second method was based on the work of Vaslestad (Vaslestad et al, 2011). Vaslestad's method involved the application of an arching factor to overburden pressures calculated for the trench. The arching factor applied is based upon the friction number S_v, which was developed by Janbu to determine friction on piles. Vaslestad's method has resulted in relatively good agreement with earth pressures measured in full scale induced trench installations, as well as results from finite element analysis programs such as CANDE (Yoo et al, 2005).

Pressure cells can be used in the field to give an accurate representation of stresses acting upon the culvert and the neighboring backfill. Finite element analysis software has been used to model an induced trench and can predict similar stress concentrations to the levels found in

the field. Field testing from Sladen and Oswell indicated that vertical loading on the culvert reduced to values between 20% and 40% of the overburden pressure from soil (Sladen and Oswell, 1988). Research performed by Vaslestad showed that vertical pressures reduced to 43% of the overburden pressure from the soil (Vaslestad et al, 2011). The intensity of load reduction was shown to vary depending on thickness and width of compressible fill, rigidity of construction materials, coarseness of backfill material, and depth underneath fill. With careful design, large stress reductions of up to 80% have been observed while using the induced trench method (Vaslestad et al, 2011).

Positive arching from an induced trench can also produce some unfavorable effects onto culverts. Vaslestad's research shows the increase of lateral pressures acting on the culvert by upwards of 58% when compared to at-rest earth pressures. This mechanism is caused by the increase of vertical pressures to the adjacent rigid soil column. Because lateral pressures within submerged soil is a function of vertical overburden pressure, lateral pressures also increase. To properly design an induced trench, the engineer needs to verify that lateral stresses do not exceed the design limits of the culvert section. This effect is more prominent at the edge of the culvert, similar to positive arching mechanics (Vaslestad et al., 2011).

II. The Influence of Groundwater

Groundwater is a concern in the design of buried structures. Field studies on existing culverts with pressure cells show that a high water table can affect bedding conditions for the base of the culvert and also alter the pressure distributions on the sides of the culvert. The exposure of culverts and bedding to groundwater allow for erosion. High lateral pressures are

developed due to corrosion related localized non-homogeneity (Oshati et al, 2012). Groundwater can also introduce uplift due to buoyancy. This is a major concern when using lightweight compressible fill material which may have a lower density in comparison to water. Uplift due to buoyancy of the compressible fill material can be addressed with the use of anchoring or providing adequate surcharge in the case of high groundwater levels.

III. Width of the Trench

The width of the trench dictates the distribution of stresses within positive and negative arching culverts. Numerical modeling of the variation of widths of the compressible zone in positive arching culverts shows that smaller width trenches display a relative overall reduction of stresses. As the span of the trench increases, the arching effect is less apparent and stresses return to near free field levels. Centrifuge testing has shown that greater vertical and lateral pressures were found on wider positive projecting culverts in comparison to induced trenches with smaller widths (Oshati et al., 2012).

In induced trenches with wider widths, the amount of shear force carried by the column of adjacent backfill is much greater, reducing the overall effect of arching which results in the settlement of more fill directly on top of the trench and the culvert. The width in which the effect to load reduction from positive arching is no longer achieved is known as the transition width. The transition width is a function of culvert width, embankment height, installation type, and soil type, and is supplemented in a table in the Concrete Pipe Design Manual. Any culverts designed with the trench width greater than or equal to the transition width should be designed as an embankment (American Concrete Pipe Association, 2011).

IV. Compaction of Fill

Compaction is defined as the densification of soils with the use of mechanical energy and is referred to as the most important component of proper embankment construction (TRB, 1990). Compaction may also involve the modification of water content and gradation of soil. Compaction is used to improve the engineering properties of the fill by increasing its shear strength, which improves the bearing capacity, reduces settlements, reduces hydraulic conductivity, and increases corrosion resistance. Compaction of fill is generally recommended for most earthwork construction, with emphasis on highways and airport runway pavements, where sensitivity to settlements may be detrimental. Compaction can be performed in the field with the use of compaction equipment, such as vibratory rollers, and is performed in multiple lifts on the order of about 12-inches, depending on equipment being used or project soils. Cohesionless soils can be compacted efficiently with the use of vibration (TRB, 1990).

The principles of compaction were developed by Proctor in the 1930's (Lundvall, 1997), where he stated that compaction was a function of the materials dry density, water content, compactive effort and soil type. Specifications of earthwork are generally classified into two different types: method specifications and end-product specifications. Method specifications are when the type and weight of rollers, number of passes, and lift thicknesses are specified prior to construction and responsibility for compaction quality lies with the owner or agency. Method specification is typically used in large compaction projects due to large investments into preconstruction engineering and testing. End-product specifications involve a certain value for relative or percent compaction, and are the generally used in the construction of highways and building foundations (TRB, 1990).

Relative compaction is the ratio of the field dry density, ρ_{dfield} to the laboratory tested maximum dry density, ρ_{dmax}, as determined by the standard or modified Proctor test. The equation for relative compaction is shown below. Depending on the project, specifications require material be compacted to achieve a certain relative compaction.

$$\boldsymbol{Relative\ Compaction} = \frac{\boldsymbol{\rho_{dfield}}}{\boldsymbol{\rho_{dmax}}} \times \mathbf{100} \qquad \textbf{(1)}$$

In a case study performed by Wyoming Department of Transportation (WYDOT), settlement of highway pavements overlying buried culverts had been observed (Lundvall, 1997). WYDOT reported that settlements were severe enough to pose hazards to driver safety and vehicular damage. Detailed investigations were conducted at 15 culvert locations, which included drilling, sampling and testing of the backfill material. The sites with the greatest amounts of settlements were located in areas underlain by cretaceous sedimentary rocks containing bentonite, which is indicative of highly compressible soils. It was also observed that the majority of settlements occurred in culvert sections that had a shallow fill height of about 5 meters (16 feet) or less. The investigations concluded that the most probable cause of the settlements were inadequate compaction, shallow cover of fill above culverts, and the use of expansive soils as backfill. Due to the variability between conditions and materials between culvert locations, there was no conclusive result, however many of the settlements could have been avoided with a more strict following of state specifications and thorough inspection of the suitability of the backfill material.

V. Geometry of the Trench

Culverts are generally constructed in a manner where the trench has a vertical backfill surface. It is possible to have ditches constructed with the use of benching and sloping techniques to stabilize the backfill and prevent any side slope failures. Field based research has been performed on trapezoidal shaped trenches to understand the effect of trench geometry on the stress distribution acting on the trench. In negative projecting culverts, the trapezoidal shaped trench increased the stresses acting on the culvert. The friction in the side slopes of the trench was minimal in resisting the additional pressures of the fill sliding and hanging on the edge of the culvert. It was noted as well that some of the mechanics behind trapezoidal trenches were not applicable when it comes to standard trench sections with vertical slopes (Chen and Sun, 2013).

Non-symmetrical slopes have also been studied and modeled. The presence of non-symmetrical slopes produces non-symmetrical loading conditions. Non-symmetrical slopes have shown to facilitate unequal stress distributions and settlements in the backfill, culvert and culvert foundation (Chen et al., 2009). Non-symmetrical slopes are dependent on individual designs and will not be considered in this thesis.

VI. Foundation Pressures

The magnitudes of the stresses acting on the supporting foundation of a culvert have been measured using data from field testing and supplemented with finite element modeling. The general trend of the stresses acting on the foundation of the culvert agree with the stresses acting on the crown and edges of the culvert. Negative projecting culverts also have an

increase in vertical stresses which are greater than the calculated free field stresses (Chen et al., 2009).

VII. Compacted Fill Material

Compacted fill material should be properly selected for use in an induced trench. The density of the material will control the magnitude of vertical and lateral stresses acting on the compressible fill and the buried structure. The particle size gradation of the material will control the mechanisms of arching and affect the overall stress reductions that are produced. In an instrumented field test of the induced trench with EPS Geofoam as a compressible fill by Vaslestad, it was found that the gradation of the material used in the backfill had a significant effect on the amount of load reduction on the structure. Using a granular backfill material brought the pressures acting on the pipe down to approximately 25% of the overburden while cohesive material reduced pressures to 45% of the overburden soil pressures (Vaslestad et al., 2011).

VIII. Extending the Compressible Layer beyond the Culvert

Spangler indicates that traditional design methods have assumed that the compressible layer is only as wide as the trench. Finite element analysis (Sun et al, 2010) indicates that increasing the width of the compressible layer beyond the trench reduces lateral pressures acting on the buried structure. The shear column supporting the load transferred from the deformed geofoam is now further away from the buried structure, allowing for dissipation for some of the transferred stresses. In field testing performed by Sun et al. (2010), lateral pressures acting on the culvert from a geofoam section with 1.5 times the width of the culvert

reduced lateral loadings on the culvert. Sun found lateral loads from an induced trench with a compressible zone width to culvert width ratio of 1.5:1 were reduced by 5kPa (.725psi) when compared to a wide negative projecting culvert section.

Sun, Hopkins, and Beckham indicated no changes in vertical stress, when comparing EPS geofoam with a width greater than the culvert width to a standard width compressible zone. Finite element models created by Kim and Yoo (2002) test the effect of extending the compressible zone width while varying elastic moduli of the compressible zone. In most tests, the maximum pressure reduction occurred at a compressible zone width ratio of 1.5 times the culvert width, except in the case of a relatively lower elastic modulus of 10MPa, where pressure reduction continued until a width ratio of 2 was met (Kim & Yoo, 2002).

Vaslestad also recommended using geofoam with a width equal to 1.5 times the overall width of the culvert (Vaslestad et al., 2011). Vaslestad found from full scale field observations that a width of 1.5 times the culvert width reduced lateral pressures on the culvert. Earth pressure cells were installed to measure vertical and horizontal stresses. Measurements of stress indicated that vertical stresses were nearly equal to horizontal stresses, which is ideal for the structural response of the pipe. This is ultimately dependent on the design parameters of the culvert. Extended width compressible fill can be manipulated to further reduce overall stresses acting on the culvert. Earlier finite element simulations extending the width of the compressible zone beyond the culvert also reduced lateral loadings on the culvert (Sladen and Oswell, 1988).

1.3 Geofoam – Expanded Polystyrene

Selection of lightweight fill material is important in controlling the amount of stress reduction due to positive arching. Geofoam (Expanded Polystyrene, EPS) is the compressible material of choice for this study because of the advantage of its superior light weight relative to other compressible materials. Geofoam is composed of pre-expanded polystyrene beads, molded and fused into blocks to be used in lightweight fill applications, as well as for thermal insulation due to its poor heat conduction properties.

I. Density

Typically, geofoam is characterized by its density, which is also a good indicator of the materials compressive strength, and deformation properties. Compressive strength, elastic modulus, and yield strength are higher for denser geofoam. The significant factor when it comes to considering geofoam over other lightweight fill materials is that it is 50 to 100 times lighter than conventional fill materials and has relatively comparable compressive strengths. Densities of EPS Geofoam used in lightweight fill operations typically range from 16kg/m^3 to 32kg/m^3 (1pcf to 2pcf). Geofoam blocks with higher densities can be produced, but cost more (Birhan, 2014).

II. Compressive Strength

Design and use of geofoam underneath fill is controlled by its compressive strength. Compressive strength of geofoam is typically taken to be the stress at which axial strain reaches 5% or 10% when subjected to an unconfined compression test. The differences between strengths at 5% to 10% are relatively small (about 10%), and both criteria have been used in

standard factored design procedures (Negussey, 2007). The stress-strain curve from the unconfined compression test of a 16kg/m^3 (1pcf) density geofoam sample is shown in Figure 5 (Birhan, 2014).

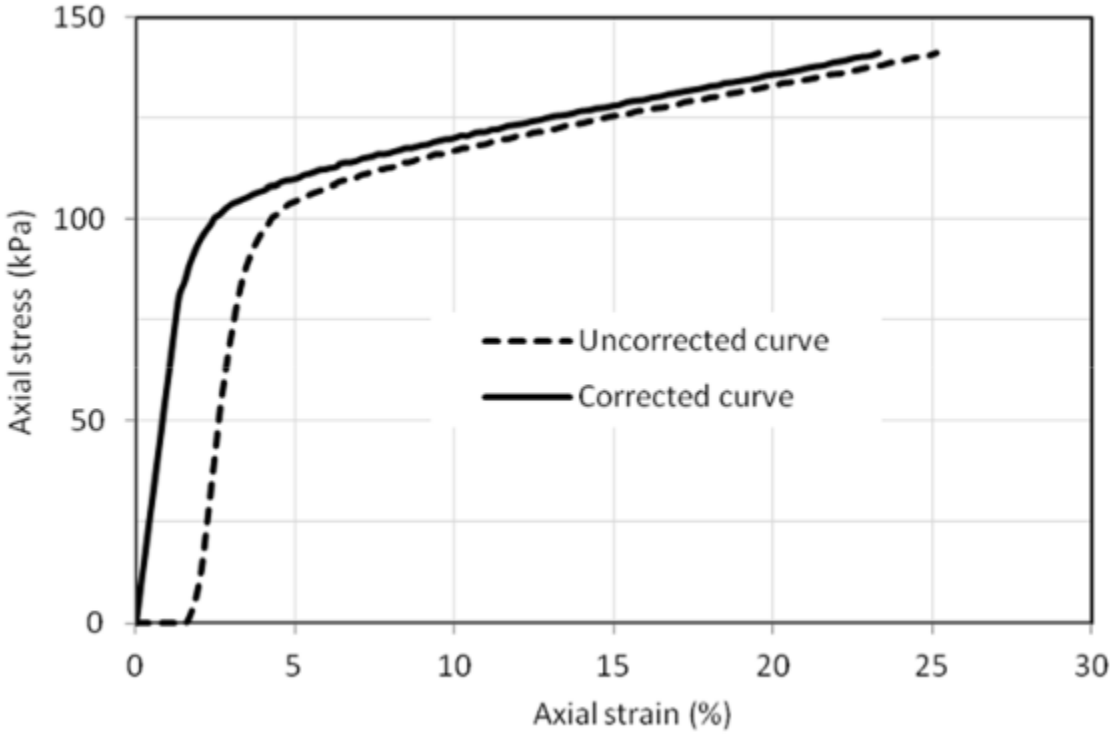

Figure 5: Stress Strain Curve from an Unconfined Compression Test (16kg/m^3) from Birhan (2014)

As shown in Figure 5, unconfined compression test results are typically corrected for seating errors as provided in ASTM D1621. The stress corresponding to the compressive strength at 10% corrected strain (110kPa, 16psi) is beyond the yield stress, and brings the geofoam into the plastic region. The working stress is taken to be 30% of the unconfined compressive strength for dead load with additional 10% considering live loads due to traffic (Negussey, 2007).

For the scope of this study, geofoam with a standard density of 20kg/m^3 (1.25pcf) is used in computer modeling and laboratory testing. All computer models are checked to ensure that

axial stresses do not exceed the corresponding design stress of 33kPa (4.8psi) for this grade of geofoam.

III. Confining Effect

EPS geofoam when exposed to confining pressures in addition to axial loading, exhibits degradation of elastic modulus (Sun, 1995). This effect is particularly important when used in a trench condition because of the increase of lateral stresses developed from the soil-structure interaction, in addition to overburden pressures. In trenches, the presence of confining pressures with neighboring soil fill should be considered in design. However, there have been no prior constitutive relationships developed to accurately capture the behavior of geofoam under confinement.

The effect of multi-directional loading on geofoam was studied by Birhan (2014) with triaxial testing. Constant axial loads were applied to cylindrical geofoam samples with a loading plate, while confining pressures were introduced by encasing the sample in a membrane and applying water pressure to vary confining stresses (Birhan, 2014). The laboratory setup for tri-axial testing is illustrated in Figure 6.

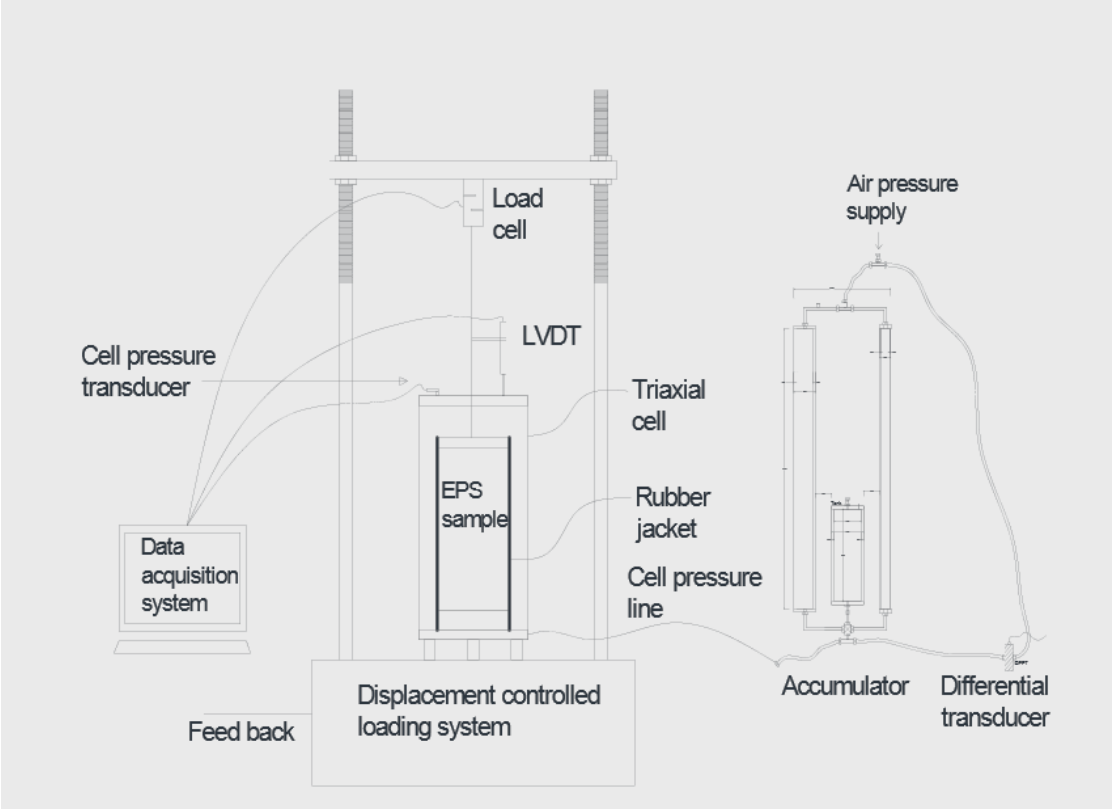

Figure 6: Triaxial Testing Setup (Birhan 2014)

The samples tested experienced more strain under confined loading when compared to unconfined samples, which indicates a weakening or degrading modulus. However, this weakening is variable depending on the amount of confining and axial pressures. Birhan (2014) represented the differences in confining and axial pressures by a deviator stress (σ_d), the difference between major and minor principal stresses (σ_1- σ_3). Varying deviator stress-strain plots from laboratory compression tests are shown in Figure 7. Samples tested had a density of 20kg/m^3 (1.25pcf), and diameter of 64mm (2.5in). As confinement was increased, deviatoric stresses produced greater strains, confirming degradation of elastic modulus, and yield stress. Birhan (2014) also found this effect to be existent, but less prominent as sample size increased.

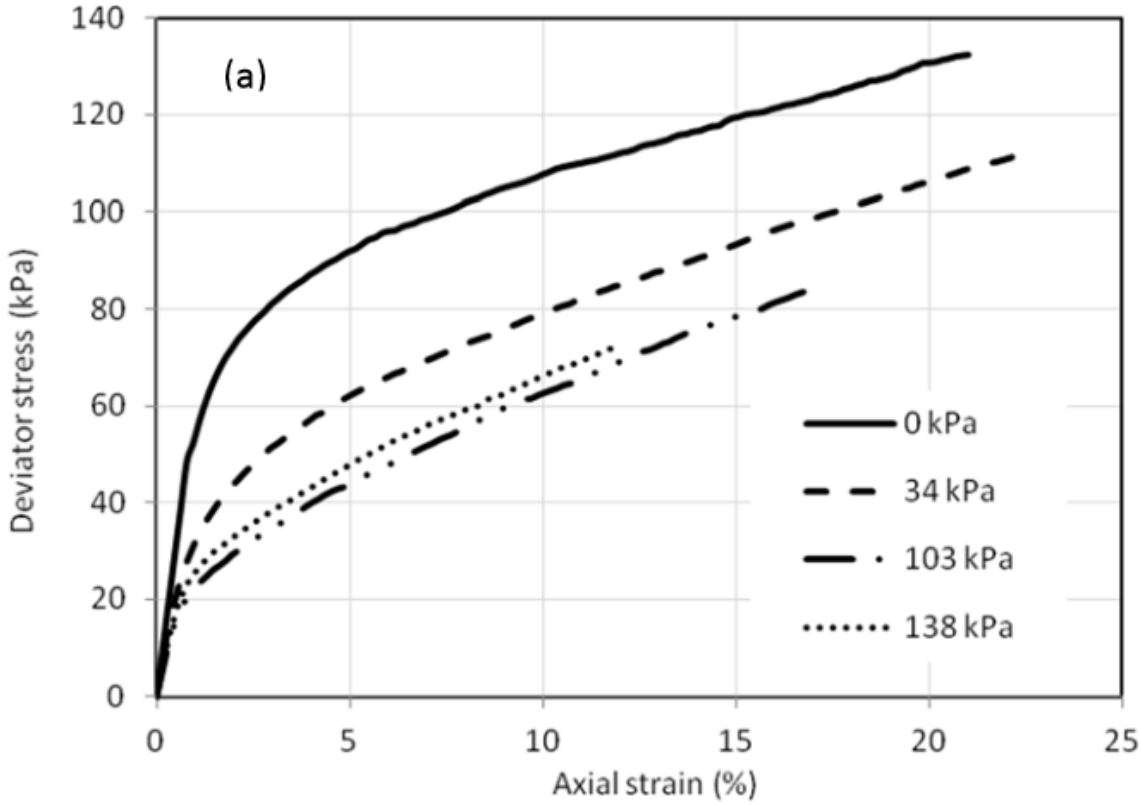

Figure 7: Deviator Stress-Strain Curve (Birhan 2014)

Equation 2 was developed by Birhan (2014) to represent the behavior of geofoam with different confining pressure levels.

$$\boldsymbol{E_t = E_{i0}\left(e^{-\sigma_3/P_a}\right)[1-(a*\sigma_d)]^2} \qquad \textbf{(2)}$$

where,

$$a = \frac{1}{(A*\sigma_{y0}-\sigma_3)} \qquad \textbf{(3)}$$

$$A = 1.5 + 0.03R$$

$$E_t = Tangent\ Modulus$$

$$R = Strain\ Rate\ (\%\ per\ min) = 10\%$$

$$\sigma_d = Deviator\ Stress$$

$$\sigma_{y0} = Initial\ Yield\ Stress = 92\ \mathrm{k}Pa\ (13.3\ ksi)$$

$$Pa = Atmospheric\ Pressure = 101.3\ kPa\ (14.7\ psi)$$

$$E_{i0} = Initial\ Modulus = 4.0\ MPa\ (.6\ ksi)$$

$$\sigma_3 = Applied\ Confining\ Pressure$$

This model uses an exponential relationship to characterize the behavior of geofoam under confinement. In conjunction with an initial elastic modulus term, the stress components account for effects that make the sample weaker in the presence of multi-axial pressures. Without confinement, the exponential term is raised to the zero power, leaving the tangent modulus to depend on initial modulus and strain rate. The relationship is for one density, which in this case was for 20kg/m^3 (1.25pcf) density geofoam. This relationship was derived from test results for small sized sample and will be used later in this thesis to characterize the behavior of geofoam under multi-axial pressures in computer modeling with FLAC.

IV. Creep Behavior

Time dependent behavior under sustained loading is an important consideration when designing with geofoam as a compressible fill. Creep deformations depend on duration and amount of sustained loading. Replacing geofoam that has deformed excessively underneath overburden pressures often may not be the most practical or cost effective solution. Designing with an appropriate stress range is the recommended method of addressing long term creep deformations. This would entail limiting the amount of overburden fill acting on geofoam.

A working stress is assigned to limit creep deformations over time to acceptable values. Norwegian design approaches are commonly used to establish a working stress, based upon the

stiffness of geofoam. This approach limits the working stress to 30% of the compressive strength at 5% strain from an unconfined compression test. An additional 10% of the compressive stress would be allowed to account for transient live loadings (Negussey, 2007). Laboratory creep test results have been reported by (Sun, 1995; Anansthas and Srirajan, 2000; Sheeley, 2000; Srirajan et al., 2001;) to confirm the validity of the Norwegian approach. Results from testing exhibited negligible deformations over time when samples were loaded to stress levels less than 30% of the compressive strength at 5% strain. Additional testing indicates that stresses up to 50% of the compressive strength of geofoam at 5% strain are the limit for producing significant creep strains. The results of laboratory testing from (Srirajan et al., 2001) are shown in Figure 8.

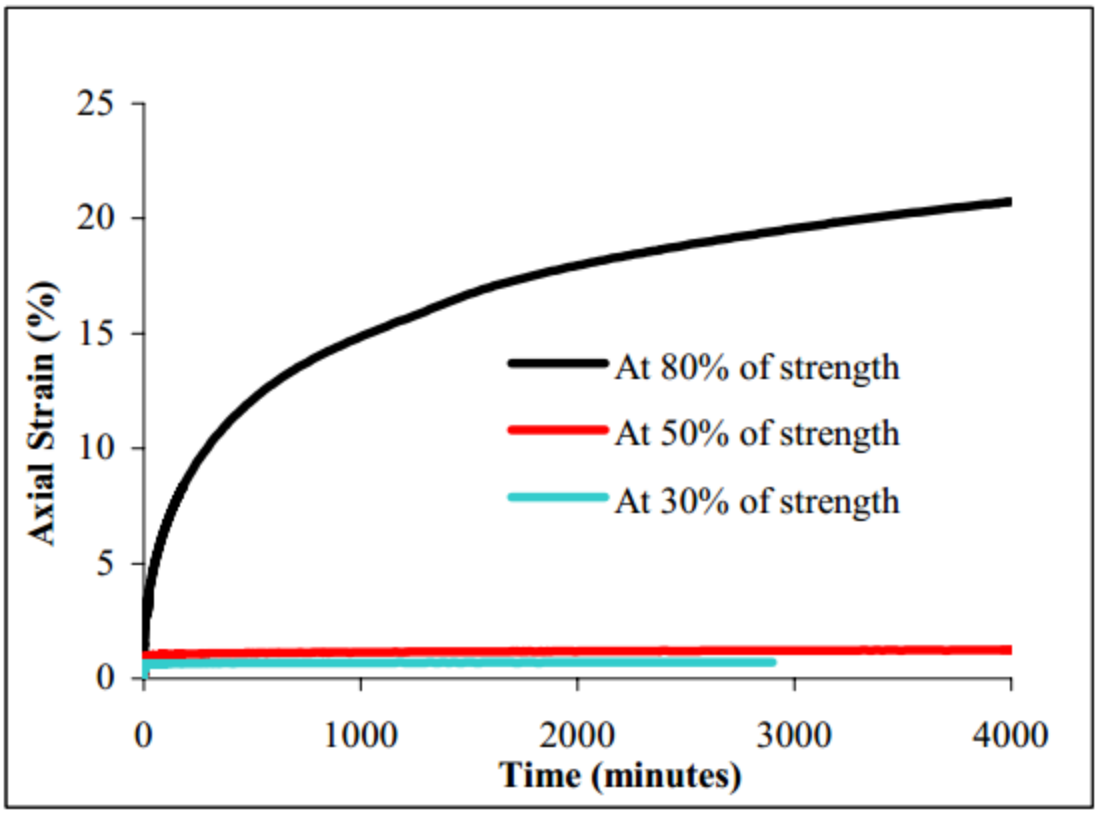

Figure 8: Creep Laboratory Testing of Working Stress (Srirajan et al, 2001)

Time dependent creep strain deformations have also been observed in the presence of confining pressures. Creep tests were performed on samples with inclusion of confining pressures. Results from these creep tests indicate that confining pressures significantly affected the creep behavior of geofoam, leading to much larger strains over time. This effect was also much more pronounced when lower density geofoam samples were used (Birhan, 2014).

Research indicates that properly designed induced trenches with geofoam as the compressible fill have served their intended service life, and are expected to remain effective over time. Field observations performed by Vaslestad (2011) on a full scale induced trench with geofoam as the compressible material showed that after 3 years, there were no increases in vertical earth pressures or compression starting from the end of construction. There was however, a small increase in deformation over time, much of which occurring immediately after the end of construction. Vaslestad's research only considers a smaller, thin compressible area. This same relationship is not valid for thicker, longer spanning trenches (Vaslestad et al., 2011).

A study on the long term behavior of an induced trench with silty clay as the compressible fill material, was performed by Spangler in 1927. The loads were measured over a period of 21 years, until the year 1948. After 21 years, there were no reported substantial increases or decreases in loading upon the culvert (Spangler, 1973). Field monitoring of an induced trench with geofoam as a compressible fill was performed by Sladen and Oswell (1988). Their research indicated that long term settlements would be small after monitoring settlements and stresses over a span of 4 years.

Sun, Hopkins and Beckham (2010) measured stresses and settlements in an induced trench with geofoam as a compressible fill material over a span of 5 years. The majority of settlements occurred during the early stages of culvert construction, when fill was being placed and compacted. Settlements in the soil prism above the trench rapidly decreased with increasing time. The initial settlement was referred to as primary compression, and leveled off when the construction of the overlying embankment was completed. The secondary compression followed right after primary compression, and exhibited time dependent creep behavior. The secondary compression followed a linear trend and could be extended to predict settlement of the geofoam over time. Over the span of 27 years, a settlement of 1 inch was predicted, which can be considered insignificant (Sun et al., 2010).

V. Mixing of Densities

Projects with geofoam as lightweight fill are often designed to have the same density material used throughout. Most studies on geofoam have only considered single density usage. However, it is possible to have mixing of different density blocks, either due to poor quality assurance or improper design. The effects of mixing different density geofoam have been studied (Liu & Negussey, 2015) and indicate that this condition can contribute to excessive settlements. Load tests were performed on samples of uniform density and mixed densities under a rigid loading plate. The uniform density tests used geofoam with a density of 20kg/m^3 (1.25 pcf). Using a displacement controlled loading setup, 6 samples were stacked in 2 layers of 3 blocks, and compressed to approximately 30% strains. Samples had near uniform displacements along the centerline, whereas blocks of mixed densities deformed unevenly.

Before and after loading, samples of uniform and mixed density are shown in Figure 9: Uniform Density vs Mixed Density Load Testing.

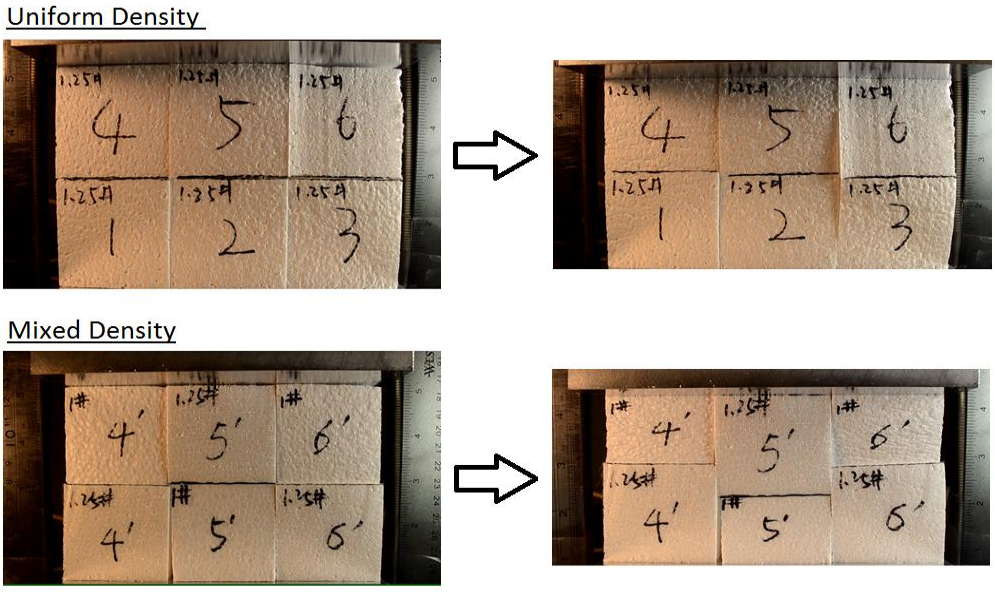

Figure 9: Uniform Density vs Mixed Density Load Testing (Liu and Negussey, 2015)

VI. Thickness of EPS Geofoam

There has been no research done strictly on the thickness of the compressible zone and its effect on the distribution of stresses. The thickness of the compressible zone is limited by the allowable loads on the culvert.

Historically, an arbitrary thickness in which the minimum would be set equal to the diameter of the pipe has been recommended (Sladen & Oswell, 1988). There is no derived explanation for this recommendation, and it is not feasible for larger culverts. Spangler and Handy recommended that thickness be selected on the basis of the settlement ratio, which is the ratio of relative settlement between the central settling soil prism and the adjacent side fill. The settlement ratio is however based upon informed intuition and empiricism

(Sladen & Oswell, 1988). It is also important that only a small amount of settlement is required in the compressible zone to activate an induced trench effect. The main benefit of having a thicker compressible zone is the replacement of a greater amount of compacted fill which reduces the overall dead loads acting on the culvert.

Chapter 2 – Computer Modeling

2.1 FLAC Modeling

I. Introduction to FLAC

Fast Lagrangian Analysis of Continua (FLAC) is a finite difference program used for advanced geotechnical analysis. FLAC can model complex behaviors, such as problems that consist of several stages, large displacements and strains, nonlinear material behavior, and unstable systems (Itasca, 2008). FLAC is capable of modeling the strains necessary to induce the trench effect, as well as the stress transfer between neighboring materials. FLAC is well suited to model the conditions under the scope of this thesis.

FLAC creates a grid of the model under study, containing numerous elements. These elements are separated into regions where each element behaves according to a user defined linear or non-linear stress-strain relationship in response to applied forces and boundary restraints. Materials have the capability of yielding and flowing and the grid can deform, which is necessary for this analysis. With the use of FISH, an internal programming language embedded within FLAC, user defined constitutive models can be created (Itasca, 2008). This is useful because a FISH program can be written to accurately describe the complex behavior of EPS geofoam under confining pressures.

FLAC uses quadrilateral elements which contain 4 different stress components, σ_{xx}, σ_{yy}, σ_{zz}, and σ_{xy} for 2D patterns. Force components are applied to each node of the element and each node is accelerated according to Newton's second law of motion. If the sum of forces is equal

to zero, then the body is in equilibrium. To solve static problems, equations of motion must be damped. Damping is performed at every node as a function of the rate of change of kinetic energy. When the rate of change of kinetic energy approaches zero, so does the damping power. The damping power is equivalent to the unbalanced force in FLAC. In all model runs, accuracy will be established by checking to see if the unbalanced force reaches a near zero value (Itasca, 2008).

II. Modeling Sections

The modeling for this thesis will only consider culverts that are symmetrical in cross-section. To reduce the overall number of elements and improve accuracy of outputs, only half of the culvert section was modeled. The majority of these models were based upon the dimensions of Carrs Creek culvert, a large bridge culvert underlying Interstate 88 in New York State. The width and thickness of the EPS Geofoam were varied depending on the mechanism under consideration.

III. Mesh & Restraints

Using the grid generation tool in FLAC, fine meshes were assigned to critical model sections to improve the accuracy of output. In all model sections, the mesh density was refined to allow for greater accuracy in the areas under study. Two different modeling sections are considered in this thesis. The first model is shown in Figure 10. This modeling section was made to study the induced trench stresses with variations in width. Y-Direction restraints were assigned to nodes along the bottom of the model to prevent vertical movements but allowing for materials to shift laterally. Along the sides of the models, nodes were given restraints in the X-Direction

to allow vertical displacement but preventing lateral movement along vertical boundaries. Out of grid displacements are zero for the assumed plane strain conditions. The culvert was modeled with restraints in both the X and Y directions to simulate a rigid structure, supported by deep piles. This is acceptable due to the large differences in rigidity between the culvert and the surrounding materials. The top nodes of the mesh were given no restraints to allow for differential displacements along the surface. The sections that contain different materials were separated by boundary lines. Due to the large differences in stiffness expected in the model, appropriate grid attachments and interfaces were assigned to the boundaries. This will be discussed in more detail later in this thesis.

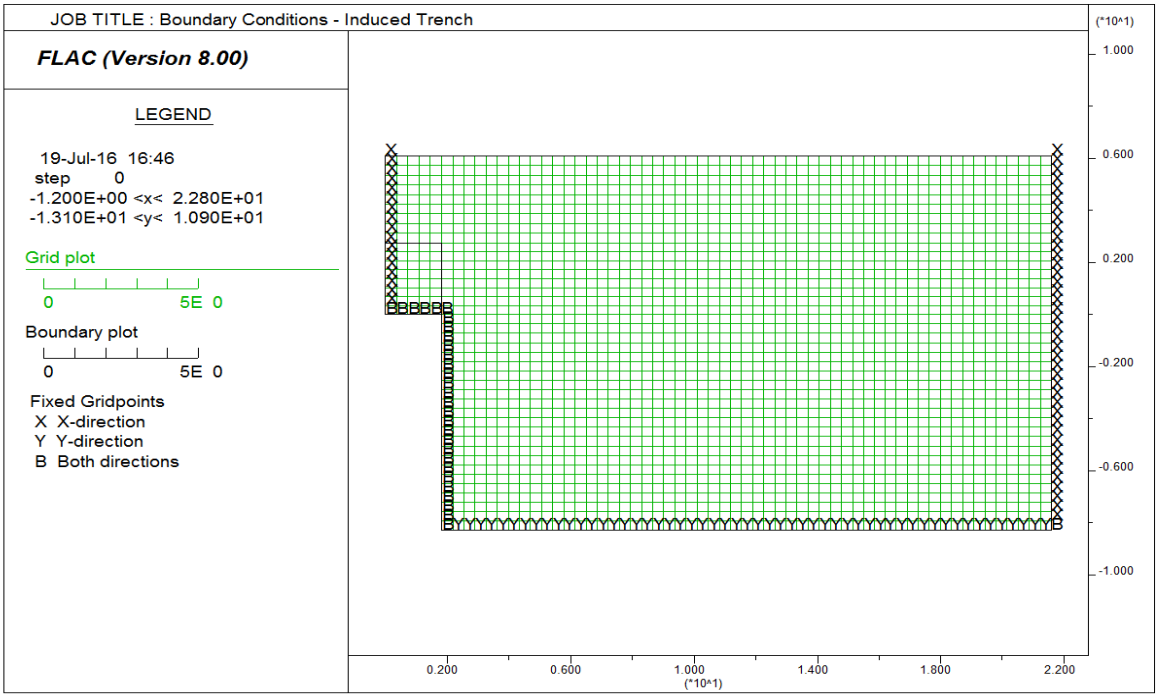

Figure 10: Induced Trench Boundary Conditions

The second model considers the cross section of a precast concrete culvert across I88 at Carrs Creek, NY, and can be seen in Figure 11. This section is similar to the culvert shown in Figure 10.

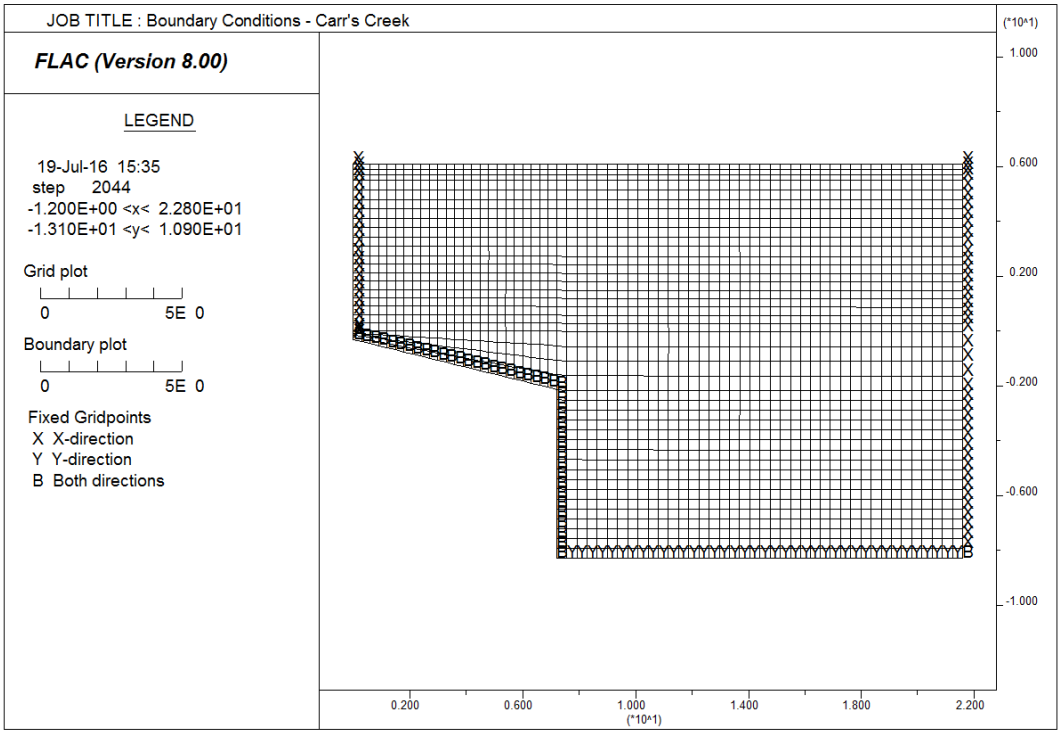

Figure 11: Boundary Restraints for Carrs Creek Model

IV. Plane Stress vs. Plane Strain

FLAC 2D has three methods of capturing the stresses and strains, with plane strain, plane stress, or axi-symmetry. The condition of axi-symmetry assumes the section to be cylindrical and have stresses and strains in a third, out of plane direction. In the plane strain condition, all strains in the out of plane dimension are zero. Alternatively, the plane stress condition, all stresses in the out-of-plane direction are set to zero. The models in this thesis represent a

plane strain condition, which is ideal for models in which the out of plane dimension is much larger than the other two planar dimensions. Plane strain conditions are ideal for two dimension cross sections of dams, tunnels and other geotechnical applications.

V. Material Parameters

The materials used in modeling sections are reflective of common materials needed to replicate an induced trench condition. The EPS Geofoam is modeled initially to be an elastic material with modulus of 4 MPa. The fill is modeled as an elastic material with Mohr-Coulomb failure criteria. The pavement overlying the compacted fill is also modeled as a different elastic material with Mohr-Coulomb failure criteria. The material parameters entered into FLAC are shown in Table 1.

Table 1: Material Properties

Material	Density (kN/m^3)	Elastic Modulus (MPa)	Poisson's Ratio	Cohesion (kPa)	Friction Angle (Deg)
EPS Geofoam	0.2	4.0	0.1	-	-
Compacted Fill	22.0	25.0	0.25	1.0	35.0
Pavement	22.8	150.0	0.3	3.0	38.0

VI. Construction Sequence

The construction sequence was performed with the cut and fill option in FLAC. To simulate compaction, the entire section is constructed in layers. These layers are built and cycled sequentially from the lowest elevation to road surface. After each layer is cycled, all displacements and velocities are set to zero. This process is continued until the very last layer

on the surface is accounted for. This process is the same for all model runs, in the same manner as for free field conditions (Itasca, 2008). The typical construction sequence for all culvert models is shown in Figure 12: Culvert Construction Sequence.

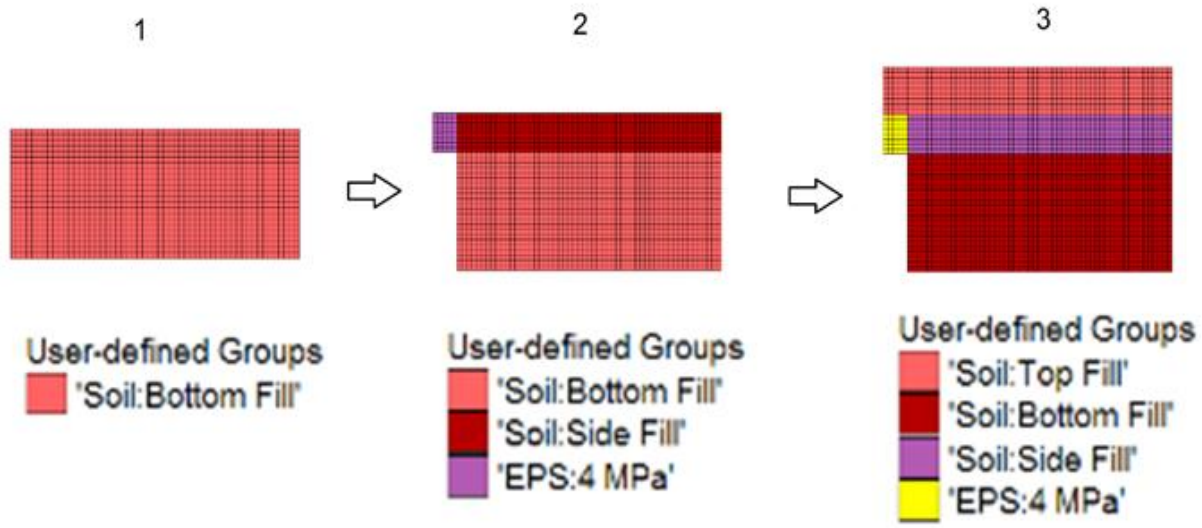

Figure 12: Culvert Construction Sequence

VII. Large Strain

FLAC supports a large strain function which allows for rezoning of grids and stresses to suppress bad geometry errors associated with large displacements. This is especially useful, and necessary with geofoam due to the large amounts of grid distortion expected when soil overburden pressure is applied. All models will be considered to be large strain for the purpose of this thesis. The large strain feature will also help improve the realism of the output (Itasca, 2008).

VIII. Interface Elements

All internal elements in FLAC models share common nodes with other elements. This is necessary for geometrical requirements within the calculations performed in the program. However, this may cause problems when materials that have major differences in properties lie right next to each other. In this case, EPS geofoam directly next to compacted soil fill will deform at a large rate. The nodes that these elements share will be between large and small displacements. The output will reflect a displacement somewhere in the middle, which results in a loss of accuracy (Itasca, 2008).

To address this problem, FLAC can model an intermediate layer between dissimilar element properties, known as interface elements. Interface elements are based upon spring mechanics. The intermediate layer is given an unbonded interface to allow for slip. FLAC requires parameters, normal stiffness, kn, and shear stiffness, ks, to solve for the unbonded interface properties. These parameters can be calculated from Equations 4 and 5 below. Normal and shear stiffness are based upon the averages of the elastic moduli and shear moduli of the neighboring material as well as the grid joint spacing (Itasca, 2008).

$$k_n = \frac{E \cdot E_r}{s(E_r - E)} \quad (4)$$

$$k_s = \frac{G \cdot G_r}{s(G_r - G)} \quad (5)$$

Where,

$$E = Material\ 1\ Young's\ modulus$$

$$E_r = Material\ 2\ Young's\ modulus$$

$$k_n = joint\ normal\ stiffness$$

$$k_s = joint\ shear\ stiffness$$

$$s = joint\ spacing$$

$$G = Material\ 1\ shear\ modulus$$

$$G_r = Material\ 2\ shear\ modulus$$

The major interface under consideration is the transition from EPS geofoam to compacted soil. This is due to the large difference in elastic modulus. All interfaces are calculated using the above equations and are assigned to the adjoining nodes based upon an average of the joint spacing.

IX. Confining Effect

EPS geofoam exhibits a degradation of elastic modulus when it is exposed to both axial and confining pressures (Sun, 1995). FLAC has no built-in function to account for this behavior, so appropriate constitutive models have been written using FISH. FISH is an embedded programming language within FLAC which allows the user to define new variables and functions. Using the confining effect model discussed in Chapter 1, axial stresses and confining stresses were considered at each node. A new tangential modulus was calculated and assigned to each element. The model section is then cycled, and displacements and stress distributions are calculated with the updated tangential moduli. The FISH file is based upon parameters derived from laboratory testing on representative samples.

2.2 FLAC Output

I. Effect of Geofoam Width

The effect of geofoam width was studied with FLAC modeling. For this section, all EPS geofoam heights remain constant and only the widths of the trench and underlying rigid culvert were altered. The height of geofoam was 9ft, reflecting three layers of geofoam stacked successively. There was soil fill above the geofoam that remained constant at 11ft to simulate a deeply buried structure. The half culvert section was initially modeled with a width of 3ft. The width of the geofoam was extended to 6ft, 12ft and 24ft to understand the overall effect of the transition of a narrow trench to a wide trench. The basic models of these sections are shown in Figure 13, Figure 14, Figure 15, and Figure 16.

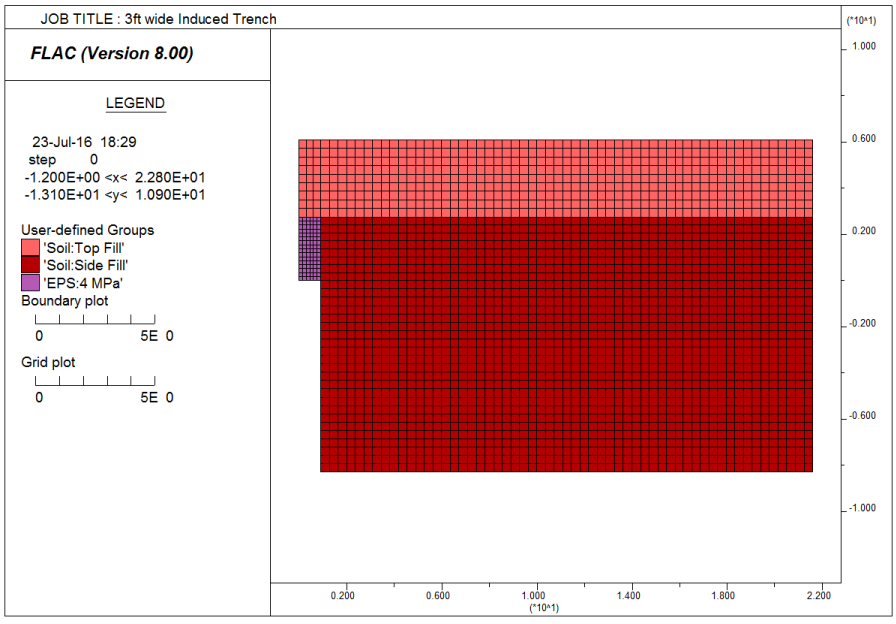

Figure 13: Induced Trench 3ft Width FLAC Model

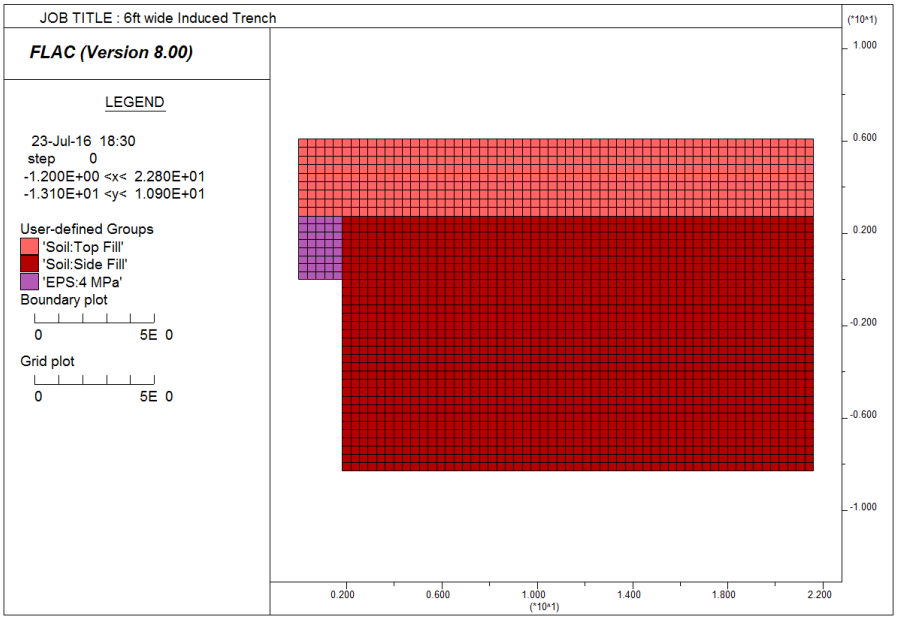

Figure 14: Induced Trench 6ft Width FLAC Model

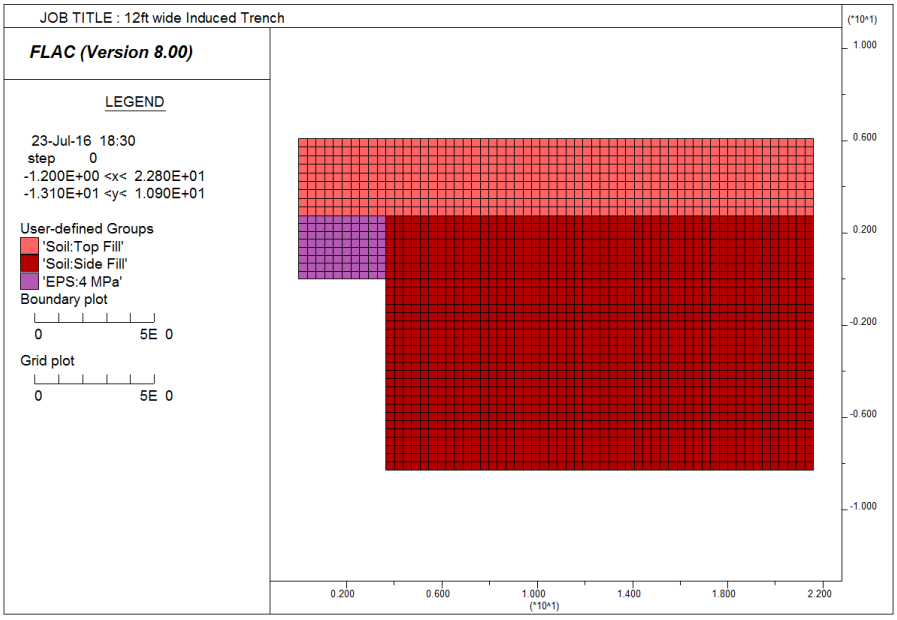

Figure 15: Induced Trench 12ft Width FLAC Model

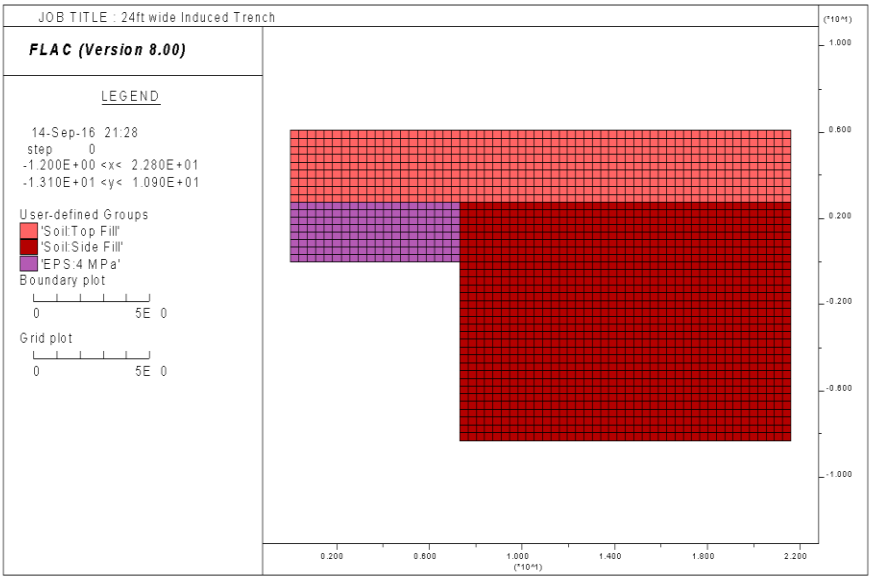

Figure 16: Induced Trench 24ft Width FLAC Model

The greatest impact of positive arching occurs with a narrow trench. As the trench width increased, the trench effect decreased at the center. In all cases, the trench effect was strongest near the edge separating geofoam and the neighboring soil fill. As width increased, the loading on the center of the geofoam increased. It is apparent that the trench effect is limited to narrow trenches for load reduction, otherwise stresses will approach free-field values.

The output for the effect of width on the induced trench is shown in Figure 17. The dashed horizontal line indicates the stress due to weight reduction by replacing the fill section with geofoam. This effect is large, reducing the loadings by nearly 50%. Starting from the center at 0 distance, deviations from the dashed horizontal grey line indicate the transfer of stress from geofoam to soil due to the arching effect. The dashed vertical lines indicate the location of the

edge of geofoam at the soil/geofoam interface for each trench width. The narrowest trench half width of 3ft has the greatest trench effect reduction of nearly 25%, contributing to an overall load reduction of nearly 80% at the center of the culvert. As the width increases, these values decrease towards the free field value for the geofoam fill, the dashed horizontal line. The 24ft half width span is a bridge culvert, and there is no trench effect near the center. The stresses at the center have returned to the stress state associated with only load reduction due to replacement of fill with lightweight fill or the free field condition for the geofoam fill. The induced trench is present at the edge or soil/geofoam interface and continues to transition to the load replacement stress over the course of nearly 6 meters (20 feet) for all trench widths.

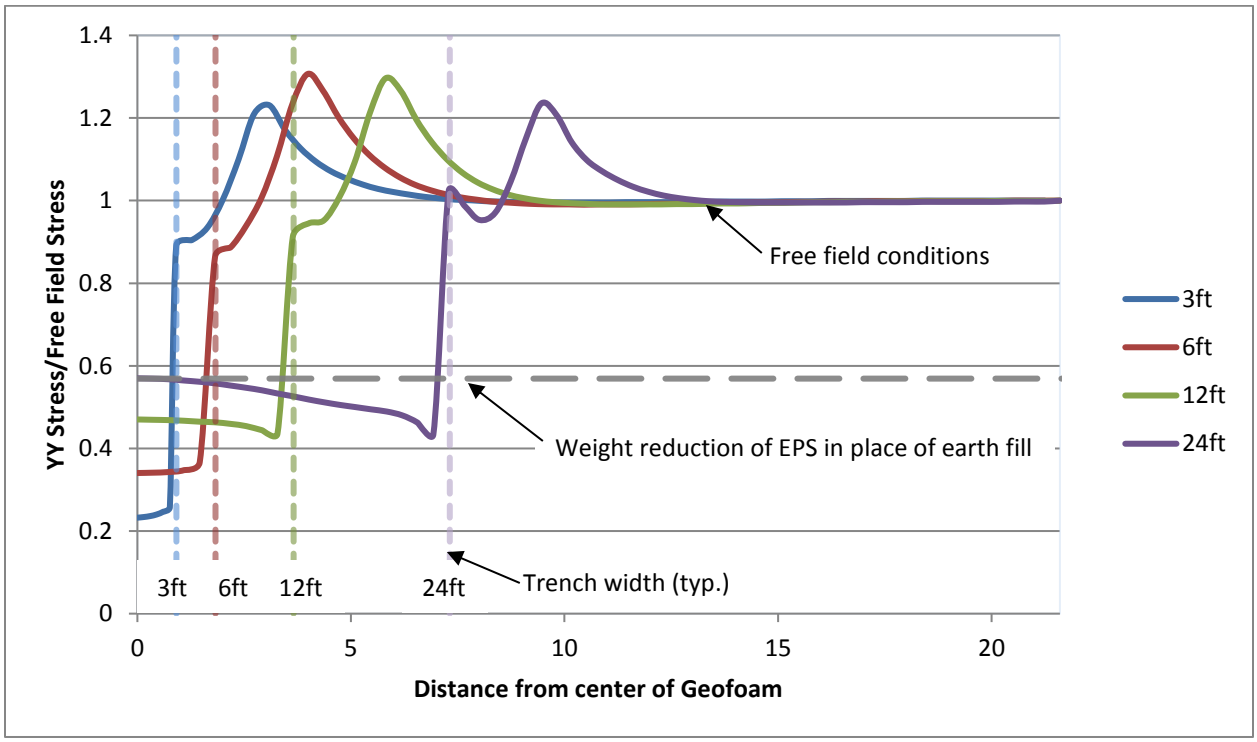

Figure 17: Trench Effect Stresses due to width of Geofoam

II. Effect of Geofoam Thickness

Thickness of the compressible fill zone has a direct effect on the stresses acting on the culvert. With a greater thickness of compressible fill, there is less compacted earth fill acting on the structure. Since EPS geofoam is approximately 100 times lighter than compacted fill, the changes in overburden pressures are significant. Models were created of a thin geofoam section with a thickness of 1.5 feet, and compared to the standard thickness under investigation of 9 feet. The pavement height remained the same in all models at 20 feet above the base of the EPS geofoam. The meshing and points of consideration can be seen in Figure 18 and Figure 19 for the thick and thin sections respectively.

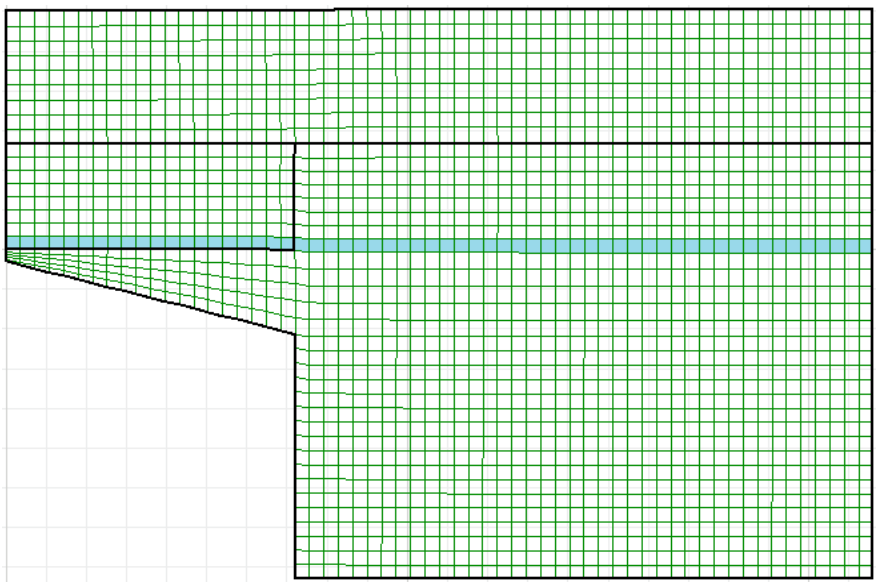

Figure 18: Thick Geofoam Section with Stresses at Geofoam Base

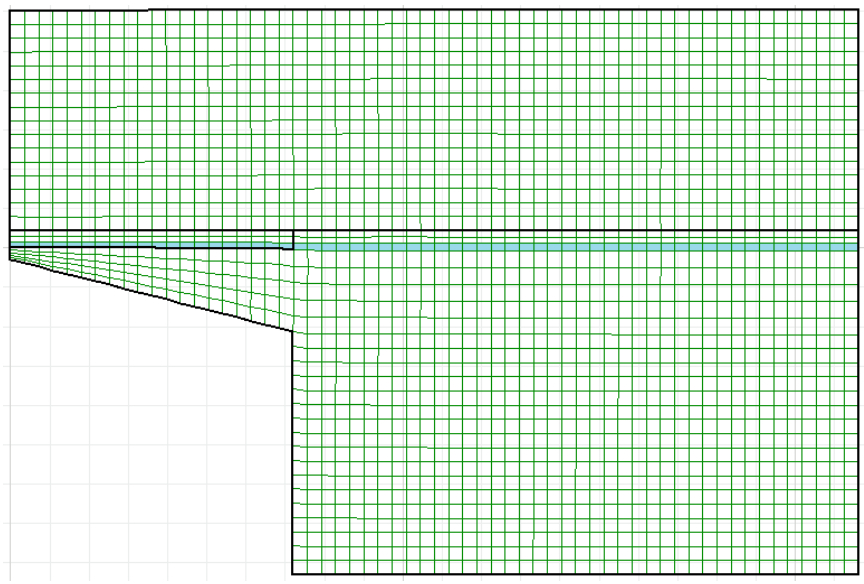

Figure 19: Thin Geofoam Section with Stresses at Geofoam Base

The stresses for these two scenarios were evaluated at the very bottom element of the geofoam. The shaded thick line in Figure 18 and Figure 19 indicate the location of where YY stresses are taken. Similarly, the YY stresses acting on the culvert are taken, along the blue shaded elements in Figure 20. These locations represent maximum stresses along the geofoam and the culvert. The stresses acting on the geofoam and the culvert are compared with the no foam condition, in which only compacted soil fill is placed on top of the culvert. The culvert geometry for these cases represents the actual shape of the I88 culvert at Carrs Creek.

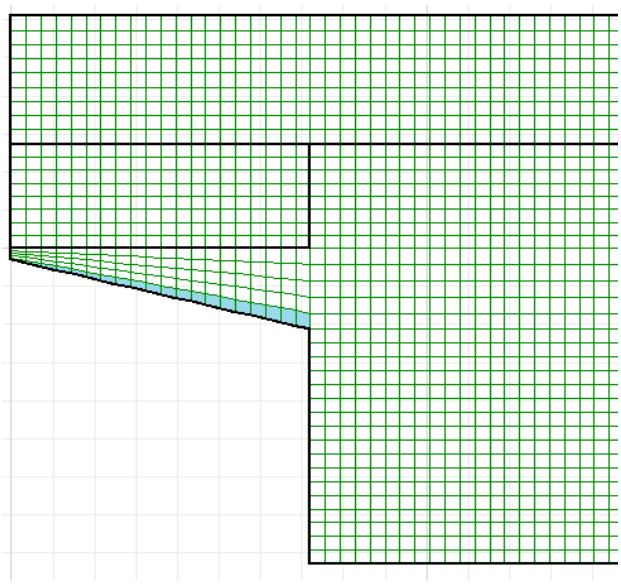

Figure 20: Location of Culvert Stress Analysis

The data output is shown in Figure 21. The stresses from the soil acting on the culvert are the greatest stresses on the culvert, as expected. Due to the lower soil fill height near the center, the stresses are the smallest at approximately 140kPa (20psi). Moving outwards from the center of the culvert, the stresses increased nonlinearly. This is from a combination of the increasing soil fill in the bedding and negative arching from the compressible soil fill deforming adjacent to the rigid culvert. At the culvert edge, the no foam condition stresses are critical, with a maximum stress of 270kPa (39psi), almost double the stress at the center.

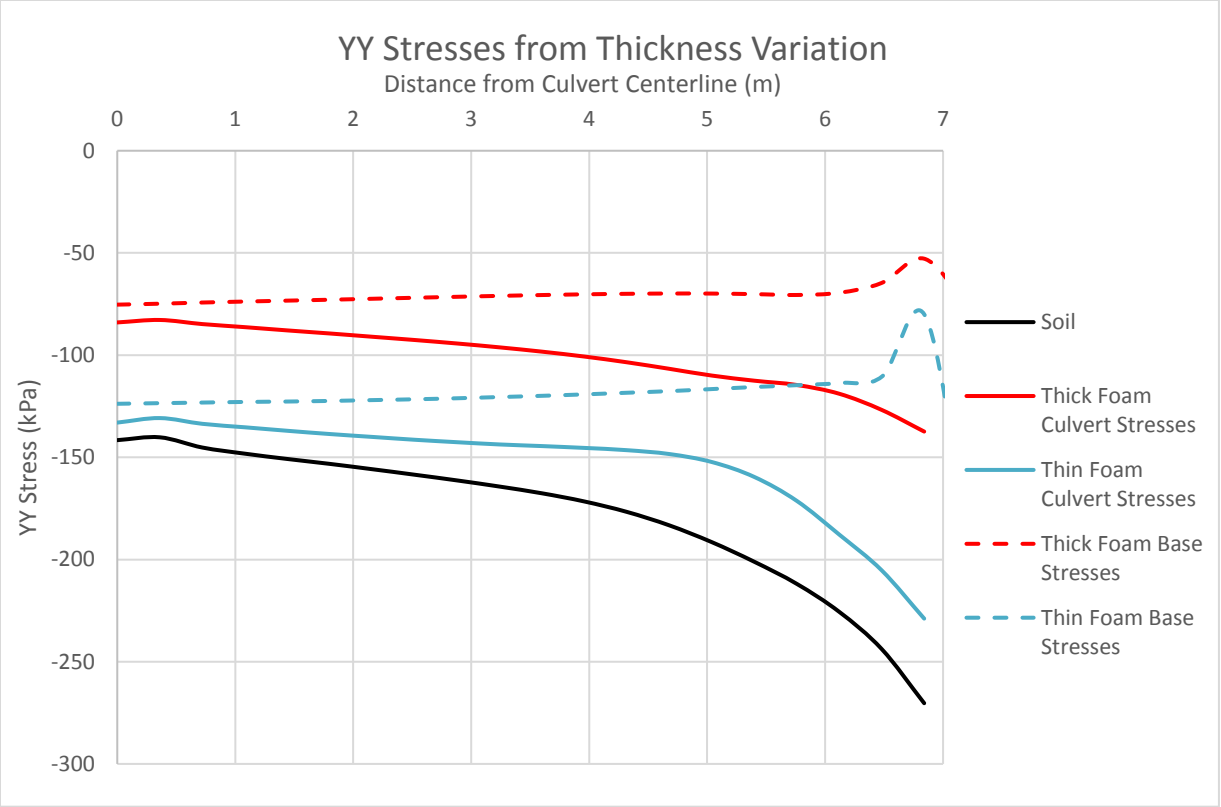

Figure 21: YY Stresses from Width Variation

The thicker geofoam section of 9ft had the greatest amount of stress reduction. As shown in Figure 21: YY Stresses from Width Variation, the centerline stresses on the culvert have been reduced to approximately 85kPa (12psi). As the distance from the centerline increase, there is greater compacted soil fill, and a negative arching effect from the rigidity of the culvert compared to the neighboring fill. These factors increased the stress on the culvert to a maximum of approximately 140kPa (20psi). The stresses at the geofoam base, along the centerline were close to values of the respective culvert stresses; however there is the presence of positive arching, which reduced stresses near the foam/soil interface. The lowest stresses along the base of the geofoam were concentrated at the edge of the geofoam, and have a value

of approximately 50kPa (7psi). It is apparent that this section is too wide to have trench effects at the centerline, and the majority of the trench effect occurs near the edge of the geofoam.

The thin geofoam culvert stresses show small differences when compared to the no foam culvert stresses of compacted earth fill only. Larger differences occurred as the distance away from the culvert centerline increased, due to positive arching. There is negative arching near the edge, and some of the stresses above the thin geofoam have been supported by the adjacent soil fill. The positive arching effect is more apparent in the thin geofoam base stress plot, where the stresses near the edge have been reduced. Just like the thick geofoam section, there is no trench effect near the centerline of the culvert because of the large span of the trench. From this plot, it is noticeable that the stresses acting on the thin geofoam are relatively large.

Changes in lateral stresses, XX stresses, from thickness variation was also considered. The results of output from FLAC are shown in Figure 22. Stresses appear to be in the same range for lateral pressures at the foam base for both thin and thick foam.

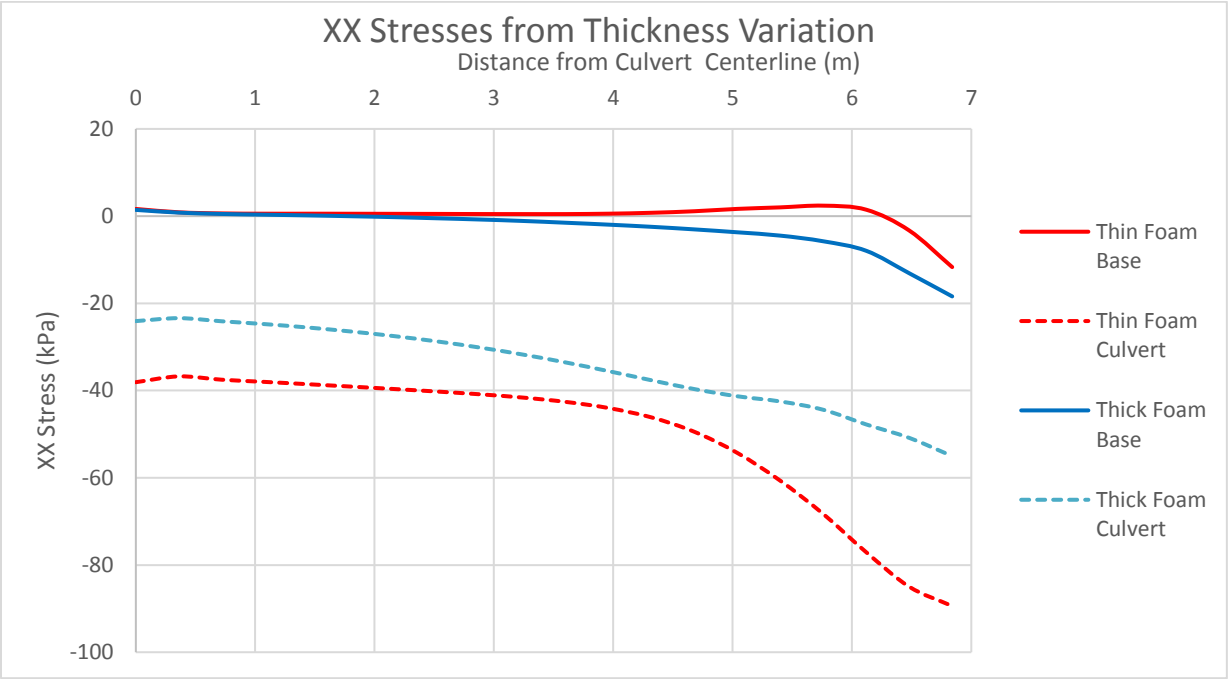

Figure 22: XX Stresses from Width Variation

The thin foam produces much larger lateral pressures against the culvert as compared with conditions for thick foams.

III. Lateral Stresses Acting on the Culvert

The mechanics of the stress transfer of a positive arching trench extend to the sides of the culvert. The stresses will increase because the column of soil adjacent to the soil fill is now supporting extra vertical stresses from the compressible fill edge. These stresses also increase the lateral stresses because they are a function of the vertical stress. These results are shown in Figures 23 and Figure 24. The non-uniform zones in Figures 23 and 24 indicate the location of the stress transfer to the side fill, where the stresses above the geofoam are supported by the soil in the adjacent column.

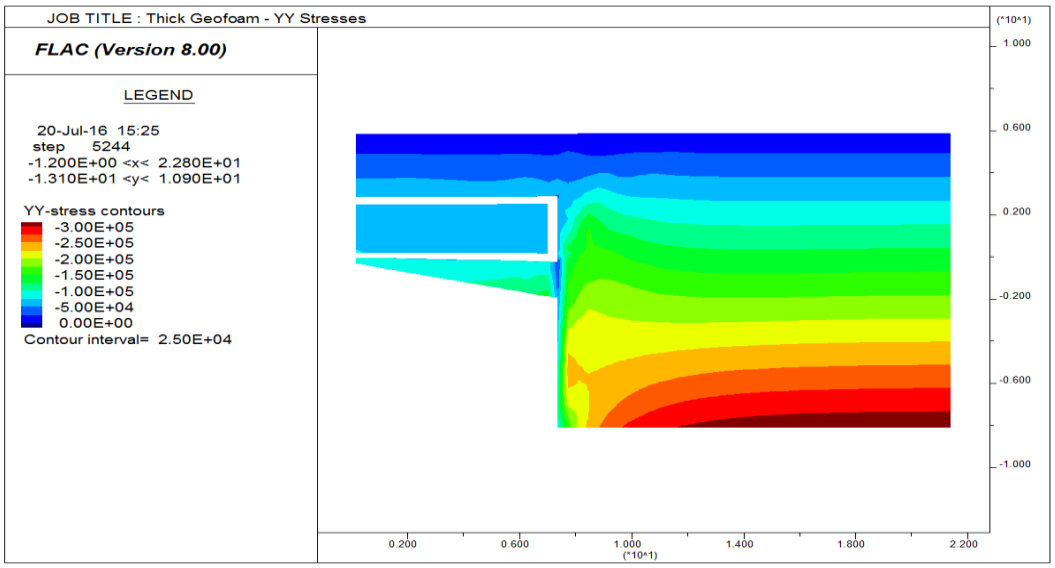

Figure 23: YY Stress Contour of Thick Geofoam

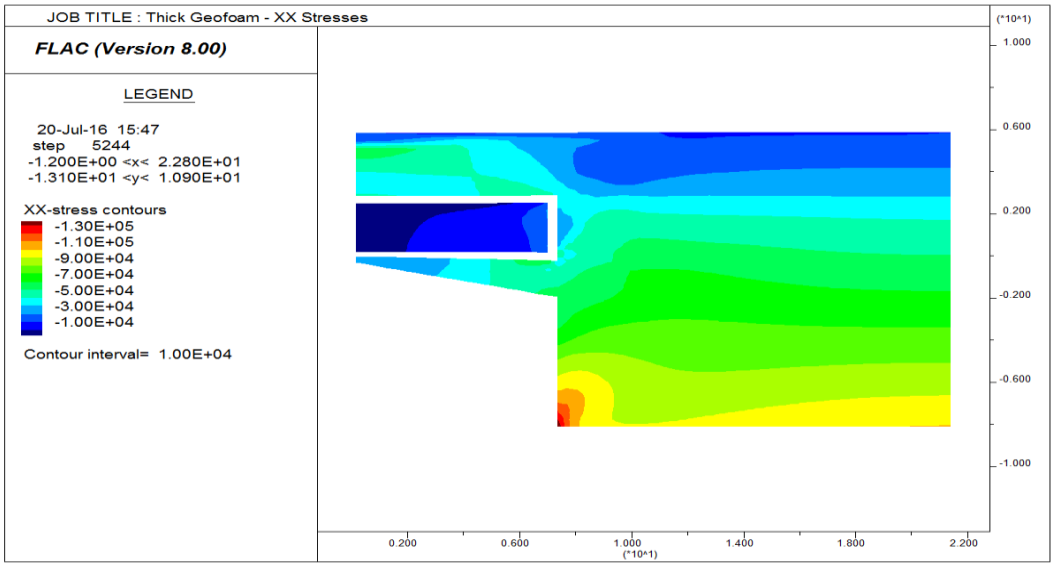

Figure 24: XX Stress Contour of Thick Geofoam

Chapter 3 – Carrs Creek Project

3.1 Background

I. Initial Failure

This chapter discusses the failure of a rapid construction project with the use of EPS Geofoam at Carrs Creek Culvert. Carrs Creek Culvert underlies Interstate 88, in Sidney, NY. The original culvert at Carrs Creek was made of corrugated steel plates and was constructed in 1974. It collapsed on June 28th, 2006 from heavy flooding during the Mid-Atlantic States Flood. The collapse resulted in the washing away of the roadway and culvert section into the Creek, and the death of two truck drivers (Figure 25). The I88 Section between Sidney and Unadilla, NY was closed and the county was declared a Federal Disaster Area. The engineers in charge of the reconstruction of the culvert were tasked to reopen I88 as soon as possible. They planned to reopen the roadway by Labor Day 2006, by rapid construction (Geotechnical Engineering Bureau, 2008).

Figure 25: I88 at Collapsed Carrs Creek Crossing on June 28th, 2006 (Geotechnical Engineering Bureau, 2008)

II. Reconstruction

During a design meeting on July 5th, 2006, the culvert designer stated that the height of the embankment fills over the culvert sections would be too large. The eastbound fill height of 21 feet and the westbound fill height of 15 feet exceeded the capacity of the standard pre-cast concrete culvert section. Thicker culvert sections could not be produced in time to meet the Labor Day deadline. This prompted for the use of lightweight fill to reduce the overall loadings on the culvert to tolerable levels. Three different options were considered for the use of lightweight fill: expanded shale, lightweight concrete, and EPS Geofoam.

The precast concrete culvert was supplied by LHV Precast of Kingston, NY. The precast section has a span of 42ft and is supported on H-Piles. The eastbound section had 9ft of EPS geofoam below 9ft of compacted soil fill and a 2ft pavement fill. The westbound section had 6ft of EPS geofoam below 6ft of compacted soil fill, and 2ft pavement fill. The median contained 6ft of EPS geofoam and different heights of soil fill with a minimum of 3ft (Geotechnical Engineering Bureau, 2008). The main elements of the reconstructed section are shown Figure 26.

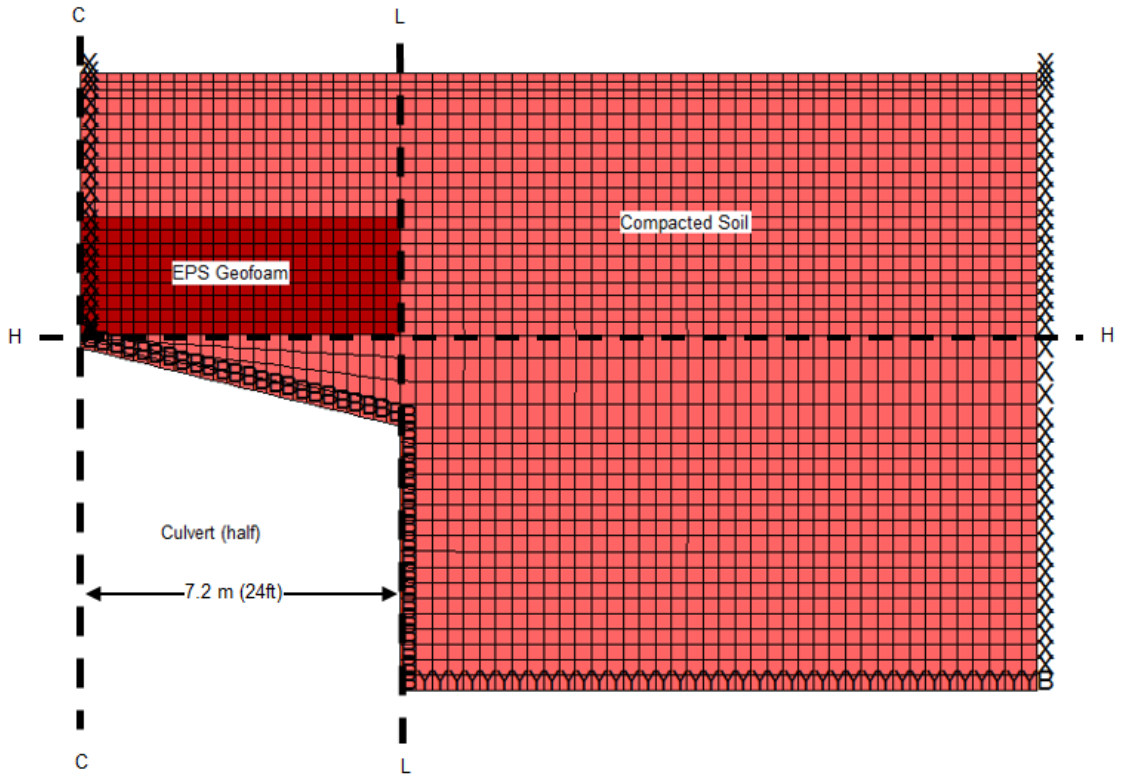

Figure 26: Reconstructed Profile of I88 Eastbound at Carrs Creek

EPS Geofoam of 1.25 pcf density was specified and installation began on August 21st. The EPS geofoam was shipped in 3' x 4' x 8' blocks to replace 9ft of fill in 3 layers on the eastbound and 6ft of fill in layers on the westbound. The top surface of geofoam fill was covered by a geomembrane to prevent direct contact with soil and water(Geotechnical Engineering Bureau, 2008).

The geofoam was placed with continuous rather than staggered vertical joints across geofoam block layers at every 8 feet in transverse and longitudinal directions, Figure 27:

Staggered Joints vs. Continuous Joints. This arrangement reduced the potential of the EPS geofoam blocks to act integrally and react more as spring square column supports.

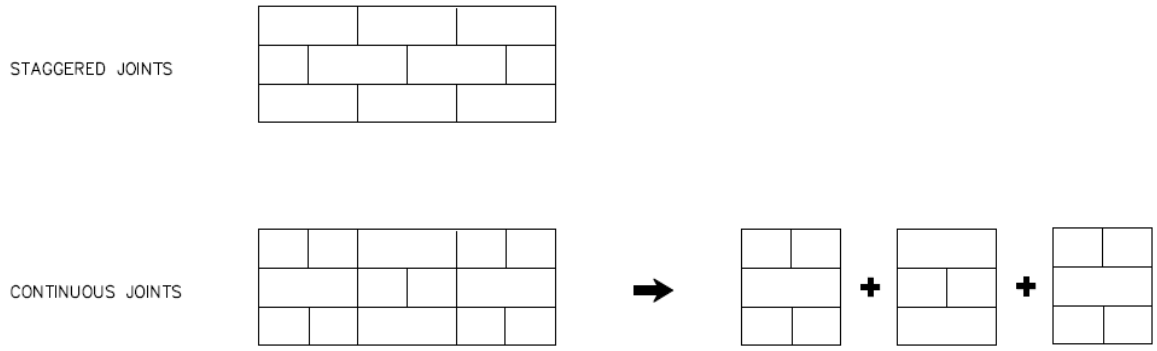

Figure 27: Staggered Joints vs. Continuous Joints

Fill height of up to 10 feet was placed over EPS geofoam at State Route 196. However, the highest fill was only applied over a small segment of the geofoam fill and a load distribution slab was provided above the geofoam surface. In the Carrs Creek Culvert reconstruction project, a load distribution slab was not provided due to the deadlines required with rapid construction. The design engineers believed the geofoam was placed at a depth low enough to diminish the live load stress increments on the geofoam, so a load distribution slab was not considered necessary. The soil above and adjacent to the geofoam was compacted with heavy equipment in wet weather conditions, and placement density of 140pcf has been reported. The continuous vertical interface between the EPS geofoam and the adjacent soil fill is unlike stepped transitions used in other NYSDOT projects (Geotechnical Engineering Bureau, 2008).

III. Settlements

Shortly after opening of the I88 westbound lanes for 2 way traffic, settlement of the asphalt surface was observed. Transverse cracks appeared on the eastbound compacted surface as

well. However the precast culvert showed no signs of distress. The settlements occurred in the EPS geofoam section of the roadway. NYSDOT decided to let the settlements continue and repeatedly repaved the section, while monitoring the settlements. They anticipated the settlements would level off in about 6 months after the initial settlement (Geotechnical Engineering Bureau, 2008).

While the settlement was occurring, trucks crossing the culvert section reported a bouncing sensation. The settlement on the eastbound section was much greater than the westbound section, which is attributed to the greater soil and EPS geofoam fill heights placed on the eastbound section. Some of the settlements on the eastbound section were recorded initially, Figure 28. Settlements continued until the geofoam was removed in May 2007, and reached 45cm on the eastbound and 27cm on the westbound (Geotechnical Engineering Bureau, 2008).

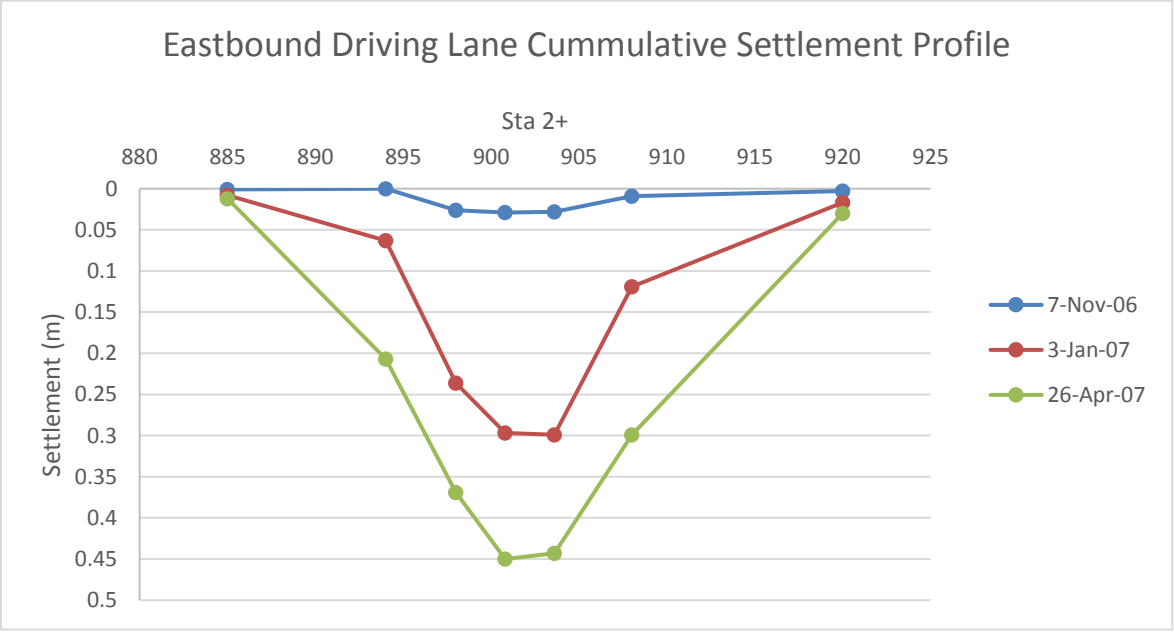

Figure 28: Eastbound Settlement Data over Time

IV. Removal and Investigation

Removal of the EPS geofoam blocks revealed large uneven deformations. In some blocks, one side was severely strained while the other side had relatively smaller deformations (Figure 29). The EPS geofoam underlying the roadways had much greater deformations than the blocks underlying side fills. Overall, the geofoam exhibited a bowl shape deformation in which the blocks closer to the centerline of the culvert were deformed much more than the outside blocks. Perched water was also observed over the geofoam surface and the geo-membrane cover. A total of 177 blocks were weighed, the dimensions were recorded and the locations were noted. Of those 177 blocks, 48 were re-measured, re-weighed after drying and stored in a warehouse for further investigation. Of the 48 blocks, only two were tested - one from the top layer of the eastbound section and one from the bottom layer of the westbound section (Geotechnical Engineering Bureau, 2008).

Figure 29: Removed Geofoam Variable Deformation (GEB, 2008)

Laboratory testing on the two exhumed blocks were performed in four independent laboratories, NYSDOT, Underwriters Laboratories, Geocomp Corporation, and IMR Test Labs. Over 100 density and unconfined compression tests were performed on 2-inch cube samples in accordance with ASTM D 1621 and 1622. The test results indicated that the exhumed blocks had met the density and strength at 10% strain requirements specified for the project. The strengths at corresponding 1% strain were lower than the values for EPS19 in ASTM D 6817, but the strengths at 5% and 10% strains met requirements. The low strength at 1% strain was attributed to possibly as a result of high amount of regrind or recycled material contained in the geofoam blocks. The material specification for geofoam was revised by NYSDOT to include requirements for strength at 1% strain (Geotechnical Engineering Bureau, 2008).

The exhumed blocks that were kept were all weighed and checked for density. Out of the 177 exhumed blocks, 29% were below 90% of the specified density. Lower density blocks were stacked with higher density and other low density blocks. The interaction effects between mixed density geofoam blocks has not been considered before. The two block samples selected for testing were among the lesser deformed of the exhumed geofoam blocks and had corresponding higher densities. The calculated densities of exhumed blocks were not adjusted to account for surface wetting, which otherwise would have made more blocks reported by NYSDOT to have been below the specified limit (Geotechnical Engineering Bureau, 2008). The revisions introduced in the NYSDOT specification were later found to have been unnecessary by a subsequent investigation of the cause of the failure (Negussey et al., 2014).

3.2 **Computer Models**

The Carrs Creek Culvert conditions were simulated in computer models. Two dimensional plane strain models were developed to investigate the likely conditions that could have contributed to the excessive settlements of the EPS Geofoam. The models used the material parameters shown in Table 1, as well as the construction sequence previously described on page 31. Only half of the culvert was modeled due to symmetry.

Relative to the geofoam block deformations, the culvert was treated as a rigid boundary and was restrained in both the X and Y-directions. A 2ft thick pavement structure overlies both the eastbound and westbound sections. The continuous joints were modeled in FLAC using boundary lines and interfaces. The geofoam was represented by elastic and exponential material models in different simulations.

I. Eastbound Model

Figure 30 is a representative model of the eastbound section.

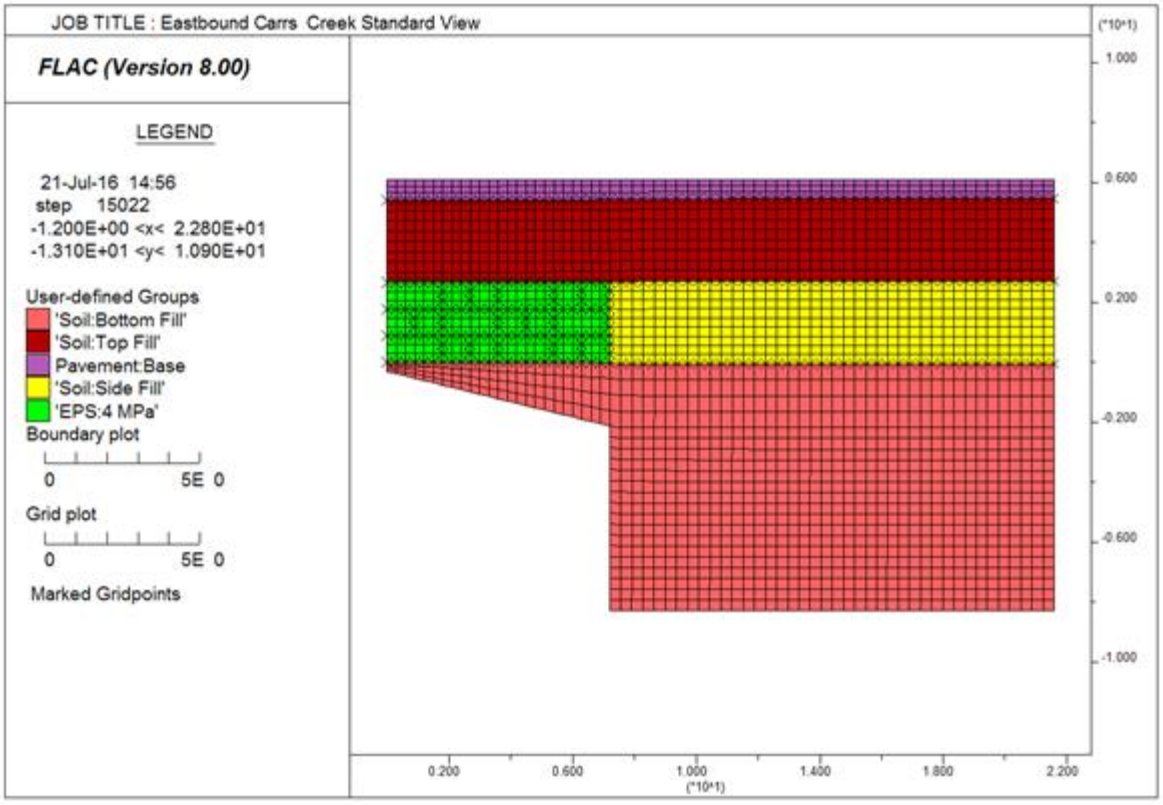

Figure 30: Carrs Creek Eastbound Model

Calculations of total stresses in the vertical (Y-direction) indicated the top surface of the geofoam was subjected to a free field pressure of approximately 75kPa (11psi). The stresses at the top and bottom layers of the geofoam are expected to remain relatively the same because of the low density of geofoam. FLAC output confirms that the stresses acting on the geofoam are in this range, as shown in Figure 31. The YY stresses were taken at the locations indicated

by the blue line. The deviations away from the free field stress are due to hanging effects from positive arching as the geofoam deforms more than the adjacent compacted soil.

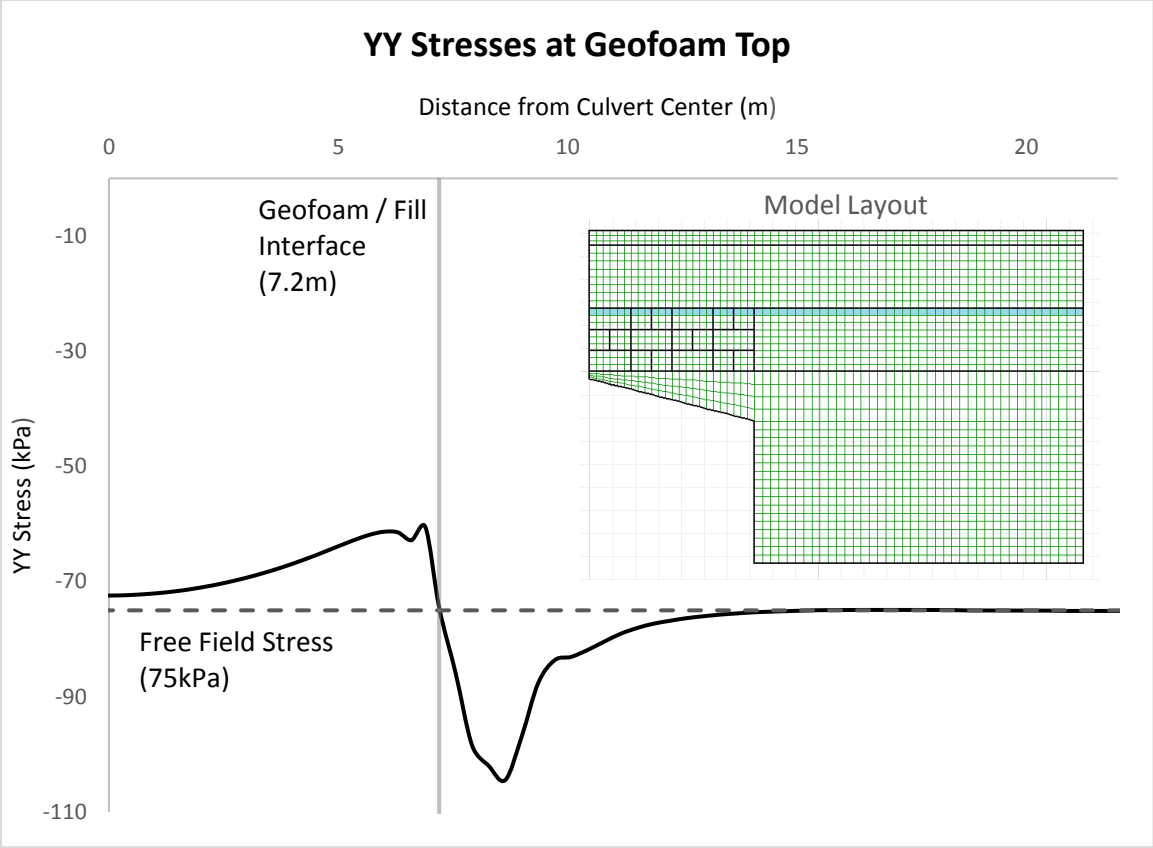

Figure 31: YY Stresses at Eastbound Geofoam Top

Positive arching is mobilized from the differences in rigidity of neighboring materials. The geofoam with an elastic moduli of 4MPa settles much more than the adjacent compacted fill of about 25 MPa moduli. The prism of soil above the geofoam fill is partially supported by down drag. The stresses on the soil fill immediately next to the geofoam increase, and eventually reduce back down to free field stresses further away from the trench. The opposite happens on the geofoam section, where the stresses are greatly reduced towards the edge and gradually return to a near free field state at the center of the geofoam. The calculated free field stress of

75kPa (11psi) reduced to about 72kPa (10psi) at the center and towards 60kPa (9psi) near the geofoam/soil interface.

The range of stresses acting on the geofoam below the eastbound lanes were above the recommended working stresses for the specified geofoam grade. EPS 19 has a compressive strength at 10% strain of about 110kPa (16psi). The working stress is generally taken to be 30% of the compressive strength at 10%, a value of about 33kPa. The overburden stresses acting on the geofoam in the eastbound section range from about 60kPa (9psi) to 72kPa, nearly double the allowable working stress. The induced trench effects were not enough to reduce the stress levels below the recommended working stress, especially since the culvert at Carrs Creek spans a large width. Large settlements should have been expected to occur in the eastbound section under the effect of overburden stresses. There are also other factors in both design and construction that could have contributed to increased deformations.

II. Westbound Model

Figure 32 is a representative model of the westbound section. There are only two layers of geofoam for the lightweight fill height of 6ft. The geofoam is modeled with continuous joints every 8ft as in the field conditions. Above the compressible fill is compacted earth fill with a thickness of 6ft. Overlying the compressible earth fill is a 2ft thick pavement section as in the case for the eastbound.

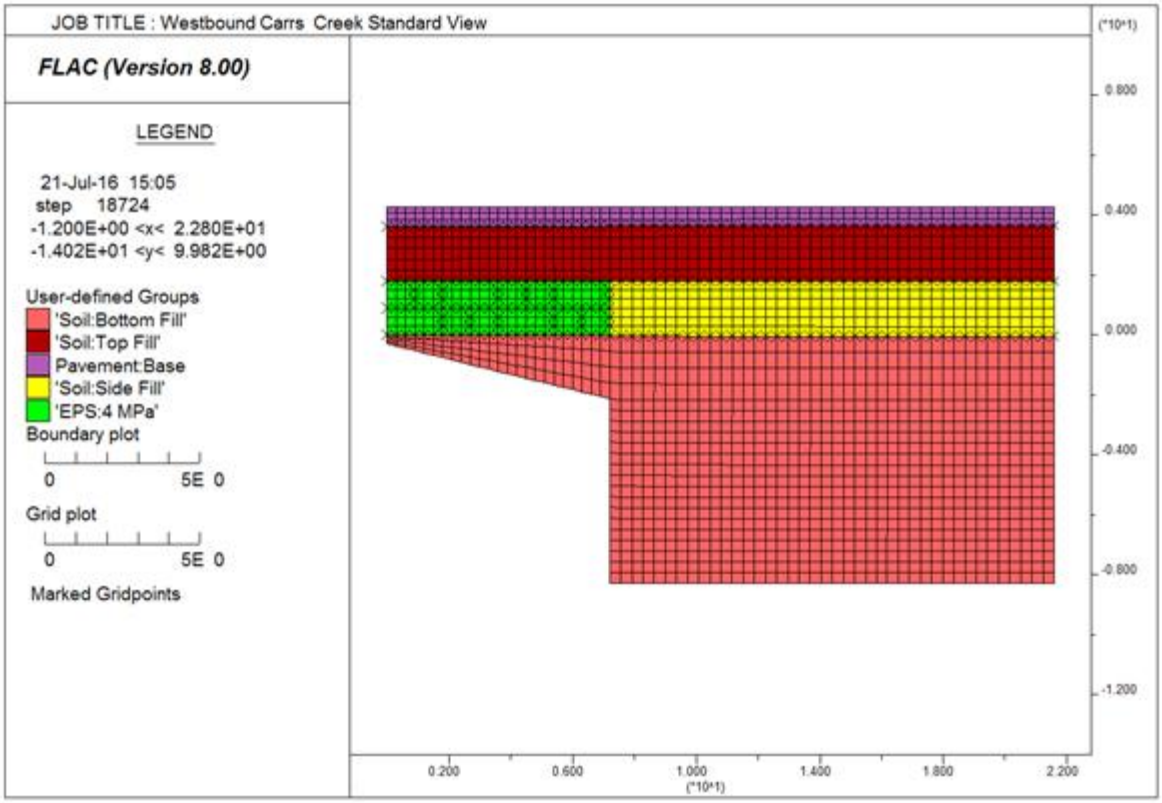

Figure 32: Carrs Creek Westbound Model

III. Median Model

Figure 33 is a representative model of the median. Similar to the westbound section, the median also contains two layers of geofoam. However, there is less compacted soil fill and no pavement section overlying the geofoam. This significantly reduces the stresses acting on the geofoam to an amount of overburden pressure of about the uplift from hydrostatic pressures during flooding. The median serves as a storm water retention pond and the section with least downward overburden pressure along the Carrs Creek Culvert Crossing.

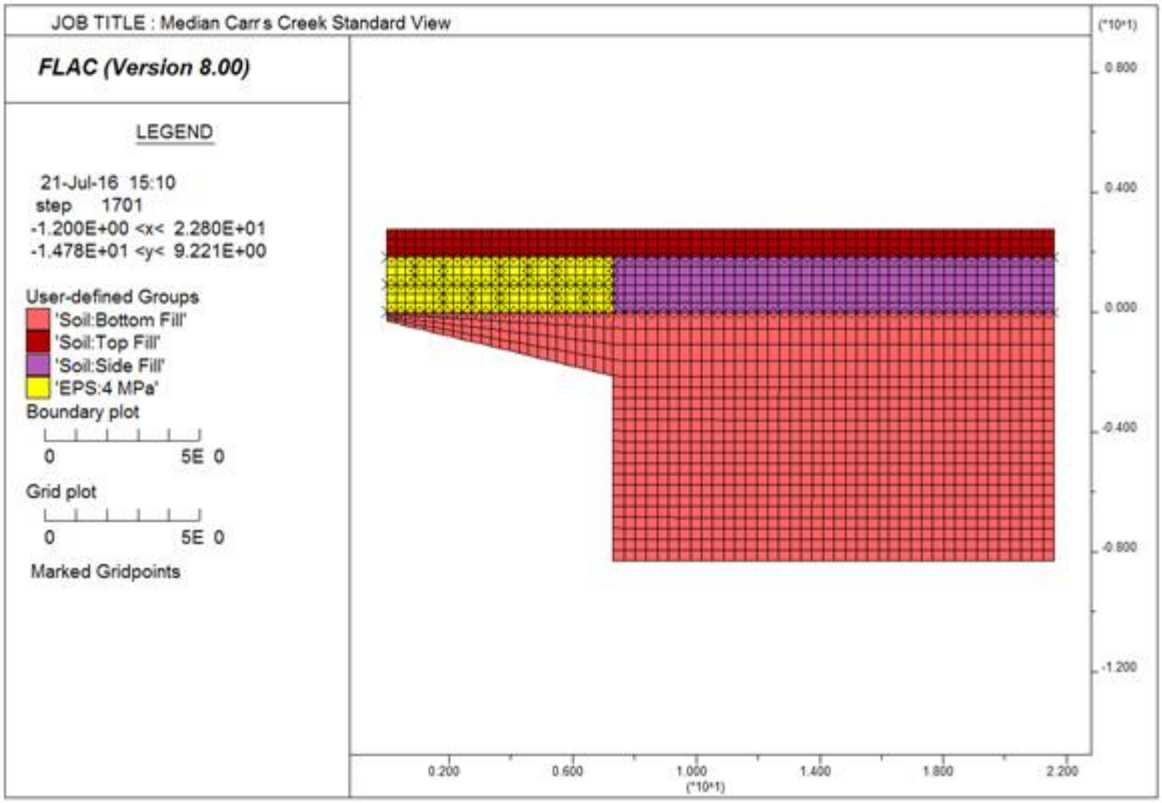

Figure 33: Carrs Creek Median Model

IV. Modeling Observed Settlements

FLAC models are capable of predicting displacements due to dead loads. Using the average elastic modulus of 3 MPa established from laboratory results, displacement outputs were compared with settlements measured in the field. The FLAC outputs produced a maximum displacement of about 2cm, which is much smaller than the 45 cm observed in the field. To improve agreement with field settlements as shown in Figure 28 (Page 51), FLAC models were generated using lower elastic moduli. These equivalent moduli were to account for the effect

of different design and construction conditions. The resulting settlements are shown in Figure 34 together with field observations made on different dates.

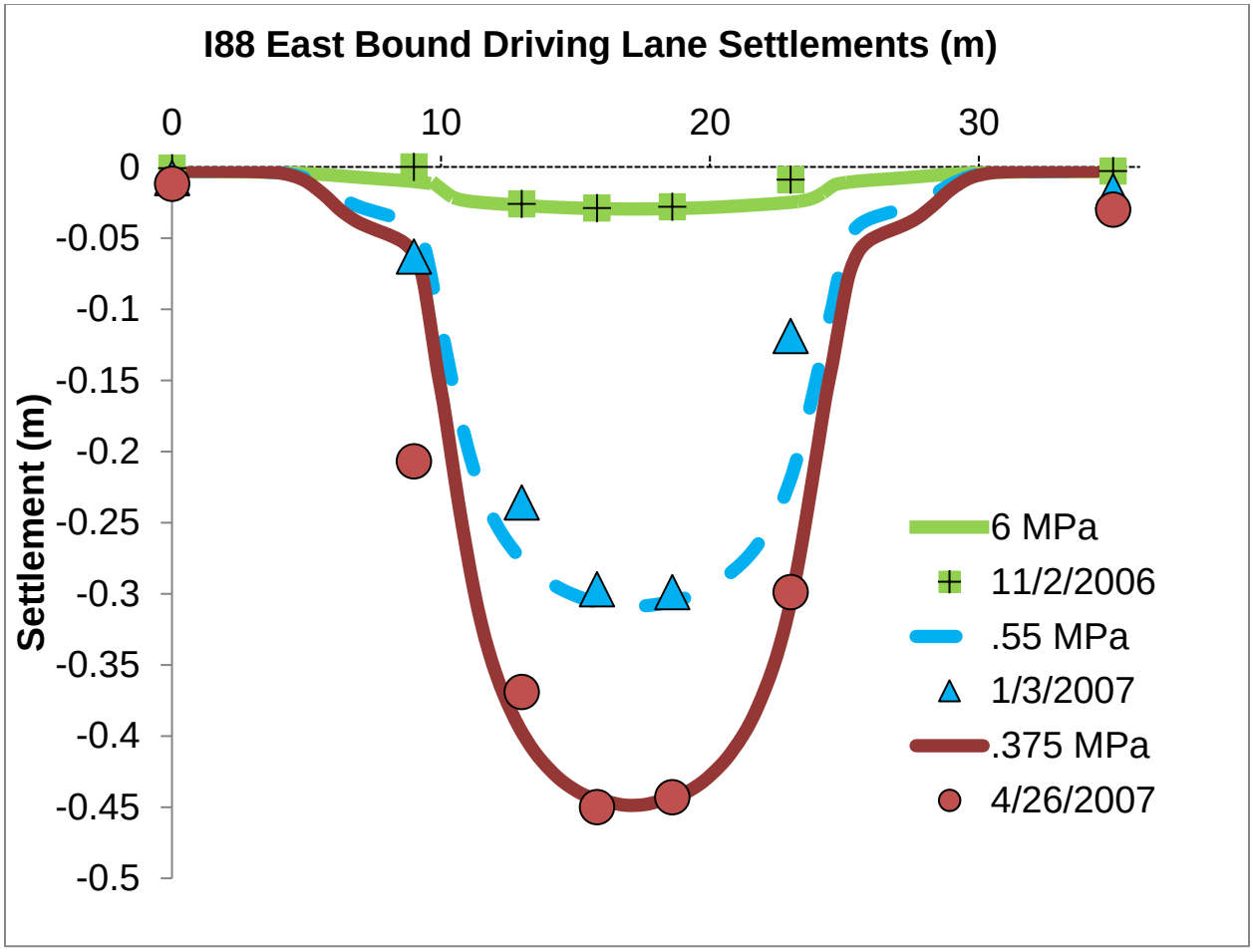

Figure 34: Eastbound Settlements and Equivalent Moduli

To match the earliest settlements from November 2006, the elastic modulus had to be raised to 6MPa. The earlier parts of the field measurements for the eastbound were recorded. The remaining two sets of equivalent moduli were much lower than 3MPa, suggesting that the combination of creep, confining pressures, mixed densities and continuous joints contributed to equivalent modulus degradation that produced the observed excessive settlements. The 3MPa

modulus determined from laboratory testing could not account for the displacements observed in the field.

V. Live Load Considerations

Photographs and data from the Carrs Creek investigation indicate that heavy equipment was used to compact soil over the EPS geofoam. These compaction stresses can be high depending on the lift thickness. Typically, a mesh reinforced concrete slab was provided to reduce stress increments on the EPS geofoam. In Carrs Creek there was no load distribution slab to attenuate compaction stresses resulting from heavy construction equipment.

Using KENPAVE, a pavement finite element modeling program (Huang, 2004), compaction induced stresses for conditions at Carrs Creek were examined. Two different sections were considered, the first being Carrs Creek with no load distribution slab underneath 6 and 12inch lift thicknesses. The second was for the same lift thicknesses but with a 4-inch-thick concrete load distribution slab over the EPS Geofoam, as was provided in previous NYSDOT geofoam projects such as State Route 196 (SR196). Both of these sections were subjected to an 18 kip single axle truck loading. Figure 35 shows the stress increments felt within the geofoam.

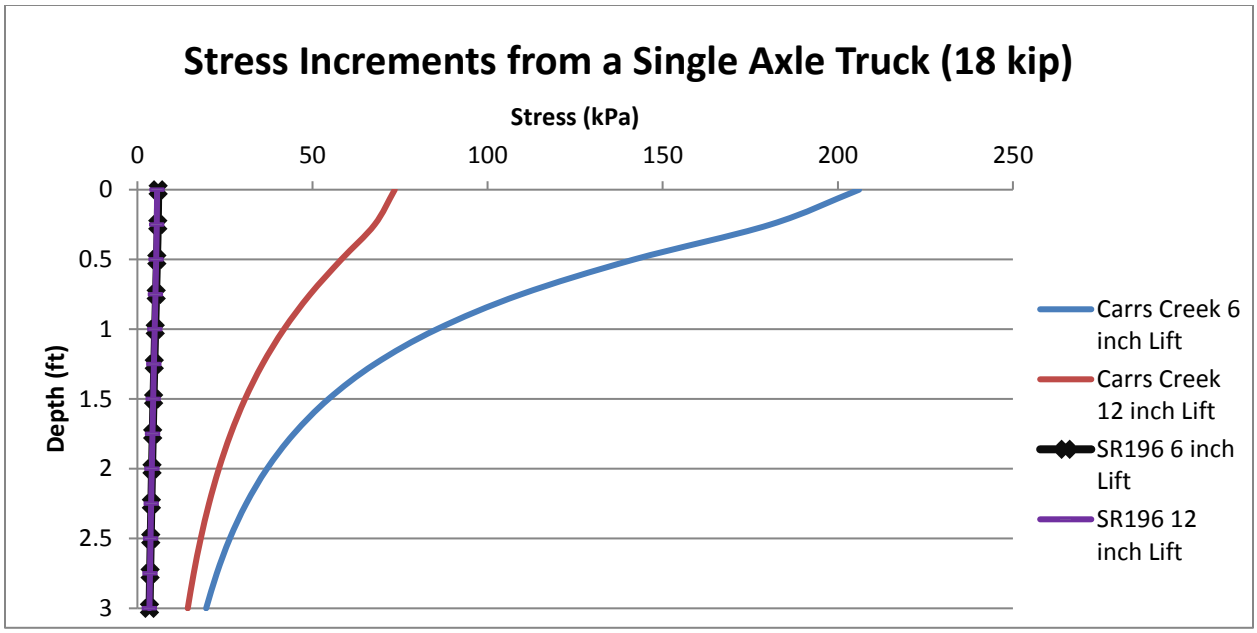

Figure 35: Live Load Stress Increments

The output for the no load distribution slab with a 6-inch lift produces the most stress on the EPS geofoam. At the surface of the geofoam, the stresses exceed 200kPa (29psi). This is much higher than the unconfined compressive strength at 10% strain of 110kPa (16psi). The 12-inch lift distributes much of the contact pressure to still excessive of about 70 kPa (10psi). Pre-stressing tends to weaken geofoam to produce larger deformations on re-loading (Birhan, 2014). In the case with a load distribution slab of 4-inch thickness, the stress increment was reduced to nearly 5kPa (0.7psi). Both the 6 and 12inch lift thicknesses resulted in tolerable stress increments on the EPS geofoam when a load distribution slab was used. In Carrs Creek, the lack of a load distribution slab caused pre-straining and modulus degradation in the upper layer of EPS geofoam.

VI. Effect of Continuous Joints

Typically, blocks are layered on top of each other with staggered joints so vertical continuous joints do not develop. The interlocking of blocks in a staggered joint layout allows for greater stress variations within the geofoam. The continuous joints are believed to cause the section to act as individual springs, especially in the absence of lower confining stresses. The continuous joints were modeled in FLAC with appropriate interface elements to allow slippage between the blocks. A section with staggered blocks was also created and cycled to obtain stresses and displacements. Figure 36 and Figure 37 show the displacement outputs from the FLAC analysis.

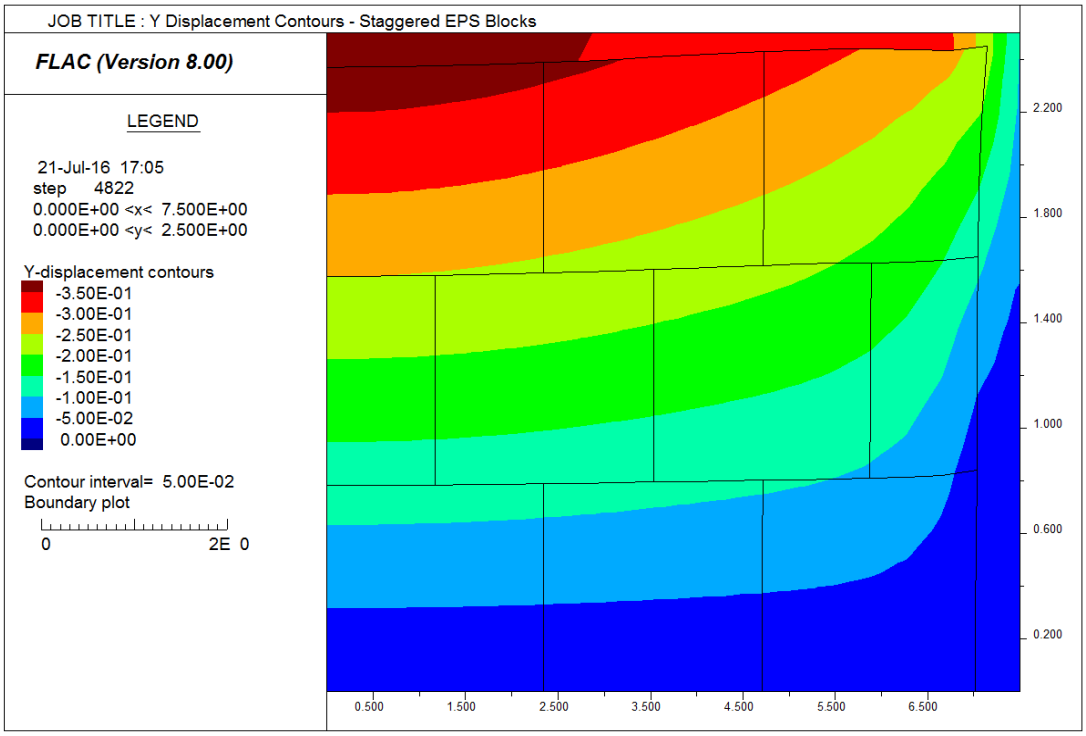

Figure 36: Y Displacements for Staggered Geofoam

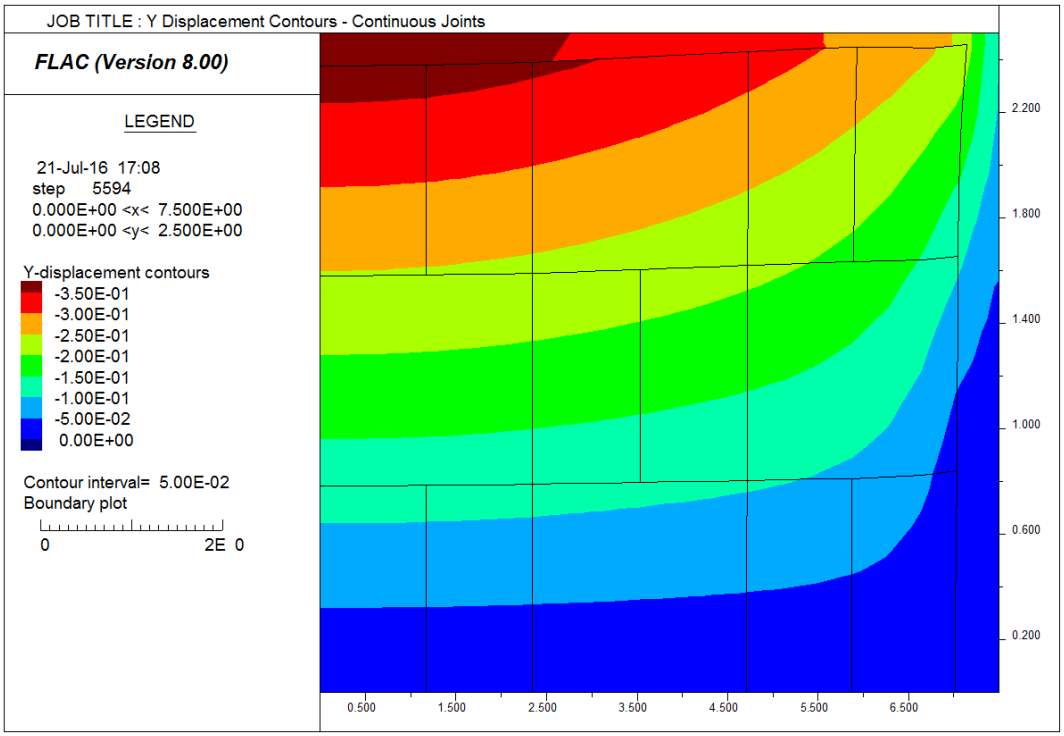

Figure 37: Y Displacements for Continuous Joints

Y displacements had the same magnitude as maximum displacements within the geofoam. The elastic modulus of the geofoam was given a very low value of .5 MPa to exaggerate displacements resulting from the condition of continuous joints. When using materials of the same modulus, displacement contours appeared to be similar and within the same range. From the displacements alone, there were negligible effects when continuous joints were selected over staggered blocks.

The stress contours from FLAC are shown in Figure 38 and Figure 39. When considering YY stresses, there were minor differences as well between the staggered and the continuous joint layout. The contours in the FLAC output show the same general range of stresses regardless of

geofoam configuration, given that the densities and elastic moduli were uniform. The only source of differences was from the interface friction existing between the individual columns of geofoam compared to a monolithic staggered structure.

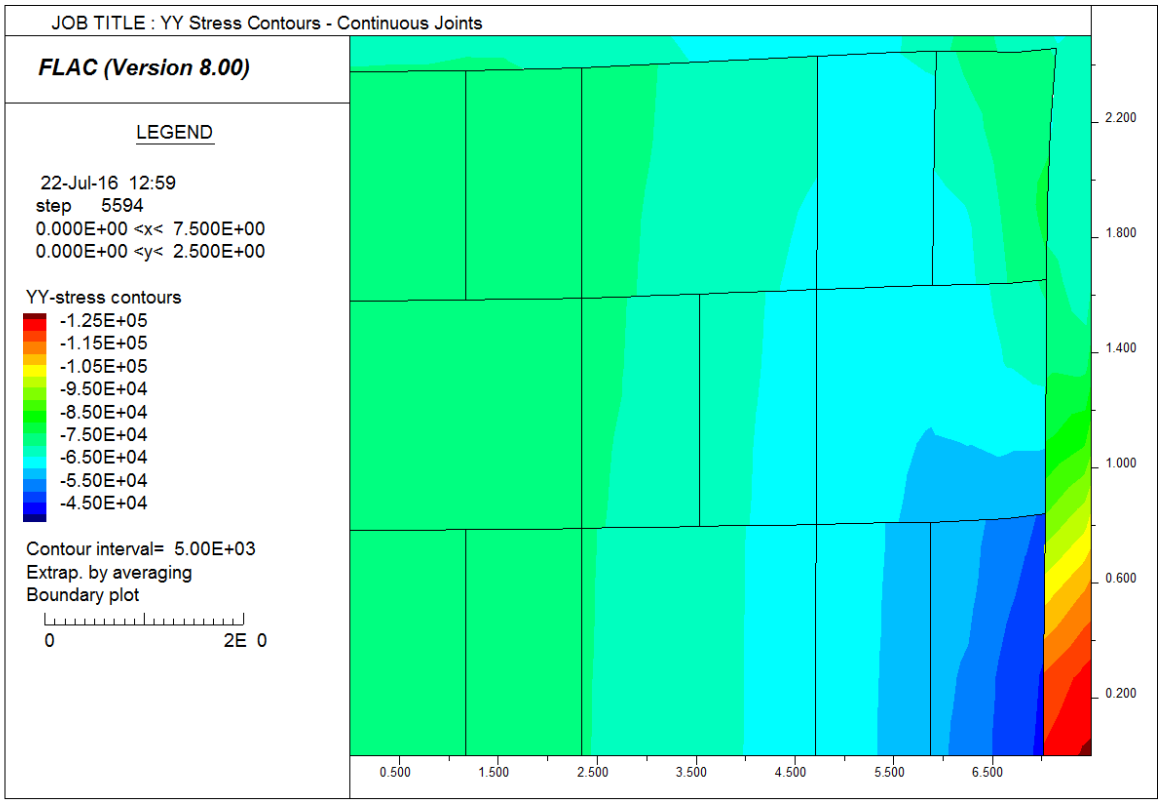

Figure 38: YY Stress Contours for Continuous Joints

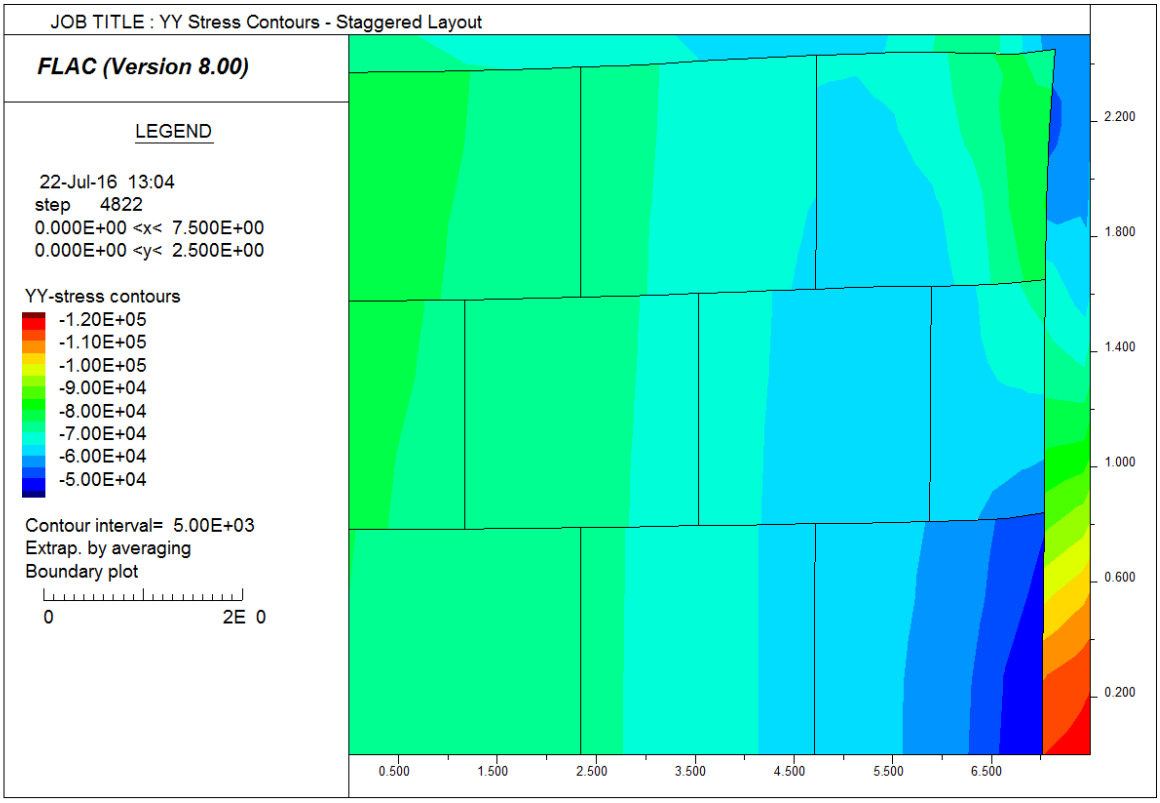

Figure 39: YY Stress Contours for Staggered Layout

Differences between the two layouts in terms of distribution of stresses in the individual elements along the top and bottom rows of geofoam are shown in Figure 40 and Figure 41. YY Stresses are very similar within the geofoam and have a maximum difference of 3kPa (.4psi), which is negligible. If the EPS geofoam blocks were of uniform density and in the presence of lateral confining pressures; the continuous vertical joints alone do not appear to have been a critical contributing factor to the failure.

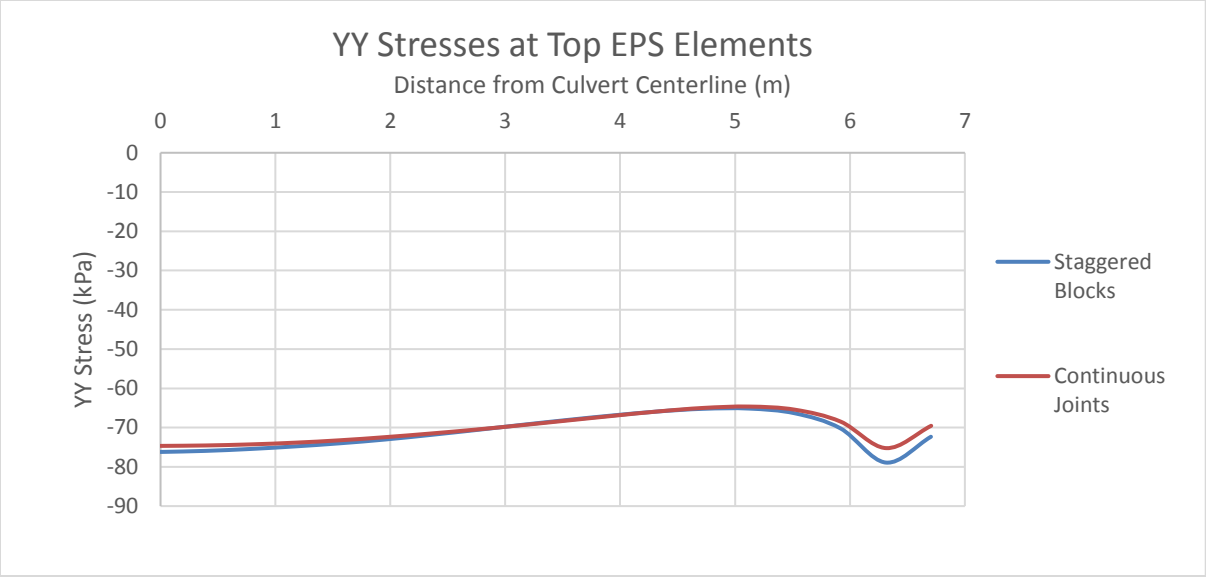

Figure 40: YY Stresses at Top Geofoam Elements

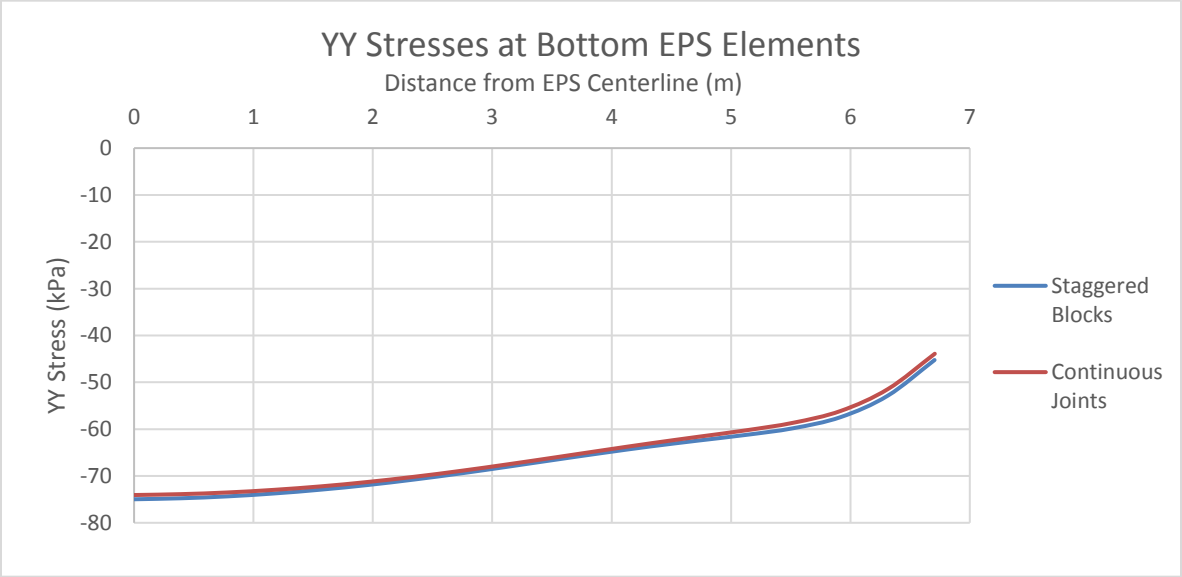

Figure 41: YY Stresses at Bottom Geofoam Elements

VII. Effect of Hydrostatic Pressures

Borehole logs show that the groundwater rose up to 2ft above the geofoam underlying the eastbound lanes. Photos taken during excavation and removal of geofoam show water was present between and on top of geofoam blocks. Groundwater was found above and below the

impervious geomembrane liner. The groundwater could have risen to higher levels following heavy rainfalls. High groundwater levels would have imposed additional all around confining pressures onto the geofoam.

At the top of the geofoam, hydrostatic pressures for water levels found in the borehole add up to about 6kPa (0.9psi). The bottom of geofoam in the eastbound section would be subjected to about 32kPa (4.6psi) and the westbound would be subjected to about 24kPa (3.5psi). Research (Birhan, 2014) has shown that confining pressures in addition to axial pressures reduce stiffness of the geofoam. Models of the eastbound section were generated using FLAC to calculate lateral pressures acting on the geofoam; XX-Stress output is shown in Figure 43 indicate a range of 10kPa (1.5psi) to 32kPa (4.6psi), when only considering a dry case.

With the presence of groundwater of up to 11ft head from the base of the geofoam, XX stresses acting on the geofoam were in the range of 15kPa (2.2psi) to 50kPa (7.25psi) as shown in Figure 43. The calculated pressures became excessive both axially and laterally. The recommended working stress for the specified geofoam is 30kPa (4.2psi), as determined in uni-axial loading. The geofoam in the eastbound section under hydrostatic pressures was subjected to pressures greater than the working stress in both axial and lateral directions. Considering confining pressure effects (Sun, 1995; Birhan, 2014) mentioned previously, there was likely degradation of the elastic modulus.

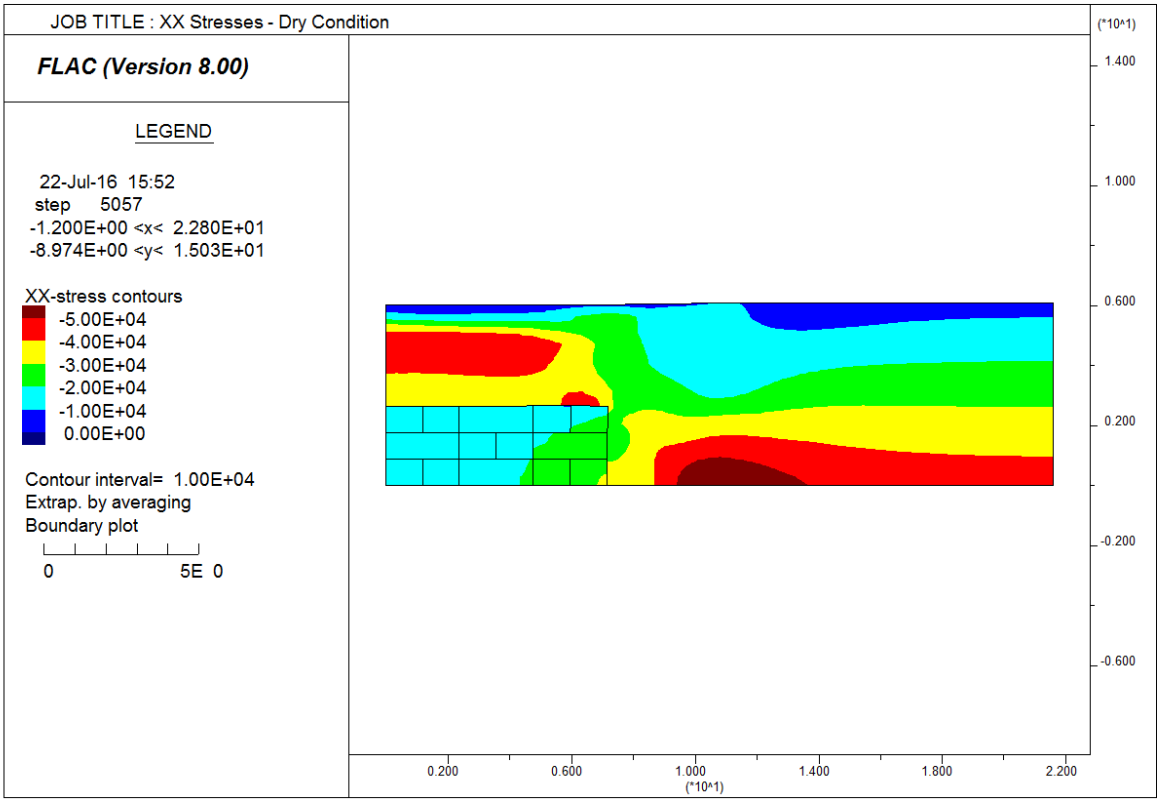

Figure 42: XX Stresses in Dry Eastbound Section at Carrs Creek

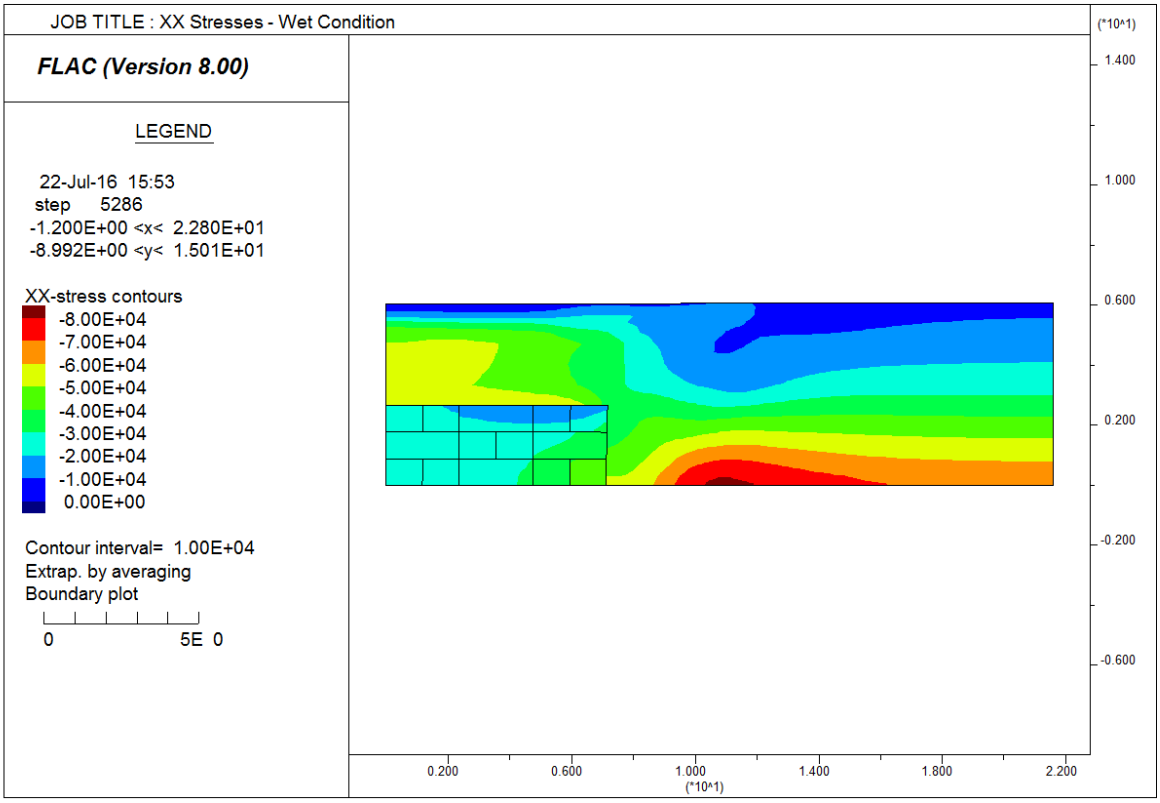

Figure 43: Hydrostatic Confining Pressures in Carrs Creek Eastbound Section

VIII. Effect of Mixed Densities

The existence of mixed densities in the geofoam of Carrs Creek was unintended. There have been no other case histories or studies that consider the mixing of different grade geofoam in the same layer. The desire to complete the project with a very short deadline resulted in delivery and installation of mixed density geofoam blocks. The lack of proper quality assurance resulted in both a broad range of geofoam densities and elastic moduli. To understand the effect of the mixing of different density geofoam, Carrs Creek Culvert was modeled with the continuous joints and different density geofoam blocks.

Densities of 20kg/m^3 and 16kg/m^3 with elastic moduli of 4MPa and .3MPa were used, respectively. These values were selected after a series of trials, to gain a better understanding of the stress and displacement differences based on modulus variations. The moduli under consideration were reflective of two extremes that may have existed within the Carrs Creek layout to produce the observed displacements. The un-deformed model layout is shown in Figure 44. The weak and strong geofoam were place adjacent to each other in a random manner to observe effects on localized stress and displacement distributions.

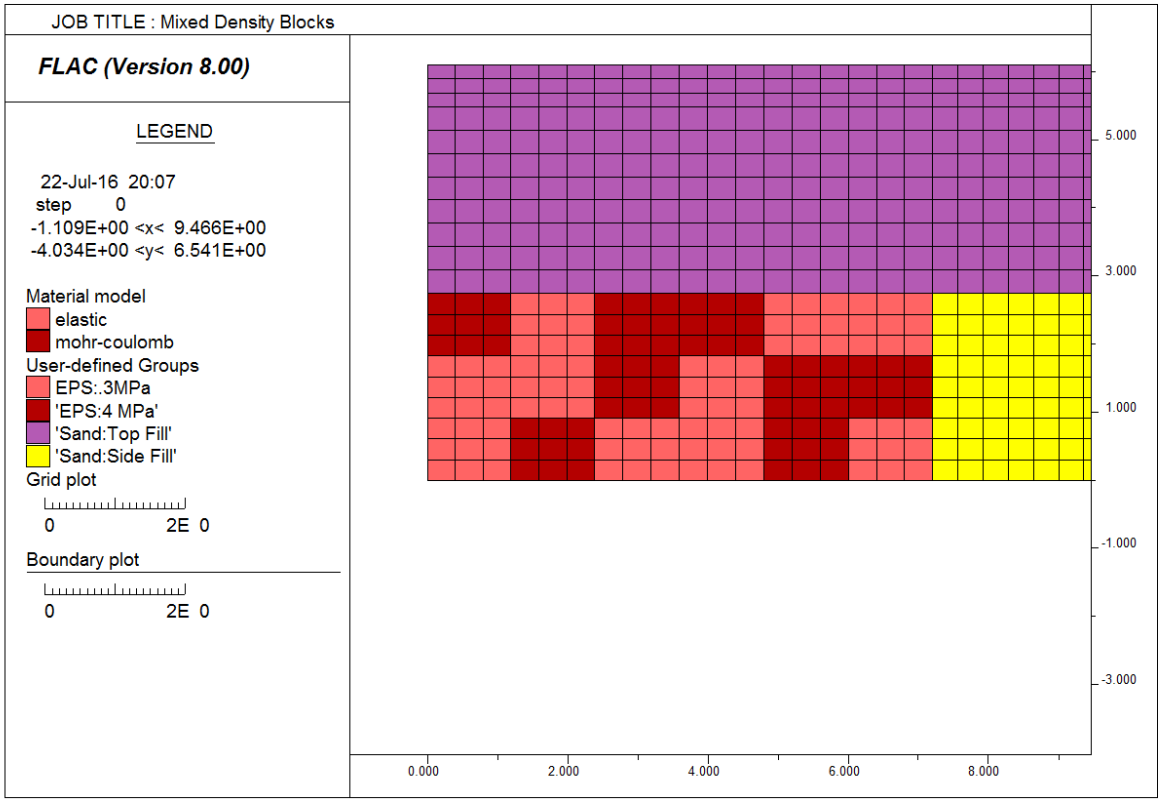

Figure 44: Mixed Density Layout at Carrs Creek Eastbound

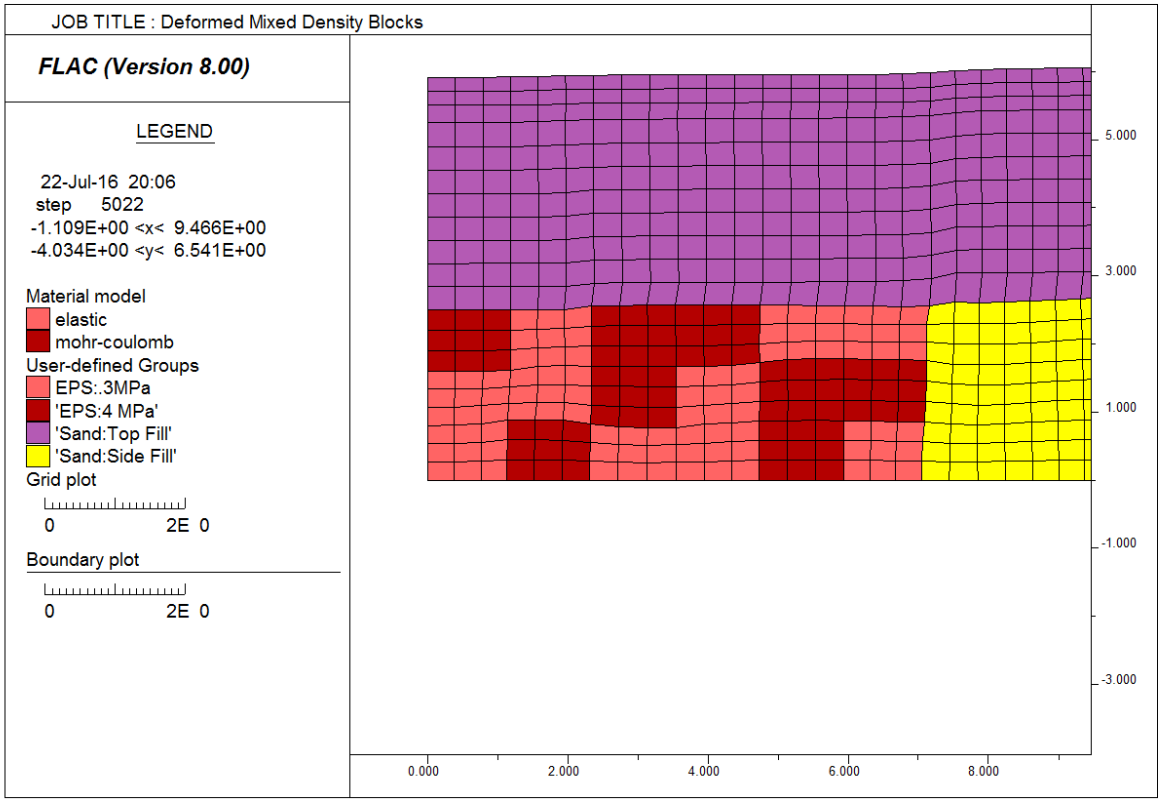

Figure 45: Mixed Density Deformed Section at Carrs Creek

Figure 45 shows the output for model cycling under self-weight. The displacements at the pavement surface indicate a bowl shape, which agrees with field observations. It is important to note that different mix of geofoam density configurations were attempted and all produced a bowl shape deformation regardless of density variations. Y-Displacement contour plots are shown in Figure 46. The mixed density layout is shown beneath the contour plot.

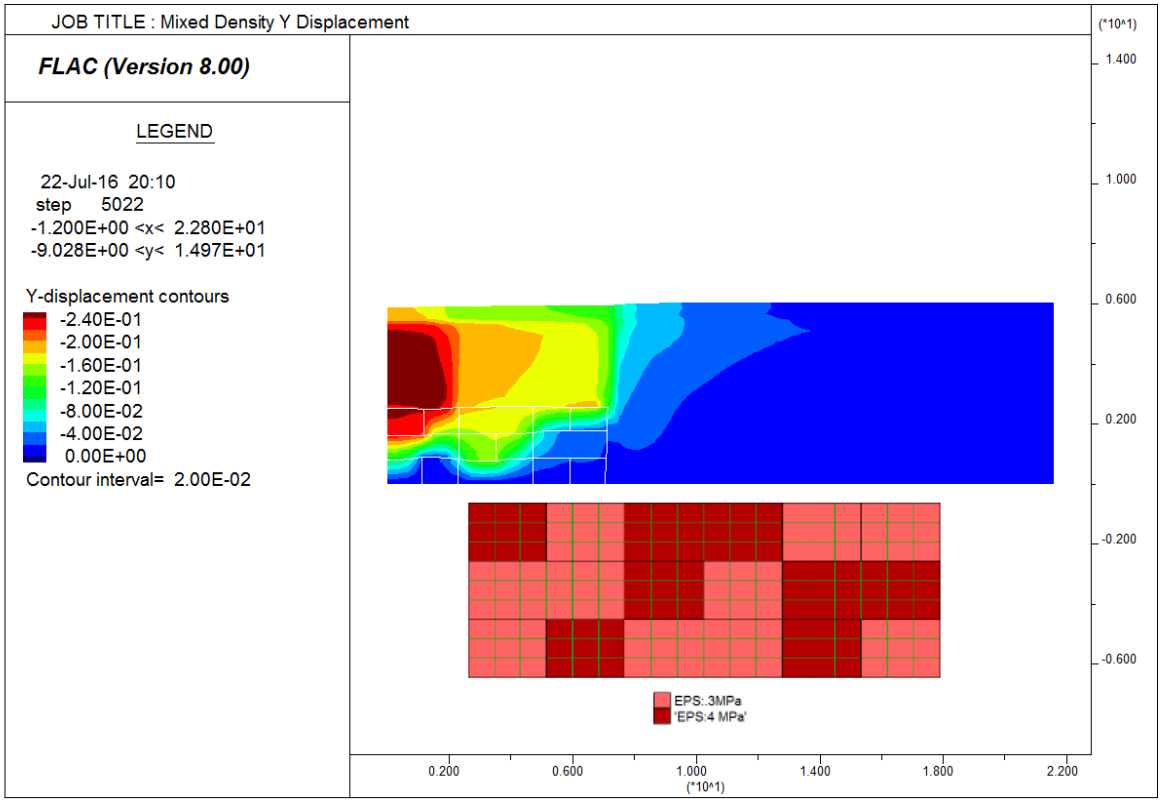

Figure 46: Mixed Density Y Displacements at Carrs Creek

The largest displacement occurred within the weaker 0.3MPa geofoam, as expected. The contour lines in the weaker geofoam blocks also show larger deformations. For example, one weaker geofoam block area contained displacements ranging from 2.5cm to 20cm. These differential displacements within one block of geofoam were consistent with the observations made during the removal of geofoam in the field. The stronger 4MPa modulus geofoam blocks exhibited much less deformations, however displacements increased towards the edge if the stronger geofoam block was adjacent to a weaker geofoam block. To further understand the

edge effects, YY Stress contours were generated as shown in Figure 47 along with the corresponding geofoam block layout.

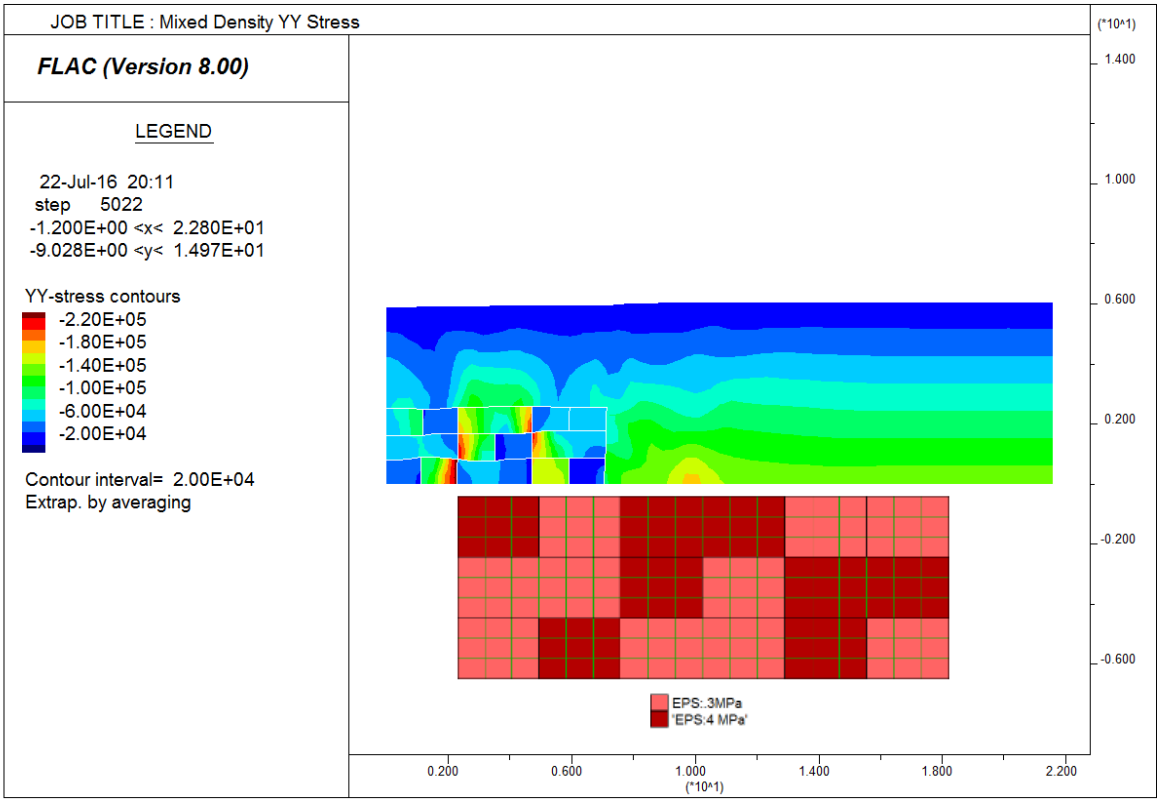

Figure 47: Mixed Density YY Stresses at Carrs Creek

YY-Stress contours for loading of mixed density blocks indicated that the greatest stress concentrations exist within the geofoam. The stresses in the geofoam were greater than the combination of the induced trench effect and the deadweight of 9ft (2.7m) of compacted fill. With just the effect of overburden soil pressure alone, a uniform density geofoam section was subjected to an overall average stress of approximately 75kPa (11psi), neglecting induced

trench effects that reduce the stresses near the geofoam-compacted fill interface. The mixing of densities facilitated the transfer of stresses to the higher density geofoam blocks. The higher contrast in modulus of 4 and 0.3 MPa for the 20 and 16 kg/m^3 densities suggests a clear trend the outcome range of 20 to 200kPa is very large. In the actual field conditions, the density range for the installed blocks was 17 and 23kg/m^3. Modulus degradation due to confining pressure effects is greater for lower density geofoam under the same when compared to higher density foam (Birhan, 2014).

The mixing of densities proved to be critical in the failure of geofoam in Carrs Creek Culvert. The lower density geofoam blocks deformed and transferred the majority of the applied Y-direction stresses to the neighboring stiff blocks. The compressive strength at 10% strain of geofoam was taken to be 110kPa (16psi), which was already an undesirable amount of strain to be present in a roadway substructure. The mixing of densities increased the axial stress to nearly double the tolerable limit, at 220kPa (32psi) in the stiffer geofoam blocks. The cellular structure of geofoam cannot accommodate these excessive stresses without producing large deformations. These large localized stresses were accountable for the differential displacements within individual geofoam blocks.

The effect of having mixed density geofoam blocks was not limited to only the Y-direction. The mechanics of stress transfer to stiffer geofoam blocks also applied in the lateral, X-direction. The XX Stresses are shown in Figure 48. Stresses in the X-direction within the geofoam range from 0kPa (0psi) to 100kPa (14.5psi). The crushing of the weaker modulus geofoam resulted in further stress concentrations on the stiffer geofoam. Lateral pressures

from the neighboring compacted soil fill and the lateral component of the excessive axial stresses contributed to excessive confining pressures.

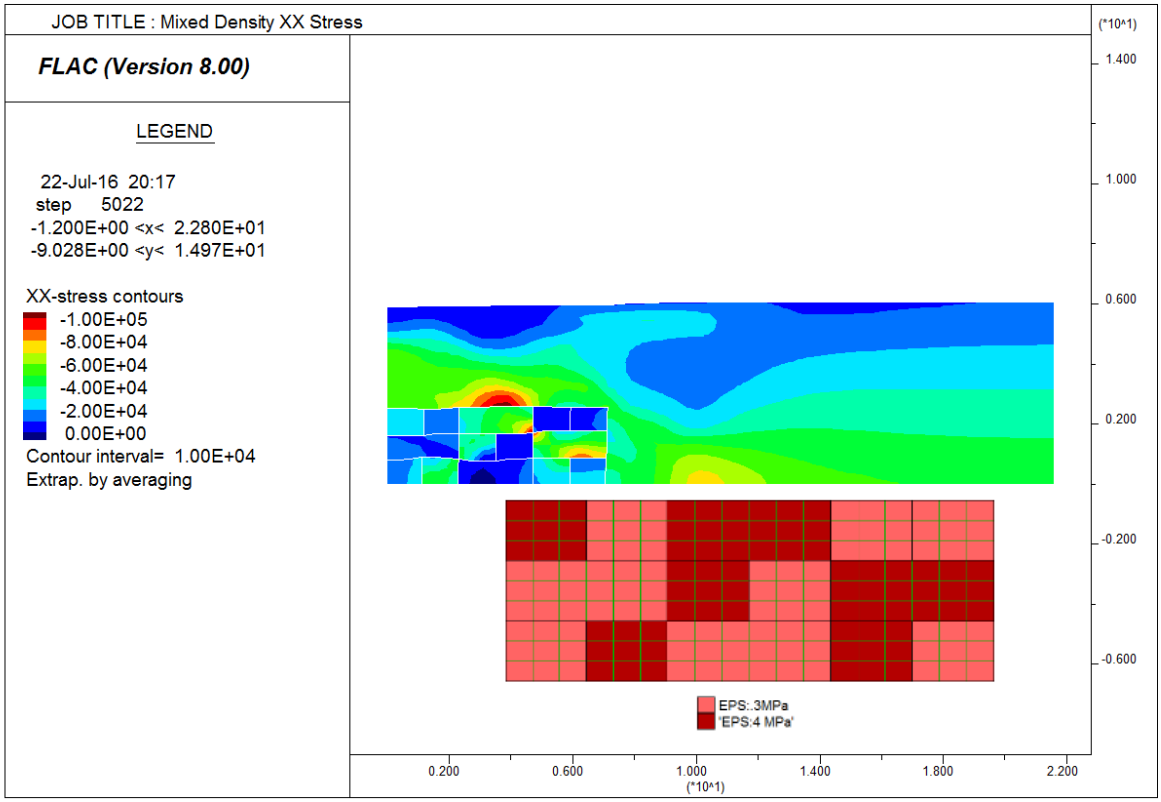

Figure 48: XX Stresses at Carrs Creek

IX. Effect of Confining Pressures

This study considered the geofoam in Carrs Creek to be linear elastic. Figure 49 shows the displacements for the elastic model for the eastbound section of Carrs Creek. The greatest predicted deformations were near the center. The maximum displacement due to dead load

using geofoam with an elastic modulus of 4MPa was approximately 1cm. These models were useful for representing stress distributions but not for displacements.

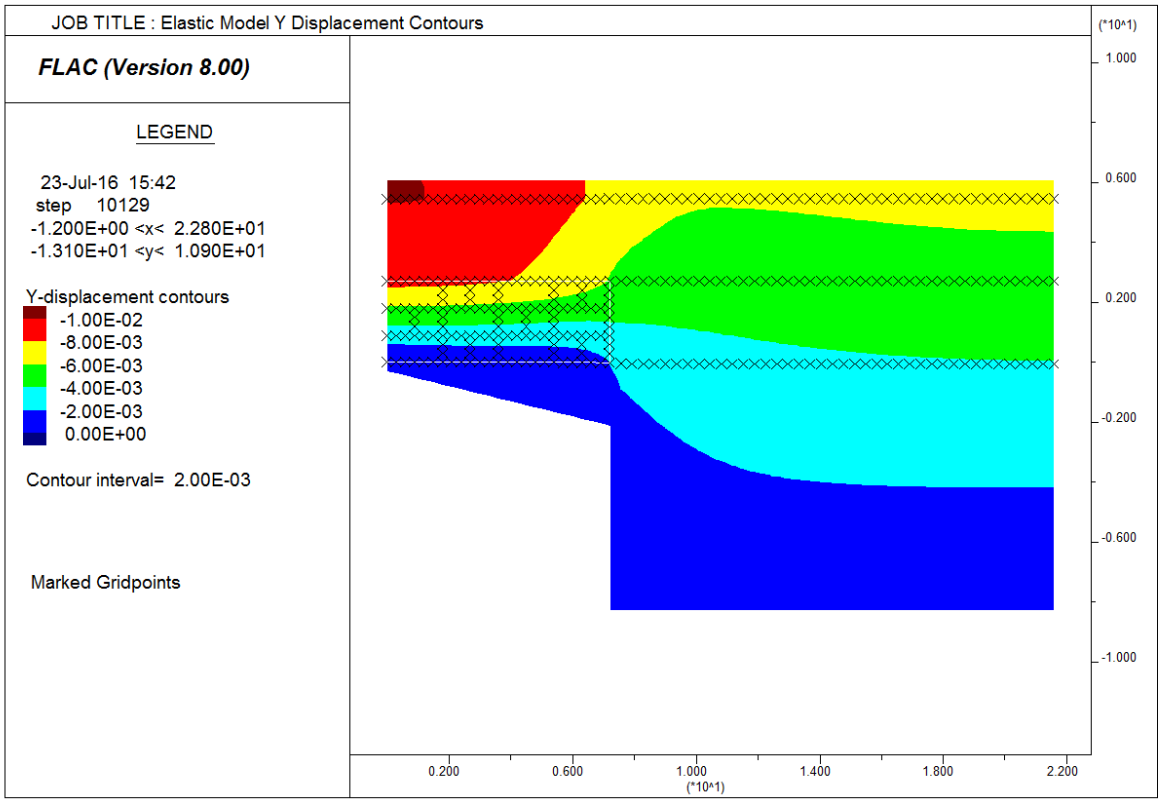

Figure 49: Elastic Model Y Displacements

To better model the behavior of EPS geofoam, alternate constitutive models were developed based upon laboratory testing. The models are reflective of the relationships shown in Chapter 2. The major effect of confining pressures is the reduction of modulus. The Y-displacements from the exponential model are show in Figure 50.

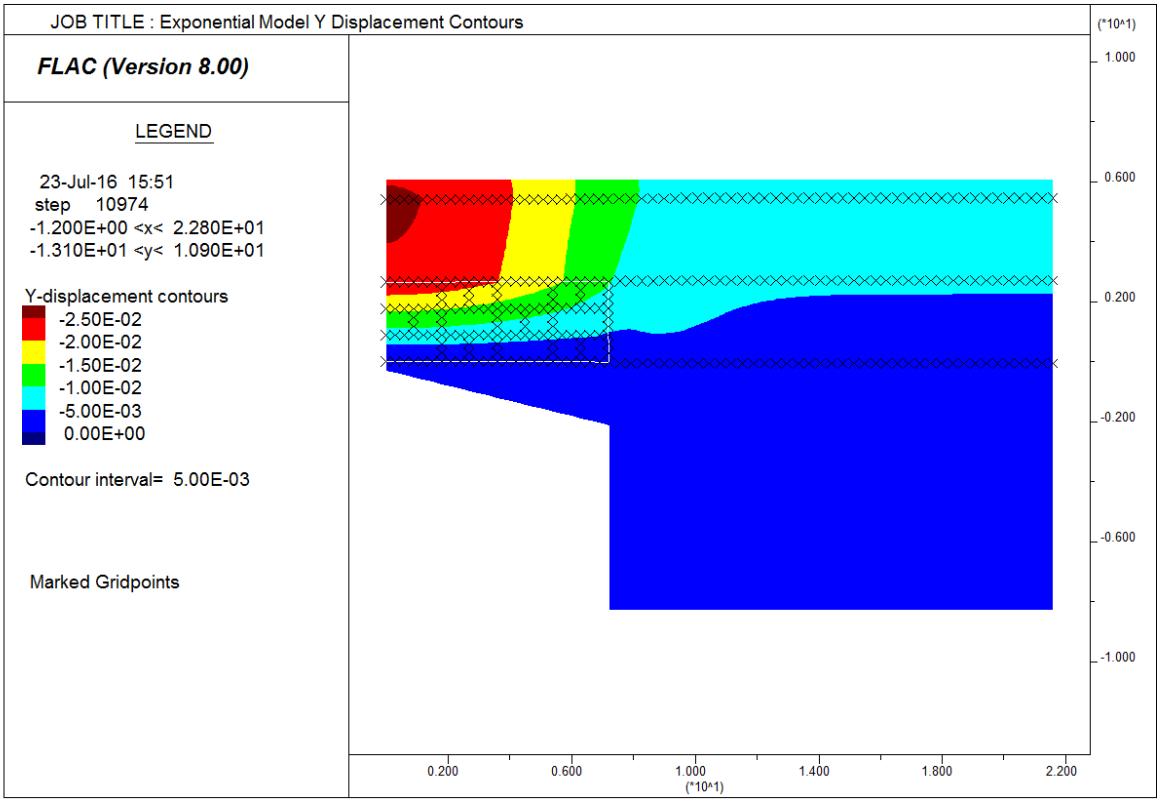

Figure 50: Exponential Model Y Displacements

The overall trend of displacements was similar to the elastic model, with the maximum displacements occurring near the centerline of the culvert. The maximum displacement of about 2 cm for the exponential geofoam model was approximately double the elastic model. The confining and axial pressures in combination with the effect of mixed density geofoam decreased the modulus of the geofoam and resulted in larger displacements but were still much lower than the displacements observed in the field.

X. Creep Behavior

Geofoam under high axial pressures exhibits time dependent deformation. This behavior is exaggerated in the presence of confining pressures. Laboratory tests conducted with both axial and confining pressures show the effect on geofoam, Figure 51. The 34kPa (4.7psi) cell used for confining pressures was within the range suggested by Carrs Creek uniform density simulation models. The 50% axial strength was 50% of the unconfined compressive strength at 10% strain of 55kPa (8psi). For Carrs Creek, the axial loading was approximately 75kPa (11psi), so these laboratory tests were for conservative estimates of loading associated with creep strains over time.

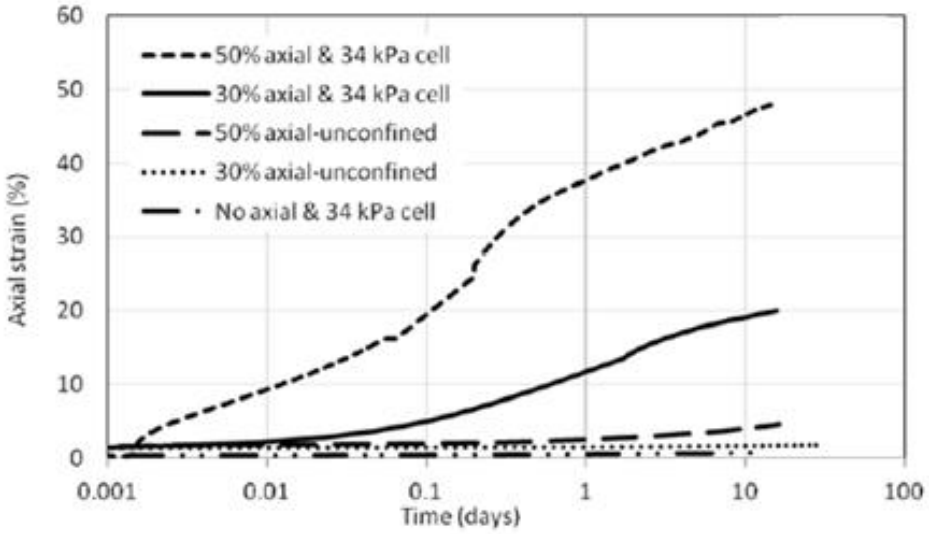

Figure 51: Creep Confining Pressure Laboratory Testing with 34kPa Cell (Birhan, 2014)

Figure 51 shows results for having no unconfined pressures or axial pressures on geofoam. With only one of these forces acting on the geofoam sample, there was very little creep strain developing over time. However when 34kPa (4.8psi) confining pressures were maintained, and axial pressures were applied, excessive creep strains begin to accumulate. An

axial pressure of 33kPa (4.8psi) will bring nearly 20% axial strains, while an axial pressure of 55kPa (8psi) will cause nearly 50% strains over 10 days.

For mixed density geofoam block arrangement, stiffer EPS blocks carried more loading as adjacent, more compressible low density blocks deformed. Such conditions increased both the axial and confining internal pressures within the geofoam assembly. Figure 52 shows creep behavior for greater confinement, with lateral pressures of 69kPa (10psi).

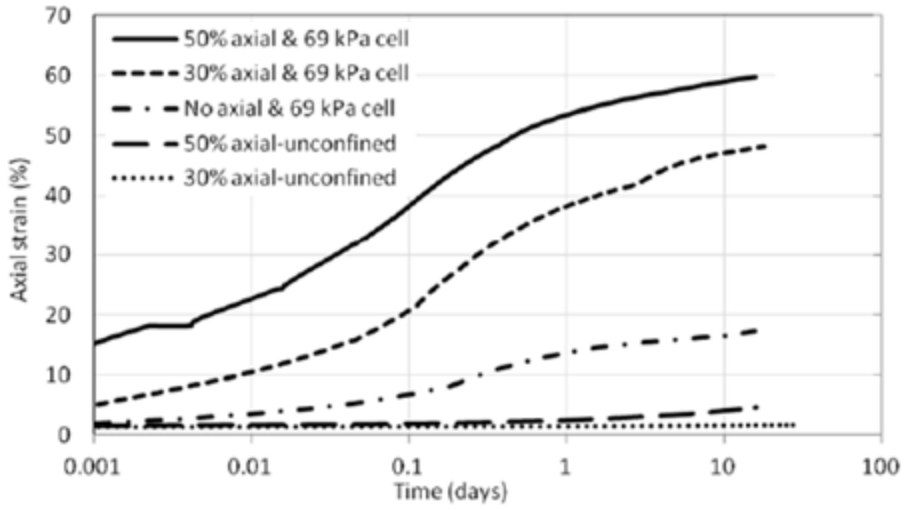

Figure 52: Creep Confining Pressures Laboratory Testing with 69kPa (10psi) Cell (Birhan, 2014)

For 69kPa (10psi) confining pressures in combination with axial pressures of 30% and 50% of unconfined compressive strength at 10% strain, strains accumulated to approximately 50% and 60% over the span of 10 days. It is important to note that the laboratory testing was done on small samples of 2in cubes. Studies of sample size effect have shown large sizes deform less (Birhan, 2014). However, the amount of strain experienced in large size block assemblies as at Carrs Creek contained additional effects of density variation. The effect of

confining pressures and additional stresses due to mixed density interacted to produce large displacements over time in Carrs Creek eastbound and westbound sections.

V. Possible Reasons for Failure of Geofoam

The major design flaw of Carrs Creek Culvert was the excessive fill heights placed on the geofoam. The stresses acting on the geofoam are shown in Figure 53. The width of the culvert was so large that the induced trench effect was minimal. There was a slight reduction of stress near the culvert-soil interface, which was much more prominent in the thicker geofoam section of the eastbound lanes. Both the eastbound and the westbound lanes had overloaded geofoam fill.

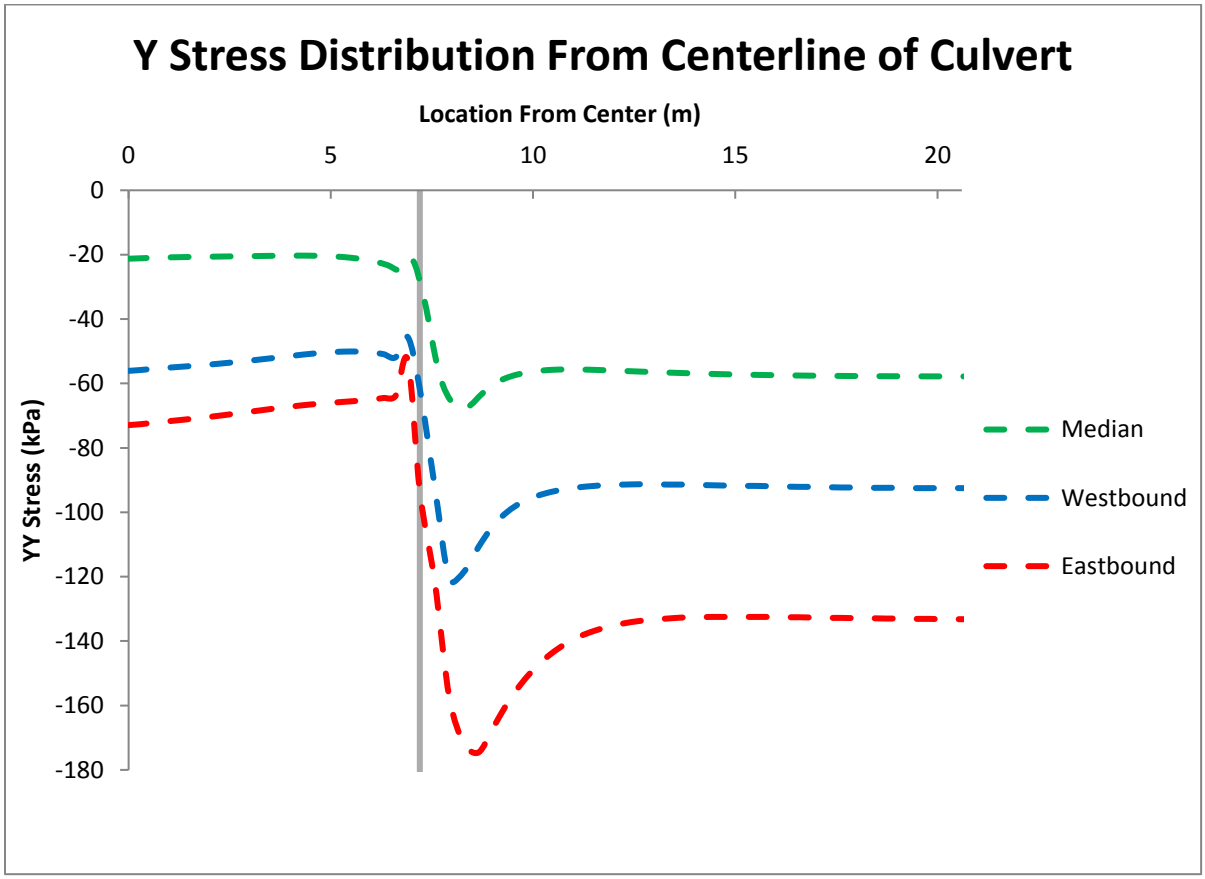

Figure 53: YY Stress Comparisons at Geofoam Base in Carrs Creek

The exclusion of a load distribution slab may have contributed to excessive concentrated point loads from heavy compaction equipment. Regardless of the lift thicknesses of 6in or 12in, stresses were large enough to induce yielding stress history within the geofoam as shown in Figure 35. With repeated cyclic loadings, geofoam undergoes modulus degradation.

Continuous joints alone had practically no effect as an individual mechanism for the geofoam failure. However, when in combination with mixed density geofoams, the continuous joint effects could have been amplified to produce excessive stresses on 8ft by 8ft plan area of individual columns of geofoam. The lack of quality assurance provided a large range of density variation within geofoam, and this needs to be considered in future projects.

Poor drainage and associated higher hydrostatic pressures also contributed adverse effects for the failure. As hydrostatic pressures increased, the all-around confining pressures increased. The amount of soil fill above the geofoam was adequate to resist uplift due to buoyancy in both the eastbound and the westbound sections, however the center of the median was potentially vulnerable to uplift movement during periods of flooding. The low amount of compacted earth fill provided low resistance from uplift due to buoyancy. There were indications of block movement and uplift, such as discoloration between block layers on excavation and removal. Due to the low density and closed cell nature of geofoam, it is important to design with provision for proper drainage.

As shown in Figure 7, bi-axial loadings caused modulus degradation. The dead weight by itself was significant. In combination with mixed density effects, hydrostatic pressures and

possible pre-straining from heavy compaction equipment, confining and axial pressures exceeded allowable design limits for EPS geofoam. These large stress increments also enabled accumulation of time dependent creep deformations, Figure 28. Multiple mechanisms were responsible for the failure of the geofoam within Carrs Creek.

VI. Proper Design

The as built Carrs Creek Culvert had vulnerable sections either to overloading, below the roadways, or uplift, below the median, as described previously. An alternative design that kept the stresses acting on both the culvert and the geofoam while providing adequate resistance to uplift everywhere is shown in Figure 54. This new design features proper drainage, reduced soil fill by increasing the geofoam, a load distribution slab underneath roadway sections, staggered vertical joint and a stepped transverse transition at the soil foam interfaces.

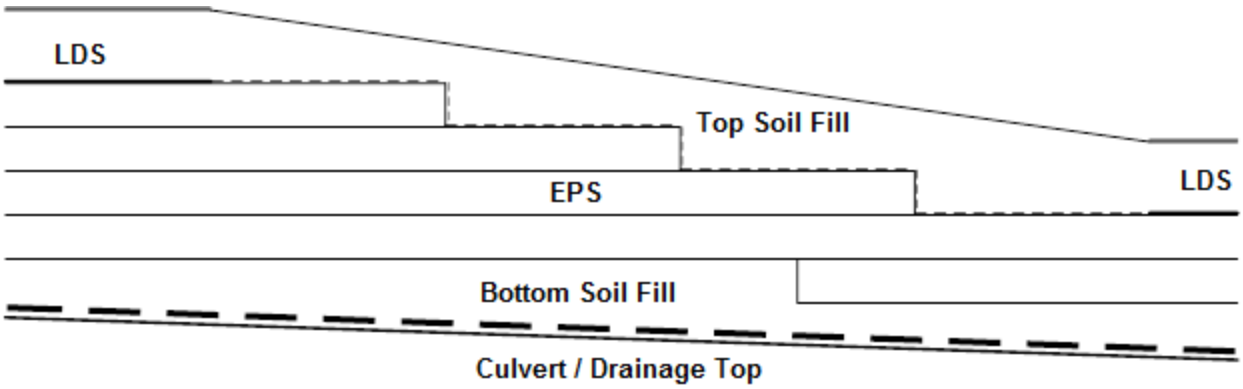

Figure 54: Adjusted Design Longitudinal Profile (Negussey et al., 2014)

Proper drainage would have a significant effect on the amount of pressures acting on both the geofoam and the culvert. Effective drainage would eliminate the possibility of uplift in

the median section during periods of temporary ponding. Proper drainage would be accommodated by using free flowing, coarse fill as a bedding underneath and to the sides of the geofoam, together with lateral and collector drain pipes for the east and westbound cross-sections (Negussey et al, 2014).

The geofoam section has been revised, and major changes have been made in both the eastbound, westbound and median section. The eastbound now contains 4 layers of geofoam blocks, making the total height of geofoam to be 12ft, and 3ft of compacted soil fill would be placed below the geofoam. This reduces the amount of total compacted soil fill required to maintain roadway elevation. The amount of fill and pavement above the geofoam comes out to a total of 5ft. As mentioned previously, the geofoam will be layered in such a manner that there will be no continuous joints. The adjusted design for the eastbound section has been modeled with FLAC and is shown in Figure 55.

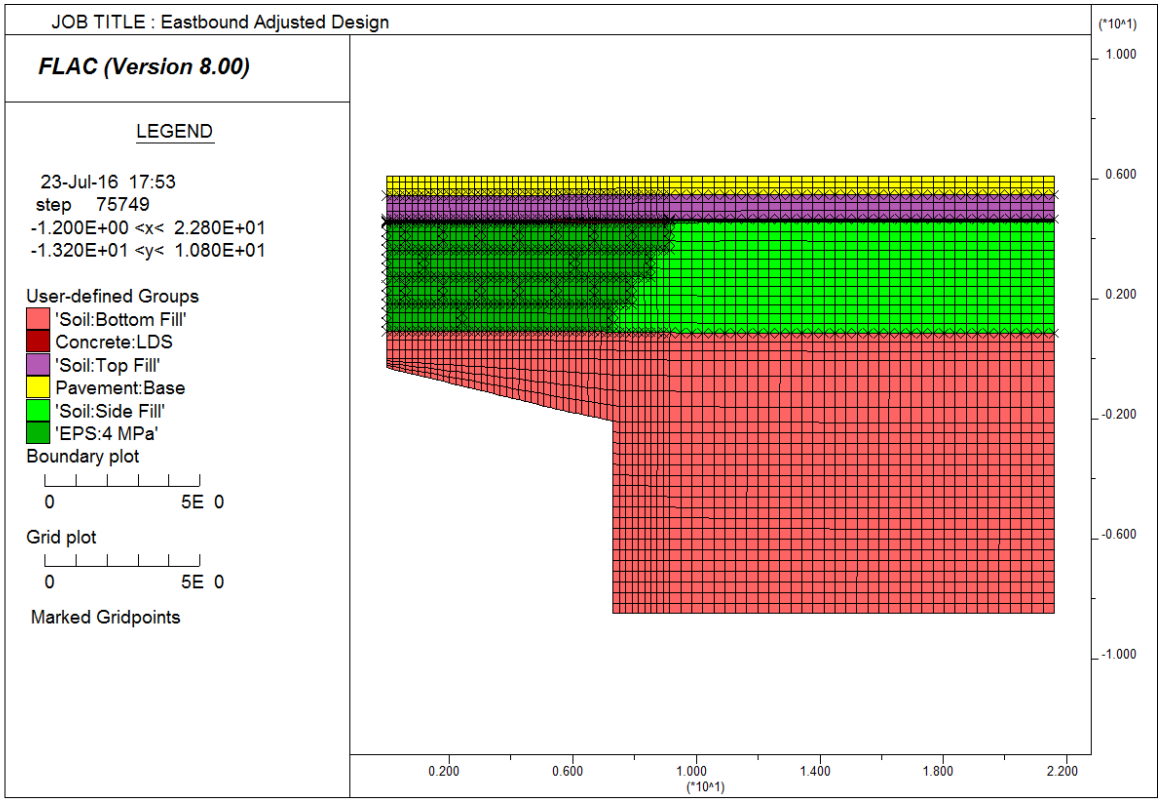

Figure 55: Eastbound Adjusted Design

The roadway lanes support vehicle traffic, so a concrete load distribution slab is cast over the geofoam areas below road lanes. The decrease in compacted fill will decrease pressures due to dead loadings but will increase live load stress increments. These live load stress increments will be attenuated by the concrete load distribution slab. The layout of the geofoam blocks are shown in the FLAC model, Figure 55. Instead of blocks being cut in half to form two 8ft long blocks, entire 16ft long blocks would be used. These blocks are stacked longitudinally every other layer and without continuous vertical joints.

The 4 layers of geofoam fill in the eastbound section transitions to 2 layers of geofoam fill in the westbound section in 3 and 2 layers steps within the median. The median sections are modeled in FLAC as shown in Figure 56 and Figure 57. In the proper design, fill heights above the geofoam such as encountered of about 5 feet during flood levels prevent during the historic record Mid-Atlantic States Flood.

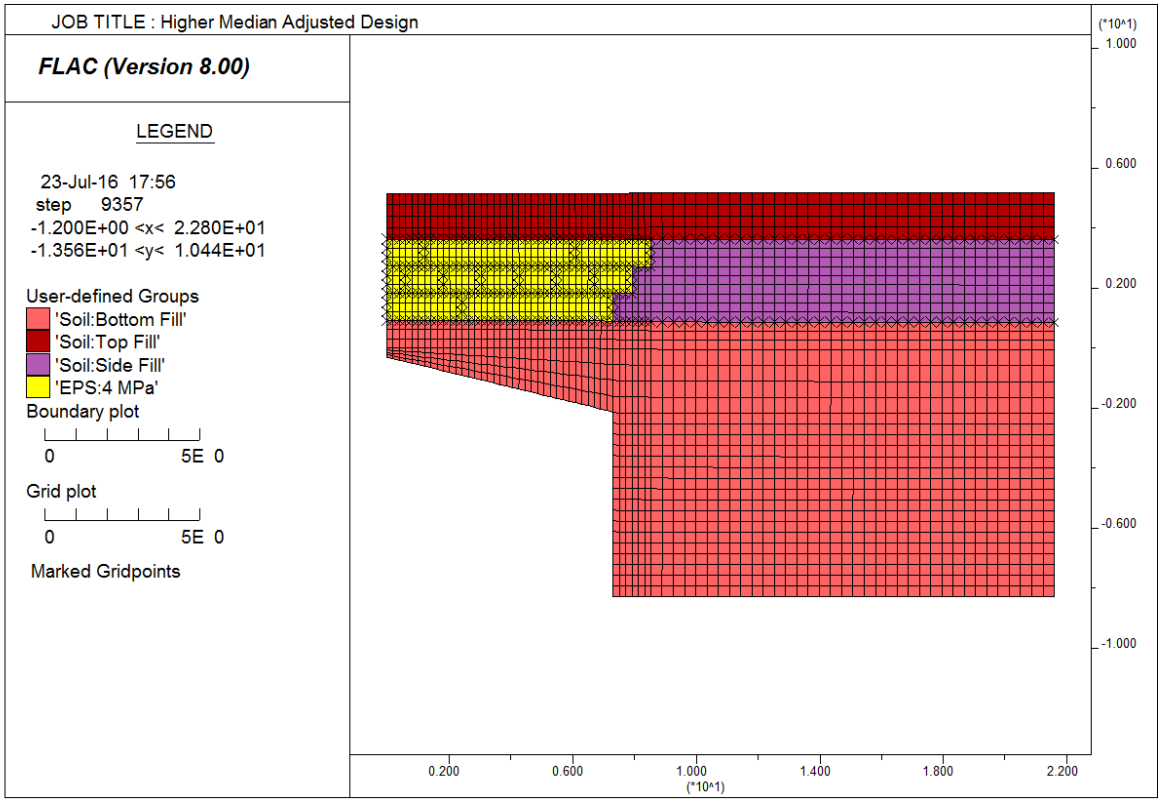

Figure 56: Higher Median Adjusted Design

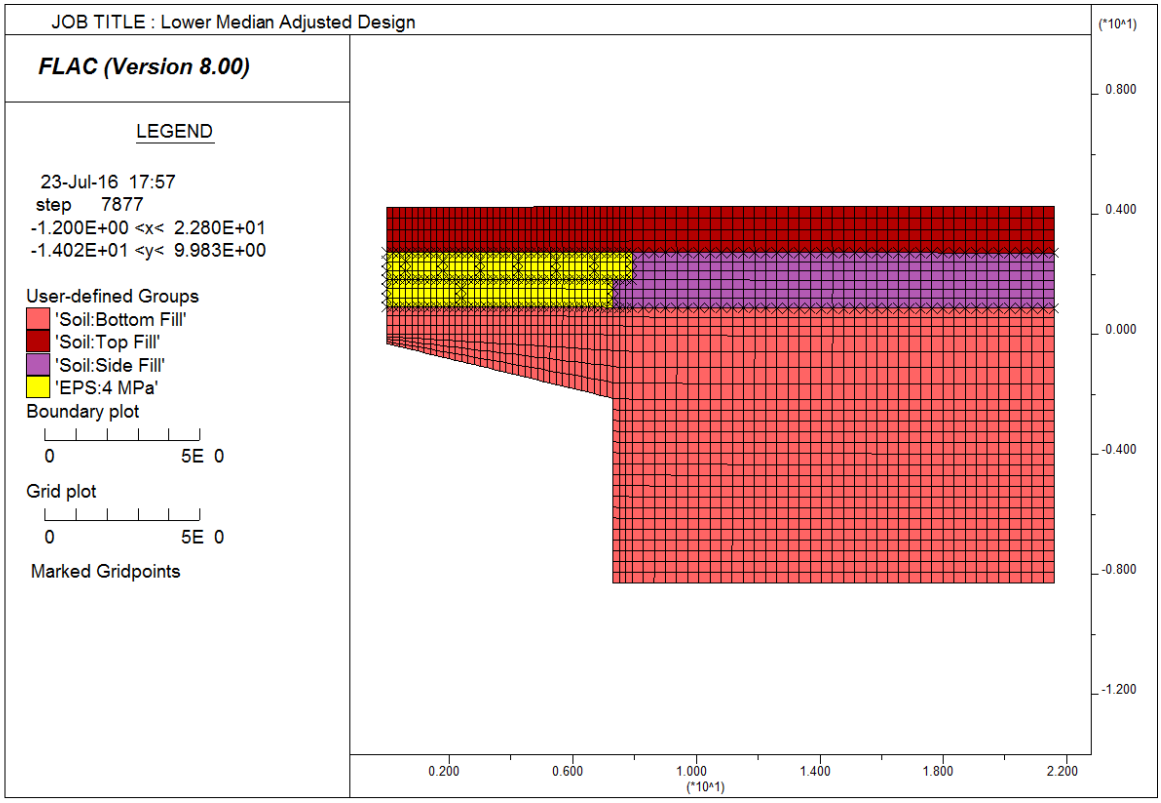

Figure 57: Lower Median Adjusted Design

The westbound section will also have two layers of EPS geofoam and will be the low point of the culvert. Sloping the embankment from the eastbound lane towards the westbound lane will prevent the pooling of any runoff in the median. The westbound section geometry is shown in Figure 58. The westbound section maintains the same elevation as the previously designed section by raising the elevation of the geofoam and putting more compacted soil fill beneath. In this adjusted design, the culvert underlying the westbound section carries the same amount of dead load as compared to the eastbound and the median. A concrete load

distribution slab is placed below road lanes and on top of the EPS geofoam to decrease live load increments from heavy vehicles.

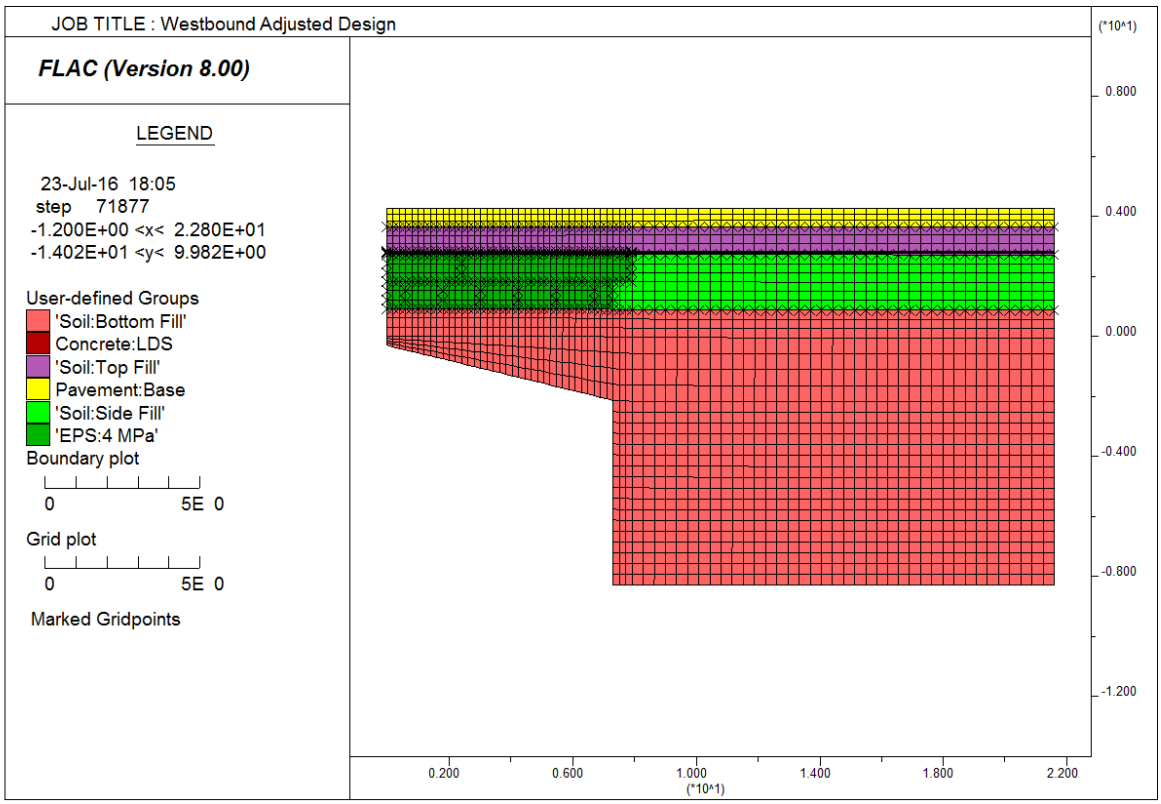

Figure 58: Westbound Adjusted Design

The effect of reducing the soil fill thickness over the geofoam was to reduce vertical stresses on the geofoam. With only 5ft of compacted fill and pavement overlying the geofoam blocks, stresses were reduced to a tolerable level of approximately 35kPa (5psi). This stress remains constant along the majority of the redesigned geofoam sections except for the soil-geofoam interface where stresses ranged from 8kPa (1.16psi) to 20kPa (2.9psi). Stress levels of

the elements along the eastbound top and bottom row of geofoam fill surfaces are shown are shown in Figure 59.

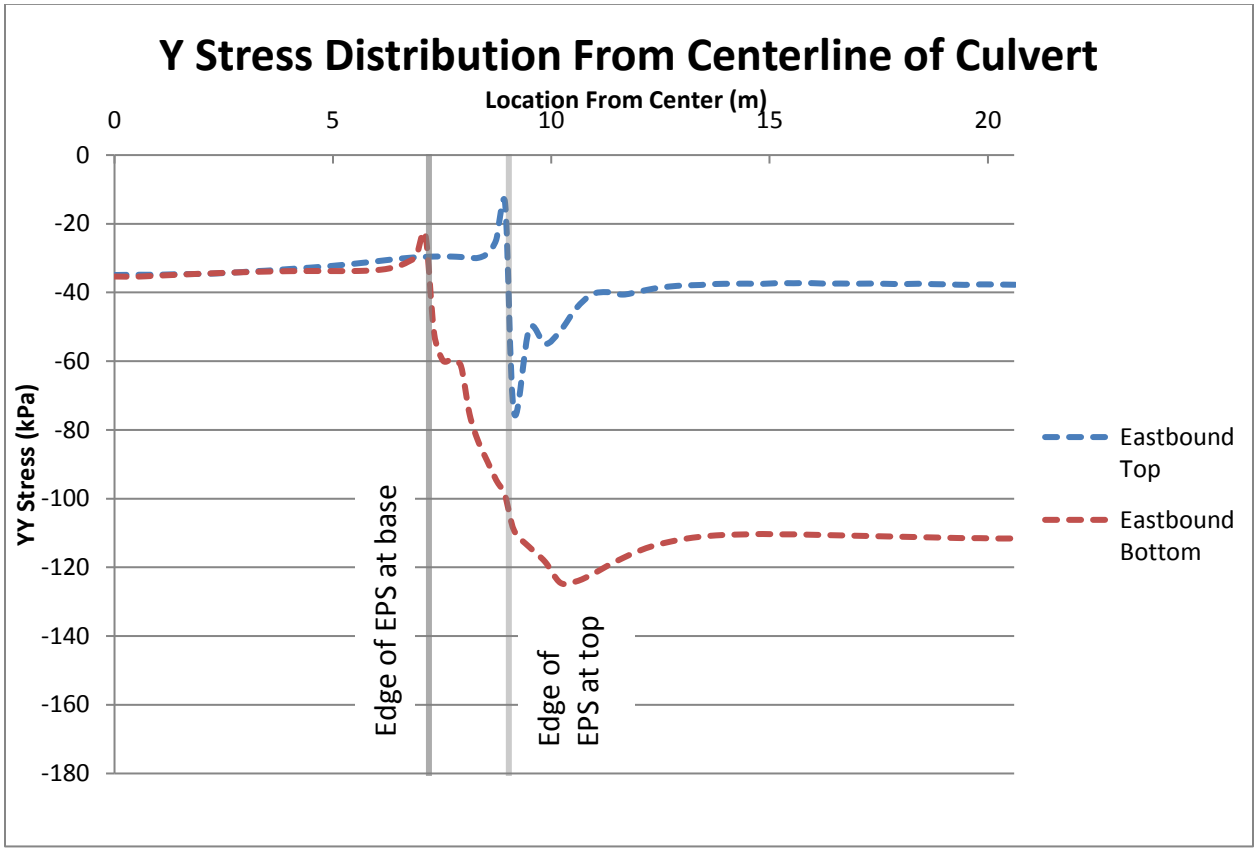

Figure 59: YY Stress at Top and Bottom of Geofoam

Figure 59 also shows negligible stress difference between the top and bottom profiles of geofoam blocks overlying the culvert because of the light weight of the geofoam blocks. Positive arching effects developed in the transverse soil/geofoam interface region. It is important to note that the sections were redesigned so that the stresses acting on the culvert remain uniform, despite differing fill heights underlying the east and westbound lanes and also in the median sections. This was accomplished with the use of geofoam, and should be beneficial to increasing the service life of the culvert.

A comparison of stress profiles for the as built (O) and alternate design (A) are shown in Figure 60. As stated previously, all stresses acting on the revised culvert section are roughly the same due to the approximately equal amounts of fill provided in the re-design. The stresses in the eastbound and westbound sections became much smaller than for the as built section of Carrs Creek. Similarly, the amount of shear stress carried by the adjacent soil column became smaller, due to the decrease in compacted fill heights. The eastbound would contain the largest amount of fill. The as built section of the median has the least vertical stresses and was likely vulnerable to uplift in the presence of storm water accumulation. The stresses in the median section are increased in the redesign.

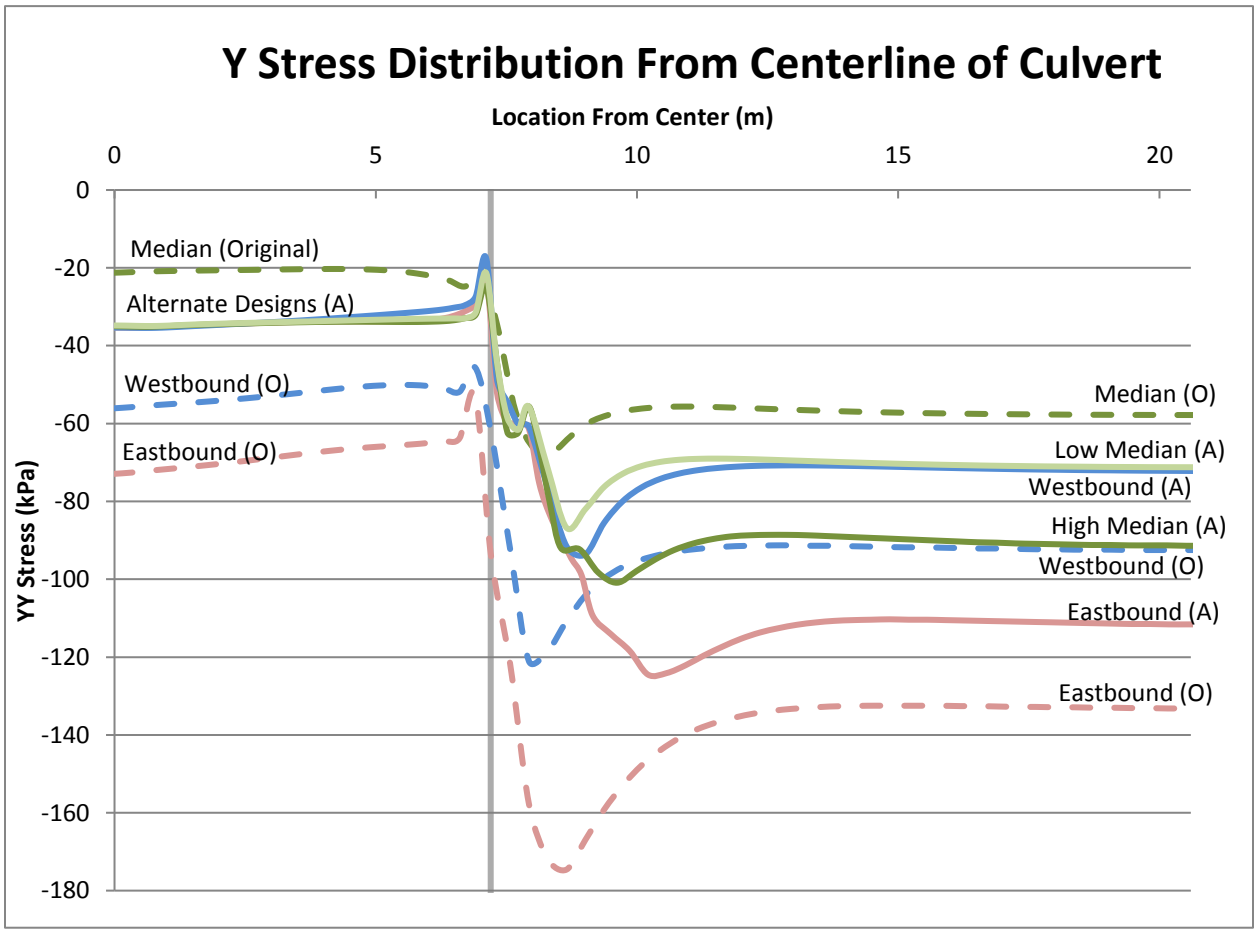

Figure 60: Y Stress Distribution from Centerline of Culvert along the Geofoam Base

It is important to have quality assurance testing on geofoam blocks and reject blocks that do not meet density requirements. Mixing different densities of geofoam contributed to large amounts of stress and strain, as seen within the excavation at Carrs Creek. Hydrostatic pressures have been minimized by providing interceptor and collector drains in the re-design. Table 2 presents comparisons of maximum stresses for the as built and re-designed sections. These values were derived from FLAC output and give a good understanding of the worst case scenario considering each condition. In the previous as-built conditions for Carrs Creek, stresses on geofoam could have accumulated to 160kPa (23.2psi) axially and 70kPa (10.2psi) laterally. The revised design section decreased stresses to 36kPa (5.2psi) axially, and 22kPa (3.2psi) laterally. With proper design, geofoam can be used in structures with large amounts of fill, while keeping overall displacements at a minimum. For mixed density conditions, higher density geofoam blocks carry more load than lower density blocks.

Table 2: Cumulative Stresses on Geofoam

	As Built		**Revised Section**	
Factor	**Axial Stress**	**Confining Stress**	**Axial Stress**	**Confining Stress**
Dead Load	75 kPa	35 kPa	36 kPa	22 kPa
Mixed Density	+ 65 kPa	+15 kPa	-	-
Hydrostatic Pressure	+20 kPa	+20 kPa	-	-
Totals	**160 kPa**	**70 kPa**	**36 kPa**	**22 kPa**

VII. Stresses on Culvert

The stresses for the loading conditions were evaluated at both the centerline and the sides of the Culvert are summarized in Table 3. The null condition of no geofoam produced a negative arching condition which yielded much larger stresses than simply the dead weight of the fill above the culvert. The as built design had higher stresses than was allowable for the specified geofoam at the centerline. Where the geofoam grade was even lower than the specified grade, crushing and large settlements developed.

Table 3: Summary of Stresses on Eastbound Culvert Section

Controlling Mechanism	Maximum YY Stress on Center of Culvert	Maximum YY Stress on Sides of Culvert
Free Field	**140**	**175**
Negative Arching	**140**	**240**
9ft of Geofoam – As Built Section	**83**	**150**
Revised Section	**67**	**135**

The stresses at the side of the culvert in this consideration increased to 150kPa (22psi) due to a localized down drag on the relatively rigid culvert by negative arching as the adjacent compacted soil settled. The revised section was subjected to the lowest loadings, at both the centerline and the end of the culvert. The overall stress comparisons on the geofoam and the culvert for the as built, case of no geofoam, and the proposed re-design are shown in Figure 61. Note that the stresses in the geofoam are uniform and below tolerable working stress levels everywhere in the re-designed case and the maximum stress level in the culvert is acceptable.

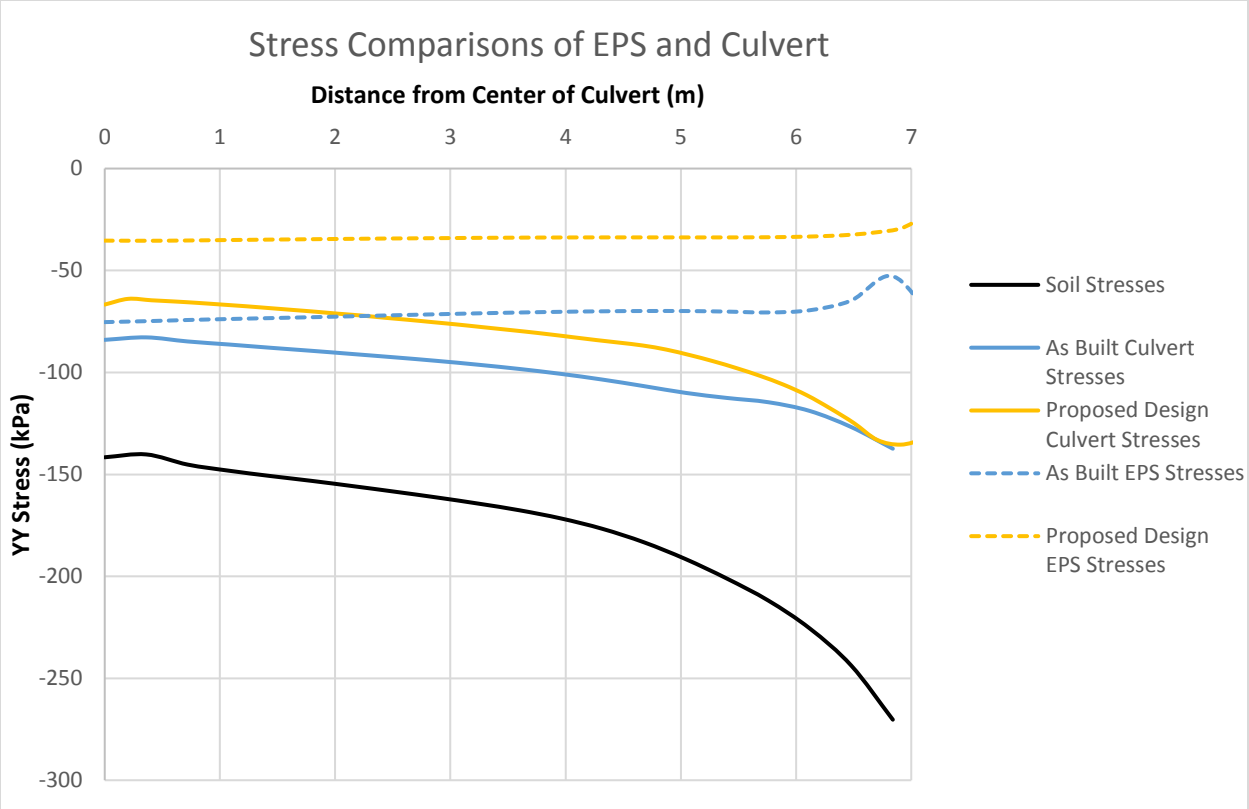

Figure 61: Stresses Comparisons of EPS and Culvert

Chapter 4 – Conclusions

4.1 Conclusions

Model studies of wide culverts with the use of EPS Geofoam as backfill in an induced trench have been performed and the following conclusions and recommendations are made.

1) As the trench width increases the magnitude of stress reduction decreases. As the trench width increases to greater than 25 ft and the culvert becomes classified as a bridge, the greatest amount of stress reduction is observed at the edge of the geofoam. Bridge culverts will not have the benefits of positive arching at center.
2) The major effect of thickness variation within the compressible fill is stress reduction due to the use of lightweight fill. The mode of arching was the same but the stress magnitudes varied due to the thickness of the foam section. This agreed with classical arching theory which only required a small amount of settlement to introduce arching effects.
3) The effect of positive arching in an induced trench increased pressures to the side columns of soil adjacent to the culvert. Both axial and lateral pressures increased from the stress transfer and should be taken into consideration in the design to prevent overloading of the culvert
4) The inclusion of a load distribution slab is essential to attenuate stresses from live loads during compaction of fill. In the case of the reconstruction of the culvert at Carrs Creek, live loads in lift thicknesses of 5 inches and 12 inches introduced loads beyond the recommended working stress of the specified EPS Geofoam.

5) EPS installation with continuous vertical joints can cause the geofoam blocks to act as individual springs as opposed to a monolithic structure. This may be detrimental in combination with other design flaws and poor construction supervision.
6) High groundwater pressures increase buoyancy effects and lateral pressures that can cause reduction of modulus in materials with cell structures such as EPS Geofoam.
7) Poor quality assurance of the supplied EPS Geofoam may lead to differential settlements in the case that different density blocks are used. Mixed density geofoam blocks can cause overstressing of some blocks beyond its recommended working stress.
8) The degradation of modulus of EPS Geofoam due to confining stress effects was captured in the FLAC models.
9) In redesigned sections, the Geofoam and soil interface was stepped to reduce lateral stresses. Geofoam can also be placed at a shallower depth with the use of a load distribution slab.

4.2 Suggestions for Further Research

This research focused on the mechanics of induced trench and effects of lightweight fill. The extremes in trench widths are considered to give an understanding of proper design considerations of culverts. The results show that there are limits to loads that can be placed on top of geofoam in an induced trench. It is possible to distribute loads in between spaced layers of geofoam blocks to instigate multiple sections where positive arching occur. The effect of successive layers of positive arching has not been studied before and could be observed in the future with both computer modeling and in field measurements. Successive layers of different density EPS stacked with earth fill In between can allow for greater fill heights to be

constructed. To also account for excessive overburden stresses acting on buried geofoam, a geogrid may be placed on top to transfer loadings to the adjacent earth fill. The combination of multiple positive arching compressible fills and geogrids can allow for deeply buried culverts to be subjected to much smaller stress concentrations.

Another consideration for further research would be to consider arching in the horizontal direction. Research done strictly on arching in the horizontal direction has not been performed before. In testing the sections at Carrs Creek there was an arching effect observed at the interface between the geofoam and the underlying rigid culvert. The extent of the horizontal stress reduction may be controlled by the thickness of the geofoam, which could act as the width component in the vertical arching conditions. The behavior of horizontal positive or negative arching would most likely be similar to the effects seen in vertical arching, but the similarities and magnitude of stresses are to be determined with further research.

References

American Concrete Pipe Association. (2011). Concrete Pipe Design Manual, www.concrete-pipe.org

Ananstha, N., & Srirajan, S. (2001). Effect of Confining Stress on Compressive Strength of EPS Geofoam. *Procedings of 3rd International Conference of EPS Geofoam*.

Birhan, A. (2014). Effect of Confinement and Temperature on the Behavior of EPS Geofoam, PhD Thesis, Syracuse University.

Chen, B., & Sun, L. (2013). Performance of a Reinforced Concrete Box Culvert Installed in Trapezoidal Trenches. *Journal of Bridge Engineering*, *19*(1), 120–130.

Chen, B., Zheng, J., & Han, J. (2009). Experimental Study and Numerical Simulation on Concrete Box culverts in trenches. *Journal of Performance of Constructed Facilities*, *24*(3), 223–234.

Culmo, M. (2011). Accelerated Bridge Construction Manual. Federal Highway Administration.

Geotechnical Engineering Bureau. (2008). 2006 - 2007 Emergency Structure Replacement Report Interstate 88 over Carrs Creek, NYSDOT, Albany

Itasca. (2008). FLAC Ver. 6.0 User's Manual. Itasca Inc.

Jan Vaslestad, N., Sayd, M. S., Johansen, T. H., & Louise Wiman, N. (2011). Load Reduction and Arching on Buried Rigid Culverts using EPS Geofoam. Design Method and Instrumented Field Tests, Norwegian Pubic Roads Administration.

Kim, K., & Yoo, C. H. (2002). Design Loading for Deeply Buried Box Culverts. Highway Research Center, Auburn University, Alabama

Lundvall, J. (1997). *Mitigation of Roadway Settlement above Buried Culverts and Pipes*., MS Thesis, University of Wyoming.

McAffee, R. P., & Valsangkar, A. J. (2008). Field Performance, Centrifuge Testing, and Numerical Modeling of an Induced Trench Installation, Canadian Geotechnical Journal.

Negussey, D. (2007). Design Parameters for EPS Geofoam, (Soils and Foundations), 161–170.

Negussey, D.; Singh, S.; Andrews, L.; Liu, C.; and Birhan, A. (2014). Investigation of the Carrs Creek Geofoam Failure. Final Report, University Transportation Research Center, Region 2.

Oshati, O. S., Valsangkar, A. J., & Schriver, A. B. (2012). Earth pressures exerted on an induced trench cast-in-place double-cell rectangular box culvert. *Canadian Geotechnical Journal*, *49*(11), 1267–1284.

Sheeley, M. (2000). *Slope Stabilization Utilizing Geofoam* (Masters Thesis). Syracuse University, Syracuse, New York.

Sladen, J. A., & Oswell, J. M. (1988). TheInduced Trench Method-a Critical Review and Case History. *Canadian Geotechnical Journal*, *25*(3), 541–549.

Spangler, M. (1941). The Structural Design of Flexible Pipe Culverts. Iowa State University Engineering Experiment Station.

Spangler, M. (1973). Long Time Measurement of Loads on Three Pipe Culverts. Engineering Research Institute, Iowa State University.

Srirajan, S., Negussey, D., & Anansthas, N. (2001). Creep Behavior of EPS Geofoam. In *Proceedings of EPS Geofoam 3rd International Conference*. Salt Lake CIty, Utah.

Sun, L., Hopkins, T., & Beckham, T. (2010). Long-Term Monitoring of Culvert Load Reduction Using the Imperfect Ditch Method Backfilled with Geofoam.

Sun, M. (1995). Engineering Behavior of Geofoam and Lateral Pressure Reduction in Substructures, MS Thesis, Syracuse University.

Taylor, R. K. (1971). *Induced Trench Method of Culvert Installation*, Illinois Division of Highways, Bureau of Research and Development.

Transportation Research Board. (1990). Guide to Earthwork Construction, National Research Council.

Voiland, A. (2013). In a Warming World, the Storms May Be Fewer But Stronger. Retrieved September 14, 2014, from http://earthobservatory.nasa.gov/Features/ClimateStorms/page2.php

Yoo, C. H., Parker, F., & Kang, J. (2005). *Bedding and Fill Heights for Concrete Roadway Pipe and Box Culverts*. Highway Research Center, Auburn University.

VITA

Stephen Singh

1841 East 48th Street
Brooklyn NY, 11234
Phone : (646) 417-3363

Education

B.S. in Civil and Environmental Engineering, 2011, Syracuse University, Syracuse, New York,

M.S. in Civil and Environmental Engineering, 2016, Syracuse University, Syracuse, New York,

Experience

Langan Engineering, Environmental, Surveying and Landscape Architecture D.P.C.
Staff Engineer – New York, NY, September 2014 to Present

- Prepared geotechnical engineering reports, construction specifications and assisted in drafting proposals for shallow and deep foundations and support of excavation systems.
- Performed special inspections of backfill placement, borings, test pits and SOE.
- Used finite element analysis software to prepare design packages.

Syracuse University
Research Assistant, Geofoam Research Center – Syracuse, NY, June 2013 to June 2014

- Created computer models in FLAC of the failure of EPS at Carrs Creek Culvert to understand major design flaws and presented findings to NYSDOT.
- Received critical acclaim from Engineering Dean's for the practicality and usefulness of research outcomes.

Syracuse University
Teaching Assistant, L.C. Smith College of Engineering – Syracuse, NY, January 2013 to June 2014

- Aided in the instruction of core classes for undergraduate and graduate engineering students, such as Transportation Engineering, Foundation Engineering, and Designing with Geofoam.
- Instructed students on how to use laboratory equipment and generate computer models of geotechnical problems.
- Responsible for grading assignments, quizzes and exams.

Honors and Awards

Nunan Research Competition Practical Application Winner, Syracuse University, 2014
Louis N. DeMartini Award for Outstanding Team Design Project, Syracuse University, 2011
Samuel P. Clemence Award for Outstanding Senior Design, Syracuse University, 2011

Skills

FLAC, PLAXIS, ANSYS, GeoStudio, SoilWorks, MathCAD, AutoCAD, Microstation, REAME, SAP2000.

Publications

Negussey, D.; Singh, S.; Andrews, L.; Liu, C.; and Birhan, A. (2014). Investigation of the Carrs Creek Geofoam Failure. Final Report, University Transportation Research Center, Region 2.